Proceedings of ESB 2009 Workshop

Movement Biomechanics and Sport, European Society of Biomechanics 2009 Workshop, June 7-9, ETH Zurich, Science City, Zurich, Switzerland

Conference Proceedings

Publication date:
2009

Permanent link:
https://doi.org/10.3929/ethz-a-010266457

Proceedings of
ESB 2009 Workshop

Movement Biomechanics and Sport
European Society of Biomechanics 2009 Workshop
June 7 - 9, ETH Zurich, Science City, Zurich, Switzerland

www.esb2009.ethz.ch

Impressum

Nadia Sigrist
Hans Gerber
Institut für Biomechanik, ETH Zürich

TABLE OF CONTENTS

Welcome

Welcome to the ESB 2009 Workshop “Movement Biomechanics and Sport” !

In many industrialized countries, musculoskeletal conditions have become a national priority in recognition of the major health and economic burdens they place on the community. While bone and cartilage have been at the center of these developments in recent years and in previous ESB workshops, the other tissues in the musculoskeletal system have received less attention from a public health point of view. However, during any type of movement, especially during sport, soft tissues within the human body are loaded too. An immediate response to such loading can be stimulation, pain or injury, whereas long-term physiological processes can include mechanical adaptation.

The organizing committee is looking forward to a stimulating workshop in 2009 with challenging topics and interesting discussions.

Background Information

In 2005 the first ESB workshop was held in Leuven Belgium at the Division of Biomechanics and Engineering Design. It was devoted to ‘Mechanobiology of Cells and Tissue Regeneration’. The second Workshop 2007 was hosted by the Trinity Centre for Bioengineering in Dublin. The theme was 'Finite Element Modeling in Biomechanics and Mechanobiology'. Both workshops were highly successful in bringing together junior and senior researchers.

Now, the Workshop 2009, is hosted at the Institute for Biomechanics, ETH Zürich. In 2009, the Institute for Biomechanics also celebrates its 20th birthday. This celebration in combination with the workshop represents an interesting platform for young researchers and senior scientists. More than 100 researchers coming from all parts of Europe are expected to participate.

In 1976, the **European Society of Biomechanics** was founded in Brussels by 20 scientists from eleven countries. It is now the largest Biomechanics society in Europe with almost 500 members. The primary goal of the ESB is to encourage, foster, promote, and develop all fields of research, progress, and information related to Biomechanics.

The **Science City** Campus of ETH Hönggerberg offers excellent conditions for this workshop. Lecture theaters, cafeterias, sport facilities as well as laboratories are all within walking distance.

Organizing Committee:

Dr. Jachen Denoth (Chair)

Prof. Dr. Ralph Müller (Co-Chair)

Dr. Hans Gerber (Secretary General)

Dr. Gisela Kuhn (Program Chair)

Dr. Silvio Lorenzetti (Chair of Scientific Committee)

Dr. Roland Müller (Local Scientific Committee)

Prof. Jess Snedeker (Local Scientific Committee)

Dr. Peter Wolf (Local Scientific Committee)

International Scientific Committee:

Prof. Aminian Kamiar

Dr. Birch Helen

Prof. Boutellier Urs

Dr. Denoth Jachen

Prof. Dominique Pioletti

Prof. Flück Martin

Dr. Linari Marco

Dr. Lorenzetti Silvio

Dr. Müller Roland

Prof. Narici Marco

Prof. Snedeker Jess

Dr. Wolf Peter

Contact:

ESB2009@ethz.ch

www.esb2009.ethz.ch

c/o ETH Zürich
Institute for Biomechanics
HCI E 355.1
8093 Zürich
Switzerland

phone: +41 44 633 62 11
fax: +41 44 633 14 53

Movement Biomechanics and Sport

The workshop has four sessions, each focusing on the short and long-term behavior of soft tissues under load. After an introductory session on the first half day, sessions on the material response, the response of the system and the system adaptation will follow.

FORMAT:

The program will combine a mixture of tutorials and state-of-the-art reviews given by leading researchers. Multiscale modeling is thought to be the line of thinking. The invited tutorial speakers are encouraged to make an effort to combine scales from micro to macro or vice versa.

Participants will further have the opportunity to present their work as an oral presentation (10 minutes and 5 minutes for questions) or as a poster presentation. This includes a poster (dimensions width 1.2m, height 0.8m) and a 1 minute short presentation including two slides.

Furthermore, special informal mentoring lecture with the title “The most important aspects when undertaking and completing a Ph.D.” is organized by the ESB.

Our main sponsors have a window for presenting their products.

The confirmed tutorial speakers are:

Prof.	Per Aagaard	University of Southern Denmark, DK
Dr.	Helen Birch	University College London, UK
Dr.	Jachen Denoth	ETH Zürich, CH
Prof.	Martin Flück	Manchester Metropolitan University, UK
PD Dr.	Jörg Goldhahn	Schulthess Clinic, Zürich, CH
Prof.	Geoffrey Goldspink	University College London, UK
Prof.	Hans Hoppeler	University of Bern, CH
Dr.	Marco Linari	University of Florence, It
Prof.	Marco Narici	Manchester Metropolitan University, UK
Prof.	Jess Snedeker	University of Zürich, CH

POSTERS

A special emphasis will be placed on student projects at both the Master’s and Doctoral levels, and ample time will be provided for showcasing student work. Posters are a great way to invite feedback on research results and engage people in constructive conversation. A guided poster session with short presentations and a chairman will be held on Sunday evening. This event includes a buffet dinner.

Awards

Awards for the best student presentation and poster will be given at the closing ceremony.

GOLD

QUALISYS
Motion Capture Systems

http://www.qualisys.com

SILVER

CADFEM CH COMPUTER AIDED ENGINEERING

http://www.cadfem.ch

SYNTHES®

http://www.synthes.com

zimmer

http://www.zimmer-orthopedics.ch

smith&nephew

http://global.smith-nephew.com/master

BRONZE

RMS Testing · Research · Consulting
www.rms-foundation.ch

Taylor & Francis
Taylor & Francis Group

www.taylorandfrancisgroup.com

Muscle loading; functional, structural and molecular implications as well as health consequences

Hans Hoppeler

Department of Anatomy, University of Bern, Switzerland, hoppeler@ana.unibe.ch

Skeletal muscle tissue is characterized by an extraordinary phenotypic plasticity. Using specific training interventions massive functional changes in strength or endurance in untrained subjects can be induced in weeks. These functional gains are the result of muscle structural modifications which have been well characterized over the last 30 years. Molecular tools enable us now to study the mechanisms of muscle plasticity. It has become clear recently that many of the structural and functional consequences of typical exercise regimes are controlled by changes in gene expression and or changes in translation as well as in modifications of muscle degradation pathways.

During exercise muscle cells are subjected to mechanical, metabolic, neuronal and metabolic signals which are transduced over multiple pathways to the muscle genome. Exercise thus activates a range of signaling cascades, the individual characteristic of the stress leading to a complex response of a network of signaling pathways. Signaling typically results in the transcription of multiple early genes among those of the well known fos and jun family as well as many other transcription factors. These can bind to promoter regions of downstream genes initiating the structural response of muscle tissue. While signaling is a matter of minutes, early genes are activated over hours leading to modifications of structure genes that are then effective over days. Repeated exercise sessions lead to concerted accretions of multiple mRNAs which upon translation result in a stepwise increase of proteins of related functional entities (i.e. all enzymes of the Krebs cycle. On the structural level the protein accretion manifests itself for instance as an increase in mitochondrial and capillary volume upon endurance training and myofibrils and associated proteins upon strength training. The molecular response to strength training (i.e. the accretion of myofibrillar proteins) is less established. We find a transient depression of transcription over 24 hours. It looks as if the main actors in strength training are the mTOR pathway and the S6 Kinase both influencing translation. It is also realized that there is crosstalk between signaling pathways; hence the outcome of concurrent training protocols for strength and endurance depend on the interactions of the key players in the signaling cascades. It seems likely that any single exercise stimulus carries a molecular signature which is typical both for the type of stimulus (i.e. endurance vs. strength) as well as the actual condition of muscle tissue (i.e. untrained vs. trained). It therefore seems feasible to use molecular tools to judge the properties of an exercise stimulus earlier and at a much finer level than is possible with conventional functional or structural techniques which require weeks of exercise before a training response can be detected reliably. The portrayed molecular approach to judging exercise interventions holds particular promise in understanding the impact of exercise in a health and rehabilitative context.

The current molecular techniques begin to paint a very detailed picture of the modulatory events involved in muscle malleability indicating distinctly different molecular reaction patterns for endurance and strength type exercise. This information will eventually be of value for the mechanistic understanding of the health benefits of exercise and for planning disease tailored intervention programs.

Muscle repair and hypertrophy following exercise and the role of Mechano Growth Factor and the IGF-1 gene.

Geoffrey Goldspink

Departments of Surgery and Anatomy, Royal Free and University College Medical School,
University of London, UK

Introduction

Macro and micro damage frequently occurs in musculo-skeletal tissues but the expression of certain genes enables them to repair and also to adapt to future increased mechanical strain. Here attention is paid to the role of the GH/IGF-1 axis in skeletal muscle and the discovery of mechano growth factor (MGF). The latter is derived from the IGF-I gene by alternative splicing and in the young is associated with increasing contractile strength in response to exercise. However, one very important medical and socioeconomic problem is why do the elderly lose muscle mass and strength? Also why do even younger individuals lose muscle mass after prolonged bed rest or during exposure to reduced gravity in space? As well from a medical standpoint – why does muscle loss occur in a range of diseases and in some it is life threatening? Therefore we should seek to understand the mechanisms so natural and therapeutic means of ameliorating the loss of muscle mass and strength can be devised.

Methods

These involve combining physiological as well as molecular methods in order to understand the cellular basis of skeletal muscle adaptation and repair. How cells detect mechanical stress is of considerable interest, particularly, how the mechano-transduction process leads to changes in the expression of certain genes the study of which has become more possible. My quest for understanding these processes commenced almost 20 years when my group used a differential display method to find which genes were expressed after stretching and stimulating skeletal muscle. This led to the discovery of Mechano Growth Factor (MGF) which is derived from the IGF-I gene by alternative splicing following muscle overload. Over the past two decades our group at University College London have collaborated with and continues to collaborate with centres in several countries that have specialized techniques and expertise, so that the role of MGF could be studied in animal models of disease and in human cell and tissue samples.

Results

Following a bout of resistance exercise the IGF-I gene is initially spliced to MGF which due to a reading frame shift has a unique carboxy-terminal (E domain) peptide for which the natural version has a short half life and is thus produced as a pulse lasting a day or so. Recent studies using human primary cultures have shown that the MGF E-peptide activates muscle progenitor (stem) cells in normal human muscle. It was found that although the initial yield of these cells was less from dystrophy and ALS patients the numbers were significantly increased by MGF C-peptide within 48 hr. During the second phase following the exercise the IGF-1 gene is spliced to IGF-1Ea. which induces the progenitor cells to enter the myogenic pathway and to fuse with the muscle fibres. With the increased number of nuclei and gene copies, IGF-I which is a major metabolic agent also increases protein synthesis for the second stage of muscle repair and hypertrophy. During ageing, growth hormone levels decline markedly and administration of hGH appears to up regulate the number of primary transcripts of the IGF-I gene so more MGF can be produced in older people by exercise. As well as understanding the gene expression involved in muscle adaptation, the unique MGF peptide offers the prospect of treating muscle wasting by increasing the number of muscle progenitor (stem) cells during the ageing process, and muscle weakness associated with diseases and injury.

References

Goldspink G, Yang SY, Hameed M, Harridge SDR, PM Bouloux. (2005) The role of MGF and other IGF-I splice variants in muscle. Chapter 14. in "Endocrinology of Physical Exercise and Sport" A volume of the Encylopaedia of Sports Medicine. Edited by W.J. Kraemer & A.D. Rogol.

Goldspink G. (2005) Research on mechano growth factor (MGF) its potential for optimizing physical training as well as misuse in doping. British Journal of Sports Medicine 39: 787-788.

Goldspink G. (2005) Impairment of IGF-I gene splicing and MGF expression associated with muscle wasting Int. J. Biochem. Cell Biol 37: 2012-2022.

Goldspink G. Wessner B. Bach N. (2008) Growth factors, muscle function and doping. Curr. Opin. Pharmacol. **8**. 352-357

Hill M, Wernig A and Goldspink G. (2003) Muscle satellite (stem) cell activation during local tissue injury and repair. J. Anat 203, 89-99

Hameed M, Lange KHW, Andersen JL, Schjerling P, Kjaer M, Harridge SDR, Goldspink G.(2004 The effect of recombinant human growth hormone and resistance training on IGF-I mRNA expression in the muscles of elderly men. J. Physiol. 555.1, 231-240.

The movement and loading during activities and its consequences on the musculo-skeletal system with a focus on soft tissues - relevant medical problems of the soft tissues

Jörg Goldhahn[1,2]

[1] Research Department of the Schulthess Klinik Zurich, Switzerland
[2] Institute for Biomechanics, ETH Zurich, Switzerland, joerg.goldhahn@kws.ch

Introduction

Acute and degenerative changes of soft tissue structures lead to significant impairments of the musculo-skeletal functions. Conditions like “frozen shoulder” with shrinked capsule of the glenomumeral joint lead to restrictions of active and passive range of motion. The opposite condition leads to joint instability. Both extremes have to be avoided during surgical reconstruction of joints. However, biological reactions show huge individual variations. Therefore the final result of reconstructive interventions at the musculoskeletal system cannot be predicted due to this uncertainty. The tutorial will exemplify both, the soft tissue condition leading to the disease and the biological soft tissue reaction during the healing process with the help of the most common degenerative disease at the hand (Carpometacarpal osteoarthritis of the thumb - CMC I osteoarthritis)[1].

Soft tissue problem leading to surgery

Although etiology and pathogenesis of the disease are not totally understood, there is anatomical and biomechanical evidence that the ligamentous structures surrounding the trapeziometacarpal joint become weaker with age, leading to instability of the thumb saddle joint and thus supporting the progress of a CMC I osteoarthritis.

The subsequent subluxation and the altered loading of the joint, both leads to painful osteoarthritic reactions of the joint, loss of grip strength, and finally impairment of hand function.

Therapeutic approach

There is a large variety of surgical procedures to treat the disease. They include ligament reconstruction at early stages, arthroscopic debridements, osteotomies or prosthetic replacements. Trapeziectomy with or without ligament reconstruction and tendon interposition (LRTI) are mainly performed in advanced stages.

The procedure includes the following steps:

- exposure and excision of the trapeziometacarpal joint
- Release of two thirdsof the flexor carpi radialis tendon proximally in the forearm
- Routing of the free end through the basis of the thumb metacarpal and suturing to itself
- Folding of the remaining tendon on itself and suturing
- Positioning of this autologous interposition material into the trapezium space
- Splinting for 3-4 weeks

Biomechanical challenge

The different steps of the procedure aim to re-establish original joint biomechanics of the trapeziometacarpal joint. However, it is not clear how much each single step contributes and how healing processes influence the functional result. On one hand patients with strong scar tissue reactions are more likely to get movement restrictions, whereas on the other hand patients with weak reactions might end up in there preoperative subluxation again.

Biomechanical tools are required to assess preoperative instability, the contribution of each surgical step to final biomechanics and to predict therapeutic success. Common measurement systems like Vicon were tested for their pre- and intraoperative use to quantify these parameters but revealed problems in terms of accuracy and handling.

Conclusions

New approaches might help to quantify efficacy of interventions as well as guide clinicians for their decision making in soft tissue surgery

References

[1] Armstrong AL et al. 1994. The prevalence of degenerative arthritis of the base of the thumb in postmenopausal women. J Hand Surg [Br] 19:340–341.

Tendon structure and function – an intricate balancing act

Jess G. Snedeker[1,2]

[1] Department of Orthopedics, University of Zurich, Balgrist, Switzerland
[2] Institute for Biomechanics, ETH Zurich, Switzerland, @research.balgrist.ch

A deceptively complex tissue

Tendon structure can vary widely depending on its intended function – and this is reflected at all hierarchical levels of organization. This tutorial will review our current knowledge regarding mechanically regulated tendon structure-function relationships across six orders of metric scale, from tissue to protein.

The tutorial will focus on how tendon is designed to bear load and ultimately how resident tendon cells govern tissue homeostasis, respond to repetitive and blunt trauma, and attempt to mediate tendon repair after injury. The importance of understanding how tendon tissue and its mechano-biology vary at different stages of human development will also be discussed.

Tendon at the macroscale

The largest extent of our knowledge about tendon regards the highest hierarchical level – the tendon itself. This is appropriate, since what goes on at the cellular level is secondary to the function of the tendon, and whether the tendon is able to optimally transmit muscular force to bone.

Optimal force transmission characteristics of individual tendons can be highly specialized; some tendons must be very compliant energy storing structures, while others are attached to short muscles with relatively small travel and must be very stiff to be effective. Further, many tendons are anatomically partitioned to permit fine muscle control necessary for precise joint movements.

The tutorial discusses the important macroscopic anatomical features that nature uses to modulate tendon biomechanical character. In particular, the importance of fascicle crimp (waviness) and relative motions between intratendonous structures will be elaborated.

Tendon at the ultrascale

Tendon regulates its functional properties via its molecular constituents (extracellular matrix proteins). From a molecular standpoint, tendon is composed primarily of water, collagen, and in much smaller quantities, proteoglycans, elastin and other macromolecules. How variations in biochemical composition correlate to material level characteristics will be introduced. Particular emphasis will be given to the role of proteoglycans, which are known to regulate collagen assembly and have been increasingly hypothesized to facilitate force transmission among the discontinuous collagen fibrils. The paradigm of proteoglycan mediated collagen cross-linking will be critically discussed.

Mechanical loading in tendon development, homeostasis and disease

Mechanical loading has been shown to provide important developmental cues, even in very early stages of embryonic development. This reliance of tendon structure and composition on mechanical loading continues into skeletal maturity where matrix remodeling processes are highly regulated by dynamic loading. Our current state of knowledge regarding mechano-regulation of tendon tissue modeling and remodeling will be reviewed. We will focus on how tendon cells sense and interpret mechanical forces, respond to those forces by the creation of the extra-cellular matrix, and thus adjust the mechanics of the tendon itself.

The tutorial will also describe mechanical implications of loading on disease and injury states (chronic and acute tendon disorders, respectively). We will further introduce how degenerative processes enter an aberrant feedback loop of mechanical overload, tissue inflammation, and progressive fragmentation of the normally highly-ordered collagen architecture.

The tutorial concludes by briefly describing emerging clinical strategies for restoring normal, functional histology in healing tendon and its insertions to muscle and bone.

Effects of movements and loading on the entire musculoskeletal system with a focus on muscle.
What causes health problems, what can be tolerated?

Dr. Jachen Denoth

Institute for Biomechanics, ETH Zürich, Switzerland

Striated muscle is - from an anatomical point of view - a complex biomechanical system. A single mammalian muscle fibre contains up to one hundred or more parallel myofibrils connected via an inter-myofibril filament network. Each single myofibril contains thousands of sarcomeres lined up as a series of linear motors.

Muscle force generation during voluntary contraction fluctuates in time and reflects the properties of the control of the motor units output (Enoka et al. 2003). As a result - from a mechanical point of view - the network "muscle tissue" sustains regulated active and passive load. (Huijing, 1997, Telley and Denoth, 2007); the stress distribution is generally inhomogeneous in space and time. The knowledge of the critical load of single myofibrils or single filaments is mandatory when discussing limiting factors in loading situations.

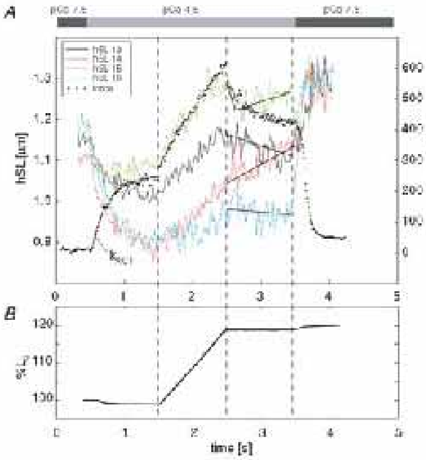

Fig. 1: Force and half-sarcomere length changes during activation, stretch and relaxation. A, the force record (dotted line, right ordinate) and the length traces from half-sarcomeres. B, the length record illustrating the ramp stretch.

It is well known that exercise involving eccentric muscle actions may induce skeletal muscle injury. Muscle force (respectively single muscle fibre or single myofibril force), muscle lengthening velocity, initial muscle length, muscle strain, and number of eccentric contractions have been found to contribute to eccentric exercise-induced muscle injury (Black et al. 2006). Force peak during moderate eccentric contraction of a myofibril exceeds isometric force by about 200% (Fig. 1, Telley et al, 2006) and accentuates the stress inhomogeneity.

Repeated eccentric muscle contractions show large over-stretched sarcomere areas and disrupted structures and contractures (Z-band tear) and loss of contractile proteins (Friden et al. 1983). Similar "inhomogeneity patches" are observed in dynamic situations in single skinned muscle fibres (own research, Fig. 2). The beginning of muscle damage lies in dynamic situations where sarcomeres are stretched into the passive scaffold. The disruption of cytoskeletal proteins within the myofibre has been proposed to result in the development of delayed onset of muscle soreness (Lieber & Friden, 2002).

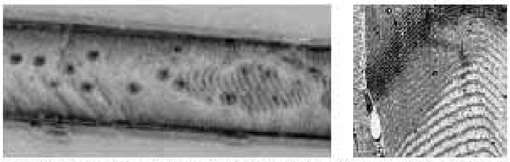

Fig. 2: Left: Phase contrast micrograph of a single fibre from the rabbit psoas muscle in a dynamic situation (J. Dennoth, unpublished data). Right: Region with highly overstretched and damaged sarcomeres (from Ogilvie, Armstrong et al. 1988 with the permission of H. Hoppeler, Uni of Bern).

Mechano-biological aspects will be discussed in this tutorial in combination with the above questions *What causes health problems, what can be tolerated?*

Acknowledgements

Supported by SNF, Nr. 315200-116611

References

Black et al (2006), J Appl Physiol 104:639-647.
Enoka et. al (2003), J Electromyogr Kinesiol 13:1–12.
Friden et al (2002), Int J Sports Med 4, 170–176.
Huijing (1997), J Biomechanics 32, 329-345
Lieber & Friden (1983) Am J Phys Med Rehabil 81 (11 Suppl.), S70–S79.
Telley & Denoth (2007), J Muscle Res Cell Motil 28 :89–104.
Telley et al (2006), J Physiol 573:173–185.

Immediate and short term response of tendon and ligament to mechanical load

Birch H. L.

Institute of Orthopaedics and Musculoskeletal Science, University College London, UK,
h.birch@ucl.ac.uk

Introduction

The response of tendon and ligament to mechanical load is governed by their complex and highly organized hierarchical structure from nano- to macroscale. At the nanoscale collagen molecules are aligned longitudinally to form fibrils which are embed in a proteoglycan rich medium to form microscale fibres. Collagen fibres in turn pack to form macroscopic fascicles and finally fascicles form the whole tendon. This composite structure results in a mechanical response which is non-linear and time dependant.

Tendons are specialized for their specific role in locomotion. Tendons involved in storage and release of elastic energy require different mechanical properties to those responsible for positioning the limb. We are interested in the relationship between the specific function of tendon and the composition and organization of the matrix. We propose that tendons are mechanically 'tuned' to their specific functional roles in locomotion.

Materials and methods

We have studied the superficial digital flexor tendon (SDFT) in the horse and the human Achilles tendon as examples of energy storing tendons. The anatomically opposing and functionally distinct common digital extensor tendon (CDET) in the horse and anterior tibialis tendon in the human were studied as examples of positioning tendons. *In vitro* mechanical testing was carried out using a servo-hydraulic materials testing machine following pre-conditioning of the tendon. Tendon structure was assessed histologically by measuring collagen crimp angle and length and collagen fibril diameters. Matrix composition was assessed using fluorometric, spectrophotometric and HPLC methods. Matrix turnover was assessed by measuring markers of tissue age, markers of synthesis and markers of degradation.

Results and discussion

The results of our work have shown differences in the response to mechanical load in the toe region, linear region and failure region of the stress/strain curve between functionally distinct tendons. The CDET (1236.3 MPa ± 209.6) had a higher elastic modulus than the SDFT (970.8 MPa ± 60.4) and failed at a lower strain (SDFT - 25.98% ± 1.44; CDET - 20.45% ± 1.60)(1). Findings were similar in human tendons where the energy storing Achilles tendon had a lower elastic modulus than the anterior tibialis tendon. The effective stiffness of the SDFT and CDET increased with increased rate of application of load demonstrating their viscoelastic nature; however at strain rates of 50%/sec and above this effect was not evident (Table 1.)

Table 1: Elastic modulus at different strain rates

Strain rate %/sec	SDFT	CDET
100	970.8 ± 60.4	1236.3 ± 209.6
50	965.7 ± 61.9	1229.5 ± 175.7
25	945.1 ± 60.5 *	1213.9 ± 180.1 *
1	888.4 ± 66.8 *	1166.5 ± 126.2 *

*Data are presented as mean ± S.D. (n=6). * denotes a significant difference relative to the test at 100%/sec loading rate.*

Collagen crimp angle was significantly smaller in the CDET and collagen fibril diameters significantly larger compared to the SDFT. Collagen crosslinks showed considerable differences between the different structures(2). Markers of matrix age and turnover suggest a higher rate of collagen renewal in the CDET than in the SDFT(3).

Conclusion

Variation in mechanical response of different tendons to the applied load is important to allow efficient functioning of these structures. This is achieved by variation in the composition and arrangement of the matrix components. Understanding these relationships is the key to understanding tendon degeneration and injury in addition to the contribution of tendon to efficient locomotion.

Acknowledgements

This work was funded by The Horse Trust, the Horserace Betting Levy Board and the Arthritis Research Campaign.

References

1. Birch H.L. (2007) *Int J Exp Pathol*, **88**, 241-248.
2. Birch H.L., Wilson A.M., Goodship A.E. (2008) *J Appl Physiol*, **105**, 1927-1933.
3. Birch H.L., Worboys S., Eissa S., Jackson B., Strassburg S., Clegg P.D. (2008) *Matrix Biol*, **27**, 182-189.

Short term mechano-regulation of muscles due to movement

Flueck M.

Institute for Biomedical Research into Human Movement and Health, Manchester Metropolitan University, United Kingdom, m.flueck@mmu.ac.uk

Introduction

Mechanical factors play a key role in the maintenance and adaptation of musculo-skeletal tissues [1]. This is most pronounced in striated muscle groups involved in posture and locomotion. These tissues undergo pronounced structural remodeling with regimens that increase or decrease their loading [1,2].

We only now begin to unravel the regulatory principles which integrate the short term alterations of mechanical stimuli into long term adjustments of tissue structure and function. Amongst those, sites of focal adhesion between the contractile cell units of muscle (i.e. muscle fibers) evolve as possible sites of conversion for mechanical stress into the cellular signaling processes which regulate the makeup of muscle cells via gene expression [3,4]. In culture this coupling of physical and chemical mechano-transduction is reflected by the activation of the phosphotransfer activity of focal adhesion kinase (FAK) through the posttranslational modification of specific tyrosine residues via phosphorylation [5].

We have tested the functional implication of focal adhesions in myocellular mechano-transduction and adaptation in rodent muscle tissue by assessing the post-translational adjustments of focal adhesion kinase (FAK) by a multi-level approach combining somatic transgenesis with physiological models of altered muscle use and loading.

Materials and methods

Animals-The experiments were performed with rodents at the University of Berne (Switzerland) and the University of Lyon (France) with the permission of the local ethical authorities. Muscles were colleted and snap-frozen for subsequent experiments.

Physiological models-Loading and activity of antagonistic hindlimb muscles, *m. soleus* and *m. tibialis anterior*, was modified with tail suspension (HU) and subsequent 1, 6 or 24 hours (R1) of reloading with voluntary activity and compared to ground controls (CTL).

Muscle transgenesis-Overexpression of FAK and co-expression of its inhibitor FRNK in *m. soleus* and *m. tibialis anterior* was achieved with injection of constitutively active expression plasmids and electropulsing.

Muscle biochemistry-Post-translational modification of FAK was monitored immunologically with antibodies against a main site of regulation of FAK, Y397, and the N-terminus of FAK in immunoblots of muscle homogenates.

Transcript profiling-Total RNA was isolated, reverse-transcribed into cDNA with specific primers and subjected to detection of transcript for major gene ontologies of muscle with microarray and polymerase chain reaction [6].

Results and discussion

FAK protein and pY397 content was reversibly altered by un- and reloading of ankle flexor muscle (Fig. 1). This response is quantitatively and qualitatively modified in plantar flexor muscle (Fig. 2).

The load-modulated pY397 content of FAK in ankle flexor corresponded to N-terminal FAK immunoreactivity in muscle fibers (data not shown).

Overexpression of FAK promoted the mechano-regulated gene expression program of slow-oxidative muscle (Fig. 2).

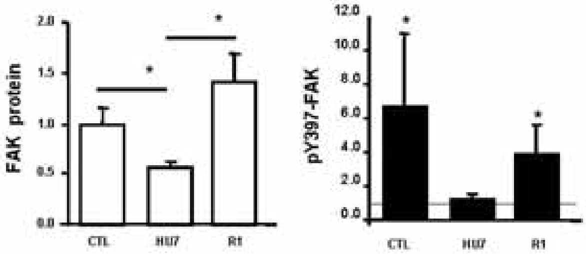

*Fig. 1: Regulation of FAK and pY397-FAK content by muscle loading in the ankle flexor m. soleus of rats. *, $p < 0.05$ vs. HU (Friedman ANOVA). n=5-6 per time point.*

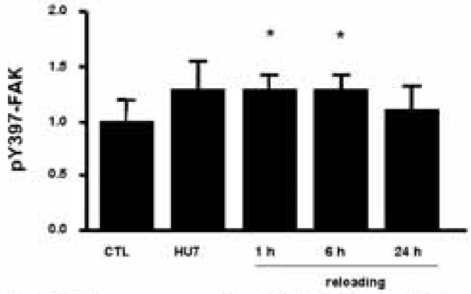

*Fig. 2: Time course of pY397-FAK regulation in plantar flexor m. tibialis anterior of mice by muscle loading. *, $p < 0.05$ vs. CTL (Friedman ANOVA). n=3-4 per time point.*

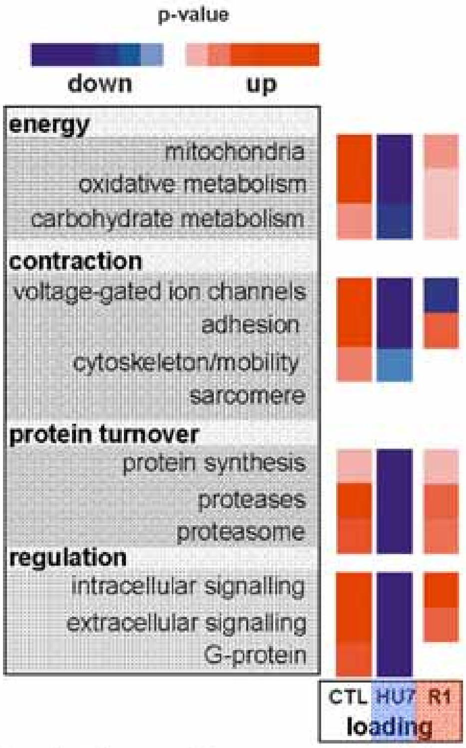

Fig. 3: Gene ontology map visualizing the load-dependent transcript regulation of major gene ontologies in soleus muscle by FAK overexpression in color coding.

Conclusion

Mechanical activation of focal adhesion kinase by muscle loading is coupled to control of the slow oxidative expression program of skeletal muscle.

A mechano-related conformational change of FAK after its phosphorylation at tyrosine 397 evolves as a molecular switch for the load-regulated FAK activation in vivo.

Differences in mechano-sensitivity of FAK pY397 content between antagonistic muscle groups imply that FAK-mediated mechano-regulation is graded by the physiological conditioning, fiber composition and anatomical origin of muscle.

These observations call for a feedback interaction of mechano-sensing via focal adhesion signaling which is involves expression of FAK.

Acknowledgements

This study was financially supported by the Région Rhône-Alpes', the Association Française contre les myopathies, and the Swiss National Science Foundation.

References

[1] Loughna PT. *et al*, Development 109: 217-223, 1990
[2] Booth FW. and Thomason DB., Physiol. Rev. 71: 541-585, 1991
[3] Fluck M. *et al.*, Biochem. Soc. Trans. 35:1312-1313, 2007
[4] Fluck M. and Hoppeler H., Rev. Physiol. Biochem. Pharmacol. 146:159-216, 2003
[5] Fluck M. *et al.*, J. Exp. Biol. 205:2337-2348, 2002
[6] Fluck M. *et al.*, Am. J. Physiol. 289:R4-14, 2005

Long-term musculoskeletal adaptations to loading and unloading in humans.

Narici M. V. [1]

[1] Institute for Biomedical Research into Human Movement and Health (IRM), Manchester Metropolitan University, Faculty of Science and Engineering, John Dalton Building, Chester Street, Manchester, M1 5GD, United Kingdom

Muscles and tendons show a remarkable plasticity in response to chronic loading and unloading. In recent unloading studies in humans, we showed that chronic unloading obtained either by bed rest (BR) or unilateral lower limb suspension (ULLS), induces a significant decrease in muscle fibre length (-8% after 23 day ULLS and 9% after 35 day BR). Concomitantly, tendon stiffness drastically decreased (30% after 23 days ULLS, De Boer et al. J Physiol 583, 2007). By contrast, in chronic loading muscle fibre fascicle length increased by 3% ($P<0.01$) after 10 days and by a further 10% ($P<0.001$) after 35 days of strength training (ST) (Seynnes et al. J Appl Physiol 102, 2007). Chronic loading also results in a significant increase in tendon stiffness (+65% after 14 weeks of ST; Reeves et al. J Physiol, 548, 2003). This rapid remodeling of muscle architecture produced by these experimental paradigms (occurring within 10 days of loading or unloading) seems regulated by changes in mechano-sensitive proteins such as focal adhesion kinase, whose content and activity increase with loading (Flück et al. Am J Physiol, 1999) and decreases with unloading (De Boer et al. J Physiol 585, 2007). Since skeletal muscle mechanical behaviour notoriously depends on tendon stiffness, muscle weakness, and its reversal by training, likely reflects a close interaction between muscular and tendinous changes.

Effects of musculoskeletal loading on the prevention and rehabilitation of muscle-tendon injury: biomechanical and neural aspects

Per Aagaard

Institute of Sports Science and Clinical Biomechanics, University of Southern Denmark,
Denmark, paagaard@health.sdu.dk

Overuse injury in tendon and muscle is frequently observed both in sports and exercise, as well as in various types of work place environment. Despite a high injury incidence the optimal treatment modalities for tendinopathies are not fully identified[12]. Within the recent years, however, the use of eccentric (ECC) exercise for the muscle-tendon complex have been found to produce moderate-to-good clinical results for the rehabilitation of Achilles tendinopathy while clinically significant treatment results also have been reported for patellar and supraspinatus tendopathy, and lateral epicondylite. Likewise, as discussed below ECC training seems to be useful for the rehabilitation and prevention of recurrent muscle strain injuries. However, the detailed physiological mechanisms responsible for the above adaptations remain to be fully understood.

Overuse tendon injury

ECC muscle-tendon loading regimes have demonstrated promising results in terms of injury rehabilitation. Thus, conditions such as Achilles tendinosis[1,9,20], anterior patella-femoral pain[21], patella tendon pain and jumpers knee[8] may show improvements in response to ECC training regimes. ECC strength training in rats resulted in increased collagen turnover and neoformation of vinculin and talin[7] that are cytoskeletal proteins involved in the force transduction between the interior of the muscle fiber and the ECM. Using microdialysis techniques we recently found indications that ECC training led to elevated type II collagen synthesis in the Achilles tendon of elite soccer players with overload tendinopathy[13]. Further, based on ultrasonography evaluation ECC training appears to result in reduced tendon swelling, loss of focal hypoechoic areas, and more regular tendon fibre structure in Achilles tendinosis patients[16]. High-frequency tendon oscillations during ECC training may be involved in the adaptive response[18]. Reduced or removed symptoms of anterior Patella pain and jumpers knee also were observed after ECC decline squat training[8,17]. Recent data from our Lab suggest that the superior rehabilitation achieved with ECC decline vs horizontal squats likely occurs as a result of greater tendon strain with this type of training[10]. Patella tendon stiffness increased in response to heavy-resistance strength training (HRST) in both young[11] and old[19] individuals, resulting in a reduced tendon strain for a given level of force production[11]. The reduction in tendon strain may contribute to a reduced risk of tendon overuse injury. Notably, we recently observed that conventional HRST (3 times/wk) using slow contraction cycles (6-s) and involving both concentric and eccentric contractions was more effective than ECC training in the rehabilitation of patellar tendinopathy[data in publication].

Muscle strain disorders

Hamstring muscle strain disorders appear to be effectively rehabilitated[6] or prevented[2,3] by use of ECC training. Notably, even athletes with a history of multiple recurrent hamstring muscle strains may show a full rehabilitation[6]. The involved mechanisms remain largely unknown but may include increased remodelling of the muscle fiber-ECM structures due to increased local IGF-1 production[4], elevated synthesis of force-transmitting cytoskeletal proteins at the myotendinous junction[7] and/or longitudinal sarcomere addition causing shifts in the passive force-length properties of the muscle-tendon complex[5,15].

References

[1] Alfredson H *et al.*, Am. J. Sports Med. 26:360-6, 1998
[2] Arnason A *et al.*, Scand. J. Med. Sci. Sports 18:40-48, 2008
[3] Askling C *et al.*, Scand. J. Med. Sci. Sports 13:244–50, 2003
[4] Bamman M *et al.*, Am. J. Physiol. 280:383-90, 2001
[5] Butterfield TA *et al.*, Pflügers Arch 451:688–90, 2006
[6] Croisier JL *et al.*, Am. J. Sports Med. 30:199-203, 2002
[7] Frenette J *et al.*, Int. J. Sports Med. 21:313-20, 1999
[8] Jonsson P *et al.*, Br. J. Sports Med. 39:847-50, 2005
[9] Jonsson P *et al.*, Br. J. Sports Med. 42:746-9, 2008
[10] Kongsgaard M *et al.*, Clin. Biomech. 21:748-54, 2006
[11] Kongsgaard M *et al.*, Acta Physiol. Scand. 191:111-121, 2007
[12] Langberg H *et al.*, Scand. J. Med. Sci. Sports 18: 541–2, 2008
[13] Langberg H *et al.*, Scand. J. Med. Sci. Sports 17:61-66, 2007
[14] Lian OB *et al.*, Am. J. Sports Med. 33:561–7, 2005
[15] Lynn & Morgan, J. Appl. Physiol. 77:1439-44, 1994
[16] Öhberg L *et al.*, Br. J. Sports Med. 38:8–11, 2004
[17] Purdam CR *et al.*, Br. J. Sports Med. 38:395-7, 2004
[18] Rees JD *et al.*, Rheumatol. 47:1493-7, 2008
[19] Reeves ND *et al.*, J. Physiol. 548:971–81, 2003
[20] Roos E *et al.*, Scand. J. Med. Sci. Sports 14:286-95, 2004
[21] Werner S *et al.*, Knee Surg. Sports Traumatol. Arthrosc. 1:162-168, 1993

Molecular basis of muscle contraction

Marco Linari

Laboratory of Physiology, Department of Evolutionary Biology, Florence (Italy) marco.linari@unifi.it

Introduction

During muscle contraction, arrays of the motor protein myosin II, organized in filaments, pull the actin filament toward the centre of sarcomere, the structural unit of striated muscle, in cyclical ATP driven interactions. Skeletal muscle is able to bear a high load at constant length or shorten rapidly when the load is reduced (force-velocity relationship) but it can also act as a brake generating a high resistive force with reduced metabolic cost, when the load is increased above the isometric force. The highly ordered organization of the contractile proteins allows the motor mechanism to be characterized with high structural and temporal resolution in an intact muscle cell by combining mechanical and X-ray diffraction techniques (Huxley and Simmons, 1971; Irving et al. 1992; Piazzesi et al. 2002; Reconditi et al. 2004). The main feature of the diffraction pattern is represented by a series of regularly spaced reflections on the meridional axis (Fig. 1), originating from the helical arrangement of the myosin motors along the thick filament. The M3 reflection, that arises from the 14.5 nm axial repeat of the myosin heads, is one of the strongest reflection during the isometric contraction. The intensity of the M3 reflection (IM3) is sensitive to the changes in the axial mass density projection of the myosin motors onto the filament axis, associated to axial movement of the motors. Because X-ray diffraction signals lack the phase information, IM3 changes can be interpreted only by using structural models. With the high collimation and flux of the beam of the third generation synchrotrons it is possible to collect the fine structure of the M3 reflection, due to the interference between the two bipolar arrays of motors in the myosin filament (Huxley and Brown, 1967; Linari et al. 2000). During isometric contraction the M3 fine structure shows two closely spaced peaks with the relative intensity of the higher and lower angle peak (RM3) about 0.8. Changes in RM3 record the extent and direction of the axial movements of the motors with subnanometer resolution (Piazzesi et al. 2002; Reconditi et al. 2004). We use sarcomere-level mechanics and X-ray interferometry to investigate *in situ* the molecular basis of the work production and the braking action of muscle.

Materials and methods

Experiments were made on intact single fibres from frog skeletal muscle (4 °C, ~2.1 µm sarcomere length) vertically mounted at the beamline BioCAT (APS, Argonne, IL, USA) between a capacitance force transducer with resonant frequency 50 kHz and a loudspeaker motor (Lombardi and Piazzesi, 1990). Length changes in the population of sarcomeres interrogated by X-rays were recorded with a striation follower (Huxley et al., 1981) adapted to the vertical mounting of the fibres. X-ray data were collected on a cooled CCD detector (active area, 4cmx7cm, point spread function, FWHM, 65 µm) placed at 2.5 m from the preparation (Fig. 1). Load/length steps of different sizes, complete in 110µs, were imposed on the plateau of an isometric contraction and X-ray data were collected during the different phases of the length/force transient elicited by the load/length step.

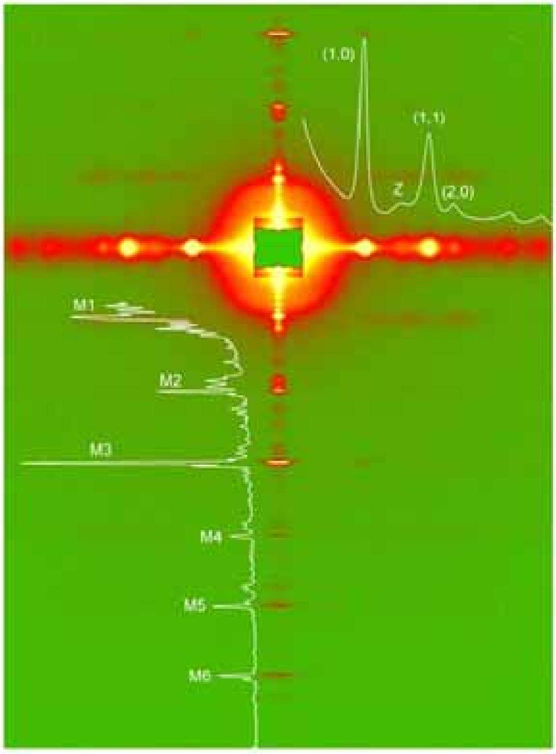

Fig. 1. *2D diagram of a single muscle fibre (4 °C, sl 2.15 µm) at rest, collected at BioCAT (APS) on the CCD detector (Phillips et al., 2002). Exposure time, 700 ms.*

Results and Discussion

During isometric contraction about 30% of the myosin motors are attached to actin and each motor bears a force of about 6 pN.

During steady shortening at high and moderate loads, the number of myosin motors attached to actin reduces in proportion to the load while the force per attached motor is similar to the isometric value. In these conditions the myosin motor remains attached for 6 nm filament sliding, then quickly detaches (Piazzesi et al. 2007). The constant force (6 pN) and stroke size (6 nm) over a wide range of physiological shortening velocities are consistent with the macroscopic efficiency of contracting muscle, providing that one ATP molecule is hydrolysed for each unitary stroke.

Step stretches of 1-5 nm per half-sarcomere cause the number of myosin motors attached to actin to increase up to twice the isometric value within 2 ms (Brunello et al. 2007). Of the two motor domains of each myosin molecule, only one is attached to actin during isometric contraction or shortening; a stretch strains the attached motor domain promoting attachment of the second motor domain, allowing muscle to resist stretch without increasing the force per motor.

Conclusions

X-ray diffraction interference between the two bipolar arrays of myosin motors in each sarcomere and sarcomere-level mechanics provide a powerful tool for investigating the molecular basis of muscle response to external load. The force-velocity relation is the result of a reduction in the number of motors attached to actin. The high resistance of muscle to sudden increase in load is due to the rapid attachment to actin of the second motor domain, promoted by the distortion of the motor already attached in the isometric contraction.

Acknowledgements

This research was supported by the Ministero dell'Università e della Ricerca (Italy), National Institutes of Health (USA), Medical Research Council (UK) and Department of Energy, Basic Energy Sciences, Office of Science (USA).

References

- Brunello, E., Reconditi, M., Elangovan, R., Linari, M., Sun, Y.-B., Narayanan, T., Panine, P., Piazzesi, G., Irving, M. and Lombardi, V. (2007). *PNAS* 104:20114-20119.
-Huxley, H.E. and Brown, W. (1967). J. Mol. Biol. 30, 383-434.
-Huxley, A.F. and Simmons, R.M. (1971). Nature 233:533-538.
- Huxley, A.F., Lombardi, V. and Peachey, D. (1981). J. Physiol. 317:12-13.
- Irving, M., Lombardi, V., Piazzesi, G. and Ferenczi, M.A. (1992). Nature 357:156-158.
- Linari, M., Piazzesi, G., Dobbie, I., Koubassova, N., Reconditi, M., Narayanan, T., Diat, O., Irving, M. and Lombardi, V. (2000). PNAS 97, 7226-7231.
-Lombardi, V. and Piazzesi, G. (1990). J Physiol 431, 141-171.
-Phillips, W.C., Stewart, A., Stanton, M., Naday, I. and Ingersoll, C. (2002). J. Synchrotron Radiat. 9, 36-43.
- Piazzesi, G., Reconditi, M., Linari, M. Lucii, L., Sun, Y.-B., Narayanan, T., Boesecke, P., Lombardi, V. and Irving, M. (2002). Nature 415, 659-662.
- Piazzesi, G., Reconditi, M., Linari, M. Lucii, L., Bianco, P., Brunello, E., Decostre, V., Stewart, A., Gore, D.B., Irving, T.C., Irving, M. and Lombardi, V. (2007). Cell 131:784-795.
- Reconditi, M., Linari, M., Lucii, L., Stewart, A., Sun, Y.-B., Boesecke, P., Narayanan, T., Fischetti, R.F., Irving, T., Piazzesi, G., Irving, M. and Lombardi, V. (2004). Nature 428, 578-581.

Additional references

- Reconditi, M. (2006). Rep. Prog. Phys. 69:2709-2759.

QTECH1005 v1.0
2009-02-09

Qualisys low latency real-time system

Author: Magnus Berlander

Introduction

This document describes the functionality and performance of the Qualisys low latency real-time system. It gives an overview of the system, specifies the total latency and lists currently supported software along with information for customer specific integration.

System overview

The image below illustrates a typical setup of an Oqus based motion capture system. Such a system generally includes:

1. 2D marker positions streamed from the Oqus cameras
2. Data fetching from any analog sources, such as force plates, EMG, EEG etc
3. Data processing in QTM, including 3D reconstruction, tracking and AIM (Automatic Identification of Markers)
4. Real-time output stream to any third party software such as Visual 3D, MotionBuilder, MatLab or any customer specific application.
5. 6DOF information can also be outputted through a D/A board in real-time.

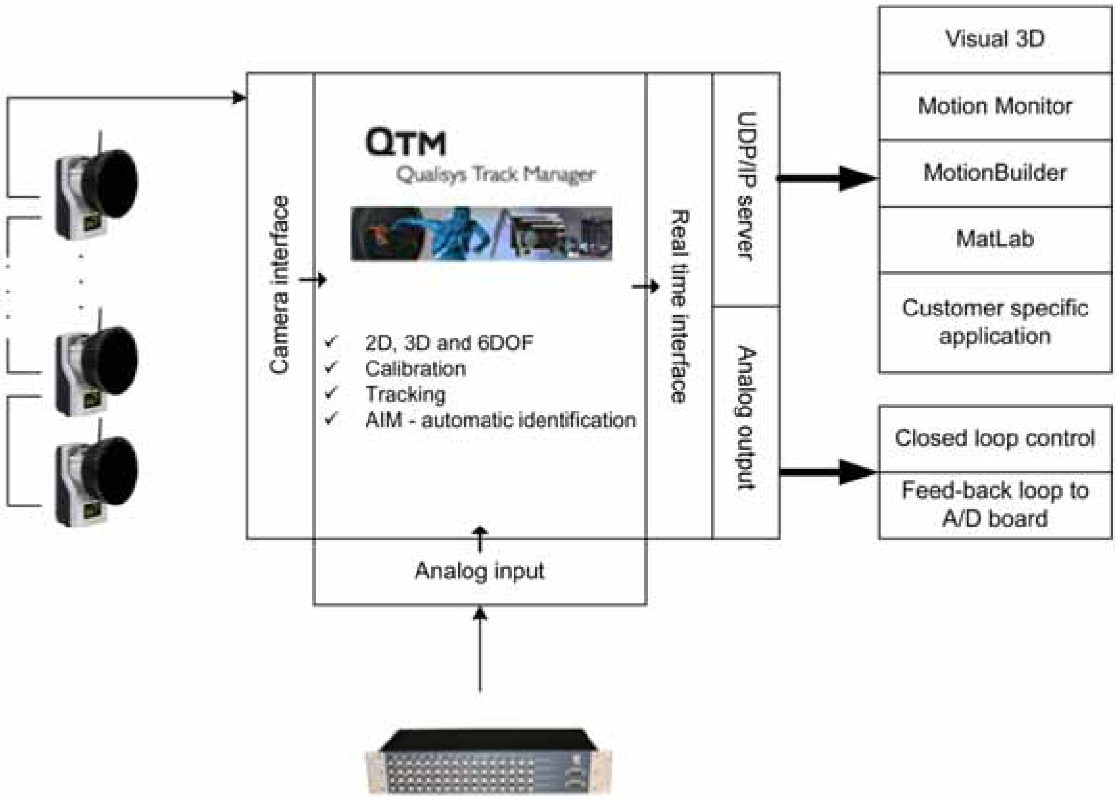

Figure 1 - Overview of the Qualisys real-time motion capture system

A Novel Method to Compute Muscle Moment Arms

Philippe Favre[1,2*], **Jess G Snedeker**[1,2]

[1] Orthopaedic Research Laboratory, University of Zürich, Balgrist, Switzerland
[2] Institute for Biomechanics, ETH, Zürich, Switzerland, pfavre@research.balgrist.ch

Introduction

Representation of a realistic muscle path is central in musculoskeletal modelling, as this directly influences the respective muscle moment arm and line of action, which are the geometric input in muscle force simulations.

Two numerical methods have typically been described to solve the essential issue of muscle wrapping on the bony surfaces. The centroid method represents the muscles by deformable line segments wrapping on bone modeled as simplified geometries, such as ellipsoids, spheres or cylinders. This method solves quickly and has been shown to deliver realistic moment arms. However, the approximate underlying geometry and fixed "via points" must be set in advance for each joint configuration, requiring a tremendous amount of preparative work1. Second, wrapping on anatomically precise bone geometries has been achieved with sophisticated 3D volumetric finite element (FE) models of the muscle2. While this approach could eliminate many artificial boundary conditions, its complexity may be excessive for muscle force estimation simulations. In fact, many models require a rapid generation of muscle moment arms, for instance when one wants to predict motions in real-time, or assess large motions such as throwing.

With the intention to combine the advantages of both methods, we have developed an intermediate technique relying on the contact detection capabilities of commercially available FE packages.

Materials and methods

The 3D surface geometry of the humerus and scapula were imported to Marc Mentat (MSC Software, Santa Ana, CA) from the Bel repository and set as rigid bodies. The bones were held fixed in the joint configuration of interest.

Ten line segments represented the rotator cuff muscles, each as a series of beam elements (Fig.1). One end of each segment was attached to the insertion site on the humerus, and the segment was oriented perpendicular to the humerus surface at the attachment site. Boundary conditions were defined to move the other segment end to the respective origin point on the scapula, deforming and wrapping the muscle strings on the bony surface. Software driven contact detection and handling of muscle and bone nodes prevented penetration. The acromion and coracoid were removed from the contact bodies to avoid wrapping on these structures. To avoid slipping, friction was introduced between the bone and the muscles. The direction of the muscle at the last point of contact with the humerus defined the line of action vector, and the moment arm was directly computed as the tangential distance to the humerus center.

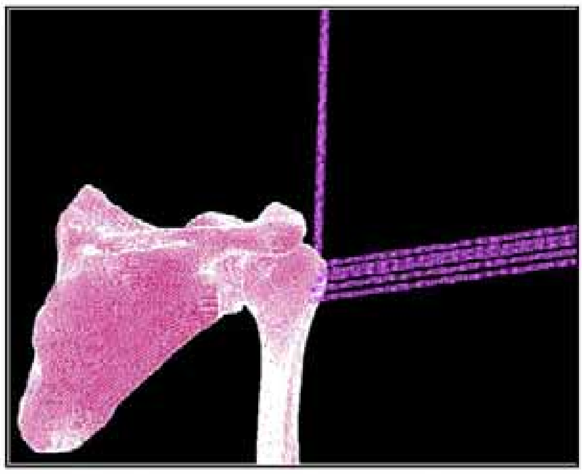

Fig. 1: Model configuration before muscle wrapping.

Results and discussion

Wrapping could be simulated in a variety of joint positions without user intervention or prior tuning of the model. An example of the muscle wrapping obtained for the arm in the rest position is shown in Fig.2.

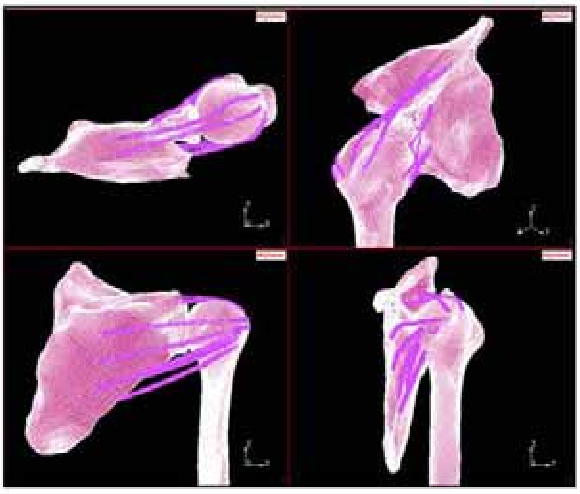

Fig. 2: Model configuration after muscle wrapping

The resulting abduction moment arms during humerus elevation in the scapular plane were comparable to published in vitro or modelling data (Fig. 3).

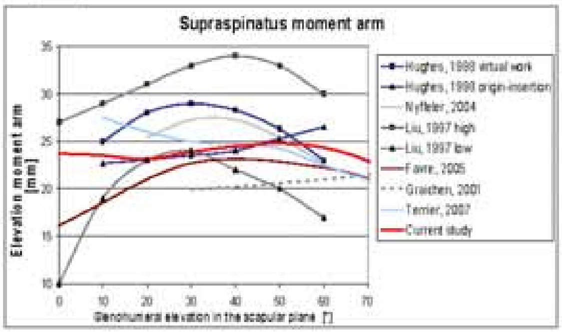

Fig. 3: Supraspinatus elevation moment arms compared to published data.

Conclusion

This method yields realistic muscle moment arms for the tested positions, solves in few minutes for 10 muscle segments on a standard desktop PC and does not require artificial underlying geometries. Most important certainly, is that the moment arms can be generated without prior measurements; the bones must simply be oriented in the position of interest, and the wrapping procedure launched. The main limitation is an arbitrarily assigned muscle-bone friction to achieve a realistic outcome. Some muscle-bone friction does exist in the physiological case as well, and this may be preferable to the use of more artificial constraints like via points or stub obstacles.

The described technique is now being extended to all glenohumeral muscles and combined with a muscle force estimation algorithm[3] to build an integrated, actively stabilized, FE model of the glenohumeral joint.

References

[1] Garner *et al*, Comput Methods Biomech Biomed Engin. 3:1-30, 2000.
[2] Blemker et al, Ann Biomed Eng. 33: 661-73, 2005.
[3] Favre et al, Clin Biomech. 20: 822-33, 2005.

A novel cable fixation technique reduces fragment dislocation in case of proximal humeral four part fractures

Baumgartner D. [1], Schlüssel, M. [1], Gerber, H. [1], Stüssi E.[1]

[1]Institute for Biomechanics, ETH Zurich, Switzerland
dbaumgartner@ethz.ch

Introduction

Proximal humeral fracture refixation in case of hemiarthroplasty is often accompanied by fragment displacement and subsequent bone resorption. It has been shown that Greater Tuberosity (GT) union to the humeral shaft reveals a better clinical outcome than non-union. The aim of the investigation was therefore an optimisation of the refixation technique with respect to a reduced fragment migration.

Materials and methods

Three different refixation techniques using titanium cables were compared: A) circumferential wire placement by two parallel slings connecting GT and Lesser Tuberosity (LT); B) cable placement similar to technique A) with additional cable supporting pins and C) cables oriented collinear to the longitudinal axis of the humerus; connecting GT and LT to the shaft (Fig 1).

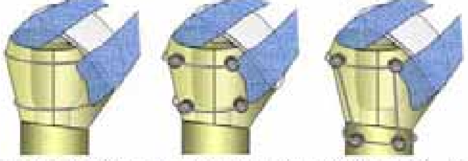

Figure 1: Different refixation techniques A, B, C.

An experimental shoulder machine simulated active rotator cuff muscle forces of m. supraspinatus, m. infraspinatus, m. subscapularis and middle part of the m. deltoideus similar to the literature[1] (Fig 2). Glenohumeral joint movement up to an abduction angle of 75° was performed. This refers to loading of 100N for SSP and DELT each. 20 loading cycles were applied.

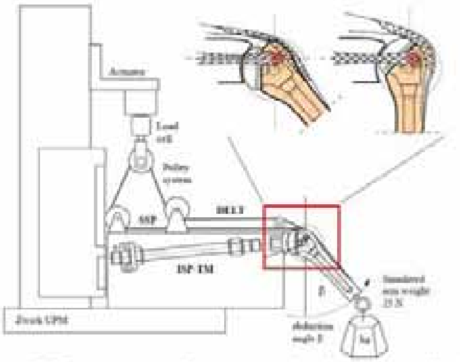

Figure 2: Test setup for muscular load application.

A standardised four-part fracture model according to the literature[2] was implemented in artificial humeral bone models (last-a-foam®, FR 6715); Affinis Fracture® prosthesis was implanted[3]. Migration between GT-shaft, LT-shaft and LT-GT was detected by an optic 3-D camera system (OptoTop, Breuckmann GmbH).

Results and discussion

GT-to-shaft migration was significantly reduced for case C) in comparison to cases A) and B). No significance was observed between A) and B) for any other measured parameters.

Migration @20cycl.	A) two slings	B) two slings+pin	C) collinear to shaft
GT-to-shaft[mm]	0.8+/-0.1	0.7+/- 0.3	0.16+/-0.1
LT-to-shaft[mm]	0.5+/- 0.4	1.1+/- 0.6	0.3+/-0.2

Table 1: Interfragmentary migration.

Cable supporting pins do not show any negative effect on the primary stability compared to the direct cable-to-bone contact.

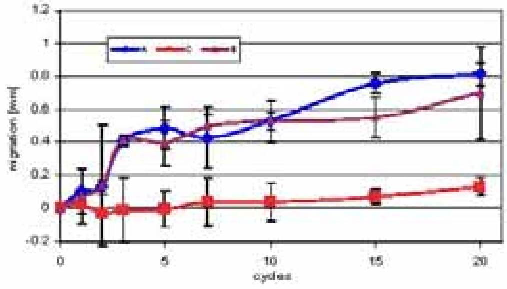

Figure 3: Relative migration during cyclic loading.

Conclusion

A stiff cable system which is placed collinear to the muscular loading direction for abduction reduces the fragment migration. A reduction of the line-pressure may reveal a positive effect on the biological healing process of the bone and thus prevent avascular necrosis.

Acknowledgements

RMS Foundation, Bettlach, Switzerland
Mathys AG Bettlach, Bettlach, Switzerland

References

[1] Wuelker N., JSES, 4: 462-467, 1995
[2] Frankle M.A., JSES, 11: 413-420, 2002
[3] Reuther F., Acta Orthop Belg, 73:179-87, 2007

Protocol for the shoulder valuation with an opto-electronic system and clinical application to the follow-up of traumatic patients

Anasetti F. [1]**, Accetta R.** [1]**, Galbusera F.** [1]**, Meersseman A.** [1]**, Monti L.** [1]**, Aziz H.N.** [1]**, Mineo G.V.**[1]

[1] IRCCS Istituto Ortopedico Galeazzi, Milan, Italy

Introduction

In this study a quantitative and three-dimensional method of evaluation for functional assessment of the shoulder during daily activity is presented, compared to a classical clinical analysis for the evaluation of the gleno-humeral functional limitation. The assessment was applied to two macro-groups of patients with displaced comminuted fractures of the humeral proximal third: both of the groups were surgically treated through a direct lateral approach to the proximal humerus [1] and with the application of a plates for the first group (Plate-Group) and of an endoprosthesis to replace the humeral head for the second group (Prosthesis-Group).

The aims of this study are: the definition of a simple and quantitative protocol for the clinical evaluation of the shoulder mobility through the use of an opto-electronic system; the assessment that a quantitative valuation referred to a motion analysis is more accurate than the subjective traditional clinical evaluation.

Materials and methods

48 patients with displaced comminuted fractures were surgically treated though a direct lateral approach: for 41 of these patients, with a mean age of 63.8 ± 18.2 years, the inter-fragmentary stabilization was achieved by locking plate system with angular stability; for 8 patients, with an average age of 69.2 ± 7.5 years, the comminuted displaced fractures of the proximal humerus required the replacement of the humeral head with an endoprosthesis without the glenoid cavity replacement due to the high risk of destabilization of this part after the implantation. Both of these macro-groups were divided into 3 groups according to post-operative period: the assessments were performed at 6, 12 and over 18 months.

The functional evaluation included the determination of the clinical index Constant Score (CS) providing an overall functional assessment of the shoulder through a 100-point scoring system [2], and a quantitative evaluation of the injured shoulder function for each group considered through the use of an opto-electronic three-dimensional motion analyzer: BTS SMART-D system (BTS Bioengineering, Milan, Italy).

Results were compared with a Control-Group of 31 healthy subjects with no history of diseases of upper limbs, with a mean age of 67.4 ± 11.5 years.

In order to assess the quantitative evaluation, a simple protocol with 16 markers was developed: 4 of these were used to define the trunk position and a trunk reference system, the others for the upper limbs (Fig. 1).

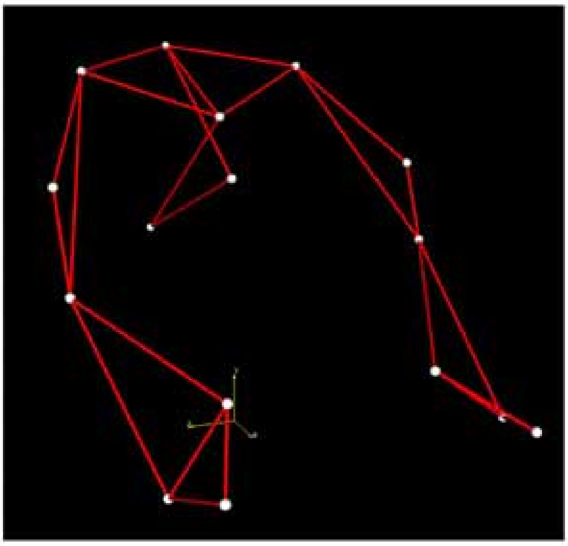

Fig. 1: Model

For the definition of the motion angles for each shoulder, anatomical planes were built with respect to the trunk reference system.

The patient was requested to perform a series of movements from which the following parameters were extracted:

A. Maximal flexion in sagittal plane
B. Maximal abduction in frontal plane with forearm turned down
C. Maximal abduction in frontal plane with forearm turned up
D. Maximal extra-rotation with elbow at 90°

For each acquisition the movement was repeated 3 times to verify the repeatability of the motion; the valuation was made on the best performance, intended as the highest width reached.

For each patient every parameter for the injured limb was compared both to the healthy one of the same patient and to the Control-Group.

Results and discussion

Table 1 shows the average values of the CS calculated for each of the two groups of patients depending on the follow-up length.

Table 1: Constant Score values for the patients' groups

Group	Months follow-up	CS
Plate-Group	6	68.3
	12	76.6
	18	78.5
Prosthesis-Group	6	46.7
	12	66
	18	41.5

Tables 2 and 3 shows the average motion analysis results for the movements for each of the two groups of patients depending on the follow-up length compared with the normality range values calculated.

	PLATE-GROUP			CONTROL GROUP
	POST 6	POST 12	POST 18	
A (°)	109.6	129.4	144.6	131.3
B (°)	98.9	106.2	112.2	115.8
C (°)	103.7	128.3	118.5	118.9
D (°)	33.7	42.0	62.3	41.9

Table 2: Motion analysis results for Plate-Group

	PROSTHESIS-GROUP			CONTROL GROUP
	POST 6	POST 12	POST 18	
A (°)	60.6	46.5	44.0	131.3
B (°)	49.4	46.3	41.5	115.8
C (°)	47.0	40.3	40.9	118.9
D (°)	26.4	23.1	22.2	41.9

Table 3: Motion analysis results for Prosthesis-Group

Conclusion

The protocol realized for the motion analysis is easy and fast to be executed; the movements are the same requested to the patient during the physiotherapic rehabilitation, thus patients could execute each movement safely in the correct way. Some patients implanted with the endoprosthesis were not able to make all the movements due to a strong physical limitation after the injury, despite of the surgical treatment.

The comparison between CS results and motion analysis ones for each single patient showed that the assessment data were not coherent: with respect to the normality, a good performance with the motion analysis in every movements did not always correspond to a high CS value. From these considerations it is possible to conclude that the CS can describe the pain condition of the patient, but for a kinematics evaluation a quantitative analysis should be preferred.

Comparing the Plate and the Prosthesis groups, both with displaced comminuted fractures of the humeral head and surgically treated through the same approach, it was possible to observe a better recovery for the first group, while a severe functional limitation was observed for the patients treated with the prosthesis. The latter group was composed by patients with a more severe fracture of the humeral head in which a plate was not implantable.

References

[1] Gardner *et al.* Bull Hosp JT Dis. 62(1-2):18-23, 2004

[2] Constant CR, Murley MB. Clin Orthop. 214:160–164, 1987

Evidence of mechanical load redistribution at the knee joint in the elderly while performing ramp and stairway locomotion

Karamanidis Kiros[1], Arampatzis Adamantios[2]

[1] Institute of Biomechanics and Orthopaedics, German Sport University Cologne, Germany

[2] Department of Training and Movement Sciences, Humboldt-University of Berlin, Germany

a.arampatzis@hu-berlin.de

Introduction

It is well established that older individuals have a high risk of osteoarthritis (OA) in particular at the knee joint [1]. Although the causes of degenerative knee joint changes are complex there is evidence that the magnitude of adduction moment at the knee is a relevant risk factor for cartilage breakdown [2]. It is also reported that older adults due to their muscle weakness reorganize their locomotion strategy (i.e. shifting the demand from the distal to the more proximal hip musculature) when performing different locomotion activities [3, 4]. However, altering the mechanics of a joint at one plane can affect the kinetics at the other planes[5]. Assuming a new redistribution of the mechanical load at the knee may cause joint loading profiles similar to those shown to be risk factors for knee osteoarthritis among the elderly. Therefore, in this study we examined the joint mechanics at the lower extremity in all three directions in a group of older and younger adults when performing incline walking as well as stair climbing.

Materials and methods

Twenty-eight older and sixteen younger adults ascended a purpose-built staircase and ramp. A motion capture system and a force plate were used to determine the subjects' 3D kinematics and ground reaction forces while locomotion. Calculation of the leg kinematics and kinetics was done by means of a rigid, three-segment, 3D leg model. To analyze the capacities of the leg-extensor muscle-tendon units, all subjects performed isometric maximal voluntary ankle plantarflexion and knee extension contractions on a dynamometer.

Results and discussion

The main findings were that the older adults reorganized their muscular output at the lower extremity in the sagittal plane, with the older adults showing lower joint moments at the ankle and knee but higher moments at the hip joint ($P<0.05$). Concerning the other two planes, older adults showed higher adduction moments at the knee and hip joint, and higher knee internal rotation moments ($P<0.05$). Furthermore, the elderly showed a more external position of the shank in relation to the thigh at the initiation of the stance phase for the two conditions examined. The reason for the higher knee adduction moment for the elderly was the higher lever arm of the ground reaction force acting about the knee joint in the frontal plane. We found a significant relationship between the lever arm at the knee joint in the frontal plane and the external hip adduction moment during ground contact phase ($0.28 < R^2 < 0.54$, $P < 0.001$) with a strong relationship between 10 and 30% of the stance phase ($R^2 \geq 0.52$, Fig. 1).

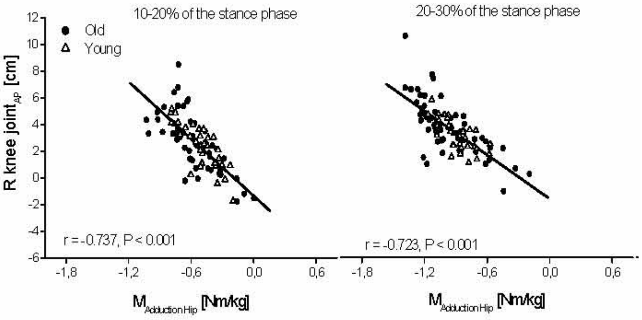

Fig. 1: Relationship between lever arm of the ground reaction force acting about the knee joint in the frontal plane (R knee joint$_{AP}$) and external hip adduction moment ($M_{Adduction\ Hip}$) during stance phase.

Conclusion

We concluded that the age-related readjustment of the muscular output in the lower extremity while stair climbing and during locomotion up an incline, initiated by the reduced muscle-tendon unit capacities (biological changes), was the reason for the higher knee adduction and internal rotation joint moments (mechanical changes) in the older compared to the younger participants. The higher knee adduction and internal rotation moments when combined with the kinematic changes in the transverse plane among the elderly give evidence that older adults redistribute the mechanical load within the load-bearing regions of the knee, increasing the risk factors for knee osteoarthritis.

References

[1] Felson et al. (2000) Ann Intern Med 17;133(8):635-46.
[2] Amin et al. (2004) Arthritis Rheum 15;51(3):371-6.
[3] Karamanidis & Arampatzis (2005) J Exp Biol 208(20):3907-23.
[4] P. DeVita, T. Hortobagyi (2000) *J Appl Physiol.*, 88(5):1804-11.
[5] Jenkyn et al. (2008) J Biomech 41(2):276-283.

Title: An investigation into the effects of a simulated effusion in health subjects on knee kinematics and muscle activity during jogging and running.

Coughlan G. F. [1]*, **Mc Loughlin R.** [2], **Mc Carthy Persson U.** [1], **Caulfield B.** [1]

[1] School of Physiotherapy and Performance Science, University College Dublin, Ireland.
[2] O'Neill's Sports Injury Clinic, University College Dublin, Ireland. garrett.coughlan@ucd.ie

Introduction

Knee joint injuries are commonly associated with activities that demand high levels of stability during dynamic movement. Depending on the mechanism and type of injury, a resultant effusion distends the knee joint capsule resulting in arthrogenic muscle inhibition, which may lead to weakness and atrophy in the surrounding musculature[1]. A lack of sufficient control and strength at the knee as a result of arthrogenic muscle inhibition can lead to the development of chronic degenerative conditions[2,3], as well as predisposing patients to reinjure[4]. The majority of the research to date on the effects of knee effusion has used a simulated effusion model to evaluate knee function of healthy subjects in static, non-functional positions. This investigation aimed to assess the effects of a simulated knee effusion on knee kinematics and muscle activation patterns during treadmill jogging and running.

Materials and methods

12 physically active subjects were recruited from the local university population for the purpose of this study. All procedures, including gait analysis, EMG and knee effusion protocol, were carried out in the university motion capture laboratory. Data was recorded in three measurement intervals throughout the testing session, twice prior to the effusion, Control 1 (C1) and Control 2 (C2), and once following the effusion, Post Effusion (PE). Ten minutes rest was allowed between the two control tests and following the injection of fluid into the knee and the PE test.

We used an active marker based motion capture system (CODA, Charnwood Dynamics Ltd, Leicestershire, UK) to acquire kinematic data during gait. Kinematic data was collected at a sampling rate of 200Hz for 20 seconds at treadmill velocities of $8kmh^{-1}$ and $12kmh^{-1}$. Surface EMG activity from the vastus medialis (VM), vastus lateralis (VL), biceps femoris (BF) and soleus (SOL) muscles were simultaneously recorded on all subjects during gait tasks. The activity was gathered using pre-amplified electrodes (model MA-317, Motion Lab Systems Inc., Baton Rouge LA, USA), which were placed, on specific sites in accordance with the SENIAM research groups' recommendations[5]. This information was recorded on a Biopac MP100A (Biopac Systems Inc. Santa Barbara, CA, USA) and analysed using its associated Acq Knowledge software (Version 3.5.7).

Following the completion of the two initial control trials, C1 and C2, the subjects underwent a simulated knee effusion procedure. The same physician undertook injections. 2ml of 2% Lidocaine was injected subcutaneously lateral to the knee joint line for anaesthetic purposes. Care was taken not to penetrate the joint capsule during the anaesthetic injection. Thereafter 60ml of saline solution (0.9% w/v Sodium Chloride Intravenous Infusion) was injected into the knee joint capsule.

Statistical analysis was carried out using SPSS for Windows (Version 12.0.1; SPSS Inc, Chicago, IL, USA). We used a general linear model three factor repeated measures analysis of variance to analyse differences in kinematic and EMG variables at each of the test intervals. In each case the dependent variable was the kinematic/EMG variable in question and the independent variables were test interval (C1, C2 and PE). Post hoc paired t-tests were then carried out to test for differences kinematic variables between individual pairs of test intervals (C1vC2, C2vPE, C1vPE). The alpha level was set at 0.05. Due to the potential for multiple comparison errors, we used a modified Bonferroni adjustment as described by Hochberg[6], to re-calculate the P value for the repeated measures and post hoc t-tests.

Results and Discussion

Repeated measures ANOVA revealed a statistically significant difference ($P < 0.004$) with a decrease in peak knee flexion in the period 250 milliseconds post HS at $8kmh^{-1}$. Pairwise post hoc comparisons revealed that the only comparison to reach the level of significance was that of a decrease in peak knee flexion 250 milliseconds post HS at $8kmh^{-1}$ during C1 versus that post effusion ($P<0.001$). No other significant differences were found in a range of variables at velocities of $8kmh^{-1}$ and $12kmh^{-1}$. This period is referred to as the initial load bearing response during the stance phase and serves to reduce the impact on the lower limb and smooth the centre of mass displacement during weight transfer, thereby reducing energy expenditure and forces on the knee joint[7].

The principal finding in this study was that minimal changes occurred in knee joint angular displacement and velocity during treadmill jogging and running following a simulated knee effusion of 60ml. However, no significant inhibition of the

Variable	Measurement Interval			
VM	C1	C2	PE	ANOVA
250ms to HS	17.42 (6.35)	17.28 (6.31)	17.27 (6.35)	0.70
HS to 250ms	58.47 (6.36)	56.10 (6.21)	62.45 (5.17)	0.05
VL				
250ms to HS	20.39 (14.42)	18.58 (10.52)	14.97 (5.85)	0.90
HS to 250ms	54.17 (9.85)	58.28 (6.85)	60.62 (6.34)	0.09
BF				
250ms to HS	44.52 (10.25)	47.26 (10.16)	46.00 (11.95)	0.42
HS to 250ms	38.89 (15.82)	41.86 (17.24)	41.42 (17.74)	0.43
SOL				
250ms to HS	14.05 (12.03)	21.29 (17.26)	23.17 (22.68)	0.34
HS to 250ms	51.64 (10.73)	52.51 (13.22)	52.64 (13.22)	0.18

Table 1: EMG Activity during the 250ms pre HS and 250ms post HS at $8kmh^{-1}$.

Variable	Measurement Interval			
VM	C1	C2	PE	ANOVA
250ms to HS	17.29 (4.95)	18.42 (4.93)	18.50 (3.86)	0.46
HS to 250ms	59.66 (3.81)	60.02 (7.43)	66.31 (3.39)	0.13
VL				
250ms to HS	17.57 (6.30)	16.98 (7.24)	17.19 (8.73)	0.36
HS to 250ms	61.87 (6.20)	60.61 (8.55)	65.69 (3.87)	0.39
BF				
250ms to HS	42.98 (9.55)	47.25 (7.80)	47.67 (12.11)	0.63
HS to 250ms	36.51 (20.04)	35.64 (19.61)	33.78 (18.49)	0.74
SOL				
250ms to HS	15.17 (14.23)	16.79 (15.90)	17.91 (20.35)	0.22
HS to 250ms	47.50 (12.44)	54.57 (10.92)	58.81 (13.01)	0.95

Table 2. EMG Activity during the 250ms pre HS and 250ms post HS at $8kmh^{-1}$.

Values are means (SD) expressed in %·ms in Table 1 and 2. The Bonferroni adjusted critical p level is $p < 0.002$ *at a 95% confidence interval.*

quadriceps muscles occurred in our study at this time. In contrast to previous studies[8,9], this investigation found that both VM and VL activity increased in the period 250 ms post HS between the C1 and PE intervals, (VM C1 = 58.47 (6.36), PE = 62.45 (5.17), VL C1 = 54.17 (9.85), PE = 60.62 (6.34)) although these results were not significant. Therefore it appears that increased quadriceps muscles activity occurred following the effusion in the period immediately post HS. This may be an attempt by the knee musculature to increase joint stabilisation to absorb full limb support and to protect the passive joint structures from harmful forces that may be increased by an effusion.

Conclusion

Based on recent research the aim of this study was to measure the effects of a high level effusion on dynamic, clinically and functionally applicable activities. We observed minimal significant changes in sagittal and coronal plane kinematics and lower limb EMG activity during treadmill jogging and running. However we cannot rule out the possibility that prolonged presence of an effusion may alter movement control about a joint through ongoing changes in feedback from joint structures. This study has implications for rehabilitation of knee injuries in that it may be possible for these patients to return to functional activity and to participate in more dynamic activities at an earlier stage in the rehabilitation process.

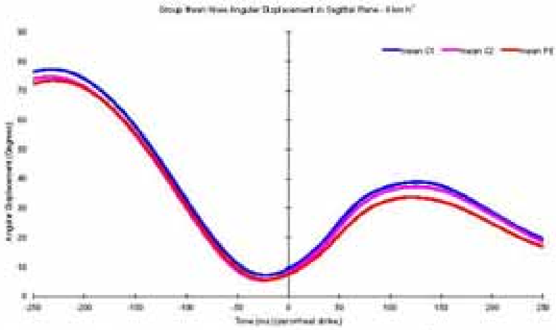

Fig 1: Group Mean Ang. Dis. In Sagittal Plane $8kmh^{-1}$

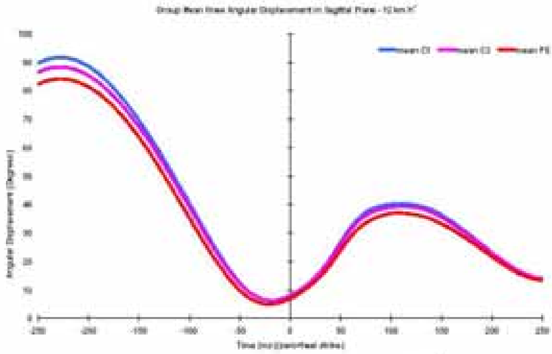

Fig 2: Group Mean Ang. Dis. In Sagittal Plane $12kmh^{-1}$

Acknowledgements
UCD Seed Funding Scheme.

References

[1] Palmieri et al., J Electromyogr Kinesiol. 14:631-40, 2004
[2] Suter E et al., Exerc. Sport Sci. Rev. 28:15-18, 2000
[3] Lewek M et al., Phys Ther. 81:1565-1571, 2001
[4] Stokes M et al., Clin. Sci. 67:7-14, 1984
[5] SENIAM Roessingh Research and Development, 1999
[6] Hochberg Y Biometrika. 75:800-802, 1988
[7] Lucareli PR et al., Clinics. 61:295-300, 2006
[8] Torry MR et al., J. Sports Sci. Med. 4:1-8, 2000
[9] Torry MR et al., Clin. Biomech. 15:147-159, 2005

Prediction of foot instability and inbalance using biomechanical measurements

Authors: Rusu Ligia[1], Marin M.[2], Dragomir M.[1], Rusu P.F.[2]

[1*] Sport Medicine and rehabilitation Department, University of Craiova, Romania
[2] Mechanic Department, University of Craiova, Romania,

ligiarusu@hotmail.com

Introduction

In sport activity performance means to have a well structure and function of musculoskeletal system. This aspect is important for create a specific profilactic training programm and also rehabilitation programm. The aim of this study is to present a comparative study of biomechanicals parameters of foot in two differents sport activity, soccers player sand field tenis players.The roleof this study is to create an immage regards functional parametres of foot specific for each sport activity, football and field tenis. The results of this study can help us to assess the risk of a possible injury and to prevent it.So after this study is possible to: prevent foot injury, prevent akle foot instability, improvement of training methods, prescribe a good orthotic system, improvement of diagnostic methods in sport activity, development and monitoring of rehabilitation programm.

Materials and methods

We study two lots of athlets: lot 1- soccers players(15 subjects, mean age 16years) and lot 2 field tenis players(15subjects, mean age 16years). We use for biomechanic assessment RSscan system, platform plate. We assess loading response at midfoot level during gait. Our recording use frame/sec 300. Parameters that we assess are: %contact(%of contact time compared to the complete stance phase), load rate(N/cms) (the speed of loading in the midfoot region), maxP(N/cm) (the maxim pressure measured in midfoot region), maxF(N) (the maxim force measured in midfoot region), %surface(an overview on the load contact surface under the midfoot), foot axis angle (related movement direction), subtalar joint angle(related to the foot axes). Regards two lasts parameters negative values means endorotation and positive values means exorotation. Our assessment is made during three phases of gait cycle: heel contact, midstance and propulsion. All these parameters help us to estimate foot balance and meta loading during gait to both lots of athletes.

Results and discussion

We present the range of values for each parameters on both sides, left and right and two lots.

Table1: Pressure parameters

Parameters	Soccers Left Right		Field tenis Left Right	
%contact	70-30	63-37	75-63	66-38
maxP	8,5-6,9	4,2-13,1	6-11,6	3,1-14,9
load rate	0,04-0,10	0,03-0,13	0,06-0,08	0,02-0,12

Table2: Force parameters

Parameters	Soccers Left Right		Field tenis Left Right	
%contact	73-30	74-73,7	78-70	69-40
maxF	321,4-315,8	191,2-275,5	277,4-902,4	145,2-620,3
load rate	1,32-0,16	1,40-0,20	2,45-6,15	0,87-46,52

%surface for soccers player are 23,4-29,2% and for field tenis players 25,3-56,9%. Also we observe negative values for foot axis angle and subtalar joint angle, range –7,37° -2,11° for lot1and positive values for lot2, means for lot1 endorotation and for lot2 exorotation.If we see all dates we can observe that in lot 2 load responding is higher then lot 1, also maxF are higher to lot2 , even if both lot have very closely values for %contact. From these dates we can to assess the prediction of an injury risk related to foot stability and balance.So we observe that at lot 1 lower risk for injury is present during heel contact and maxim intsability at left and right feet during propulsion phase(graphic1,2,3,4). For lot2 we see lower risk for injury during heel contact and midstance, foot stability during midstance phase at left side and left side intsability during propulsion phase. For right side we see to entire lot2, a high instability(graphics 5,6,7,8).

These results show to us that risk of ankle foot injuries are high in field tenis then football, that can be corelate with high loading respond existed in tenis. If we see the graphics we observe that for left side, lot1, range –45+20 and for right side 0+59.For lot2, left side 0+15, right side +7+35.

These can be corelate with high values of maxF on right side and load rate also on right side and explain instability during propulsion phase.All these results are in accord with abnormal position of foot, to exo or endorotation, that involve a high risk of instability. So we can say, in according with literature that high loading and extrem foot positions have been associated with a variety of injuries.

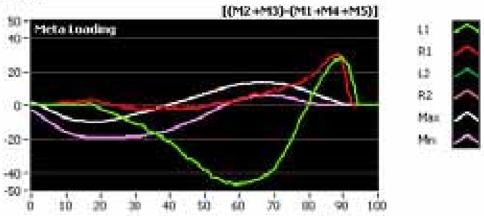

Graphic 1-metaloading and zone of lower injury risk (soccer, 18years)

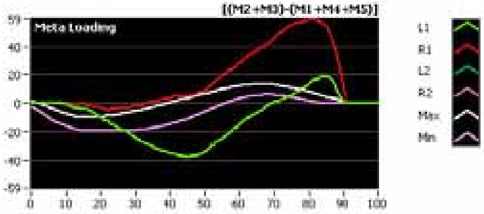

Graphic 2-metaloading and zone of lower injury risk (soccer, 16,5years)

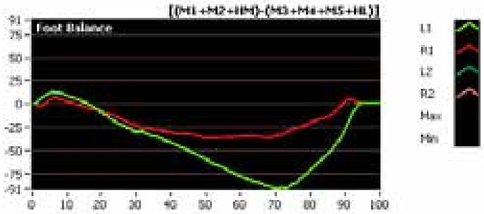

Graphic 3- foot balance (soccer, 18years)

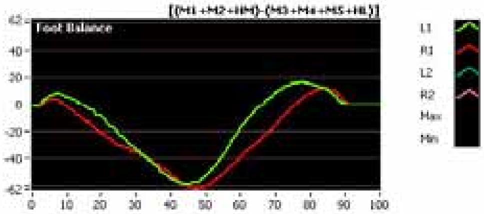

Graphic 4- foot balance (soccer, 16,5years)

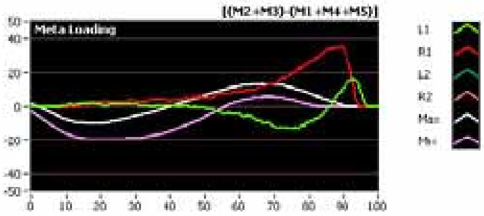

Graphic 5-metaloading and zone of lower injury risk (tenis, 17years)

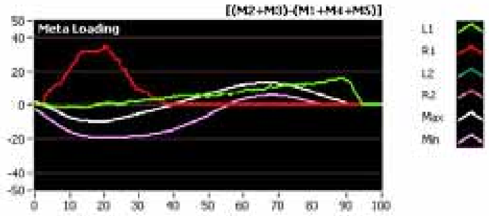

Graphic 6-metaloading and zone of lower injury risk (tenis, 18years)

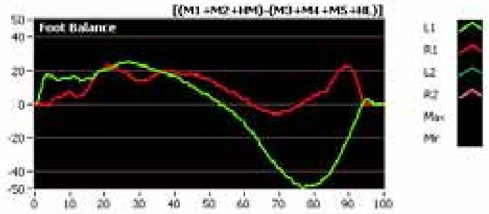

Graphic 7- foot balance (tenis, 17years)

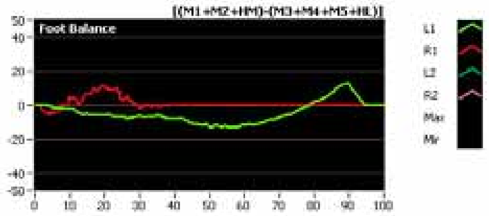

Graphic 8- foot balance (tenis, 18years)

Conclusion

In conclusion we consdier that a good assessment of biomechanic aspect of ankle foot is important not only for prevent or treatment and monitoring rehabilitation programm, but also for a good selection for each sport activity. Also is important to know the load response because that help to prepare the entire muscle chain for both side because how we see muscle inbalance between left and right, increase the posibility of injuries.

Acknowledgements

Thanks to research centre from our university.

References

[1] Hamill J., Knutzen Kathleen, *Biomechanical Basis of Human Movement*, Thrid edition, Lippincott and Wilkins, 2009

[2] Giddings V.L. at.al, Calcaneal loading during walking and running. *Medicine and Science in Sports and ExErcise*, 32, 627-634

Movement optimization of multibody system with application to long jump

Pettersson R. [1], Eriksson A. [2*]

[1] Mechanics, Royal Institute of Technology, Sweden
[2*] Mechanics, Royal Institute of Technology, Sweden, anderi@kth.se.

.Introduction

Biomechanical simulations can be a useful tool to analyze human movements like in a sport event. This provided that the model can represent the most important mechanical properties for the specific application and also find the control that represents the choice of movement. Many simulations in literature need measured movements where the trajectories are known[1]. Here, we want to be able to find optimal trajectories, from initial configuration and velocity while independent of any recorded motion. In our primary application, the athletic long jump, we want to express the optimality in terms of ballistic flight distance.

.Materials and methods

A six-segment sagittal model, linked by hinge joints, was chosen to represent the support-leg foot, shank and thigh, the trunk and the non-support leg thigh and shank. A wobbling mass was attached to the hip joint by spring and damper to represent in-plane motion of soft tissue and upper extremities. Three degrees of freedom (dof) were introduced at ground with spring and damping properties (consequently, 10 dof in total). Driving control moments were introduced to represent both flexors and extensors acting at the joints. The control moment for each joint was determined by activation, maximum isometric force, a factor for moment arm and muscle length, and a factor compensating for concentric or eccentric movement. The latter two are dependent on position and velocity respectively.

Optimization was used to represent the coordination of the movement. The muscle activations in each physical joint were chosen as optimization variables. Each displacement coordinate was described by two polynomials of 5th degree, i.e. determined by 9 parameters. These parameters are the remaining part of the variables to optimize. Then the length of CM's trajectory following a projectile motion was maximized while subjected to nonlinear constraints. The equations of motion at n_t evaluation points along the contact time serves as equality constraints, range of motion, activation derivative (Fig.1) and a constraint to ensure foot contact, were inequalities.

.Results and discussion

Supplied with published subject and motion data[2,3] the method is applied to simulate a long jump take off. The outputs are joint trajectories, muscle activations (Fig.1) and ground reaction forces. Also the contact time with the ground is determined by the optimization.

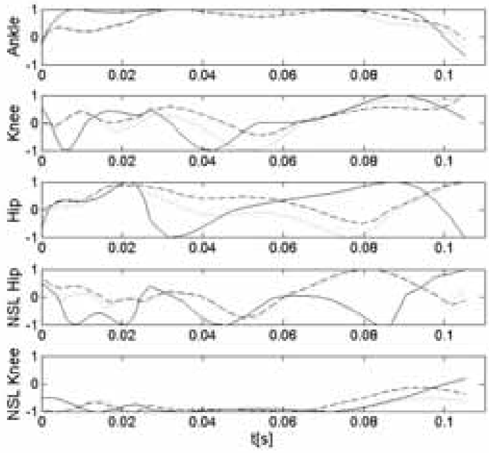

Fig. 1: Optimal activations, α, with three sets of constraints of the activation derivative, unconstrained (solid), $\dot{\alpha} < 200s^{-1}$ *(dotted) and* $\dot{\alpha} < 100s^{-1}$ *(dashed)*

Preliminary simulations show that jump length is dependent of activation rate of the muscles, footplant velocity and contact time. This resulting model leaves future possibilities to investigate parameter dependence, test of coaching strategies and technique analysis. However, there still remains extensive work to set properties of ground contact and wobbling mass connection.

.Conclusion

A methodology for simulation of optimal movement of a multibody system subjected to contact has been developed. From an initial configuration, the simulation derives suggestions of optimal movement based on the assumptions made. The simulation time, end configuration, control and interaction with the ground are all determined by the optimization.

.Acknowledgements

The authors gratefully acknowledge financial support from the Swedish Olympic committee.

.References

[1] Spägele, T. *et al.*J. Biomech. 32,521–530,1999
[2] Brüggemann, G. *et al.* Biomechanical Research Project Athens 1997, 1999.
[3] Muraki, Y. *et al.* International J. Sport and Health Science 6, 21–32, 2008

Intraarticular and muscle force reactions of the leg using different insoles

Wyss, Ch [1], Roethlisberger, M [2*], Gerber, H [2*]

[1] Laboratory of movement analysis, Kantonsspital Aarau, Switzerland, christian.wyss@ksa.ch
[2*] Institute for Biomechanics, ETH Zurich, Switzerland

Introduction

In the literature the effect of insoles is discussed controversial [1,2,3]. The aim of our study was firstly to find a correlation between kinematic, kinetic and electromyographic changes during gait caused by the application of different insoles. Secondly we were interested in the change of the intraarticular force in the knee and the change of muscle forces in the leg.

Materials and methods

We examined 10 healthy subjects using 5 different insoles alternatively with a neutral insole. The kinematic measurements were performed with a Vicon MX System (6 Cameras). Additionally we used an AMTI force platform and a Novel SF pressure measurement System, even though a Pedar (Novel) insole pressure measurement system. The EMG was measured with a MegaWin system, synchronized with the Vicon system. The intraarticular reaction forces in the medial and the lateral compartment oft the knee were calculated with the help of a finite element model (ANSYS) of the leg which is considered as a rough estimate or a simplified model not based on CT Scans. The muscle forces were determined using a slightly modified model from the repository 7.1 of ANYBODY TECHNOLOGY (Vaughan).

Results and discussion

Opposite to the literature we found that there is, for some kinematic parameters, a more or less unique change due to different insoles. The insoles with a medial wedge, for example, showed a significant decrease of eversion of the hindfoot and the insoles with a lateral wedge showed a significant increase of eversion. A more interesting result was the calculation of the intraarticular reaction force in the medial and lateral compartment of our simplified knee model. In figure 1 the pink curve shows the reaction force in the lateral knee compartment in % Bodyweight with an insole with a medial wedge. Nearly the same curve (blue line) shows the measurement with a neutral insole. A significant decreased reaction force could only be observed when we simulated a stiff ankle joint that means inversion and eversion of the ankle joint was excluded in our simulation.

Using our muscle model we found no significant change of muscle forces in the whole leg. Opposite to that we found a significant increase of all thigh extensors comparing barefoot gait with gait in shoes with neutral insoles.

Fig. 1: Reaction force in the lateral knee compartment

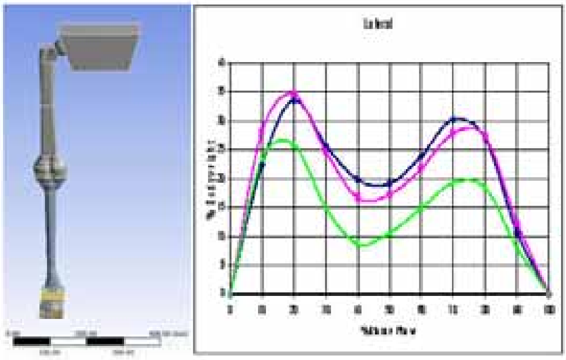

Conclusion

The findings concerning the kinematic parameters of the ankle joint confirm more or less the clinical assumptions. But the clinical conclusion, that the changing of these parameters influence the reaction forces in the knee, could not be confirmed without reservations. The results of our simulations shows clearly that the effect of an insole will be completely compensated by the ankle joint. There is no effect on muscle forces of the leg or joint reaction forces in the knee if the ankle is enough mobile. In other words: it is only helpful to use an insole, unloading the medial knee compartment in mind, when we stiffen the ankle joint for eversion and inversion with a special shoe or with an orthoses. These findings will change our clinical procedures concerning the application of insoles enormously.

Because the muscle forces are significantly increased, when gait analysis is performed with shoes, in the future it will be necessary to do the clinical gait analysis not only barefoot as hitherto. Especially important is this fact when muscle problems of the thigh are existent.

Acknowledgements

We thank gratefully the APO Schweiz and Kantonsspital Aarau AG for the financial support of this study.

References

[1] Stacoff A et al.: The Foot 2007;17:143–153
[2] Nester CJ et al.: Foot Ankle Int 2001;22:133–9
[3] Nester CJ et al.: Gait Posture 2003;17:180–7

Rat tibialis anterior muscle characterization, passive and active behaviour. 3D Finite Element Model.

Jorge Grasa[1], Mª Jesús Muñoz[2], Fernando Soteras[2], Rosario Osta[2], Pilar Zaragoza[2], Begoña Calvo[1], Manuel Doblaré[1]

[1] Centro de Investigación Biomédica en Red en Bioingeniería, Biomateriales y Nanomedicina (CIBER-BBN), University of Zaragoza, Spain.
[2] Lagenbio-Ingen, Aragón Institute for Engineering Research (I3A), University of Zaragoza, Spain.
jgrasa@unizar.es

Introduction

Great research effort have been made to understand biomechanical and neuromuscular properties of skeletal muscle. Since Hill numerous autors have developed mathematical models[1] to describe passive and active behaviour of muscle as the motor for body motion.

Computational models would have the potential to help understanding mechanisms such as damage and fatigue, both in healthy and pathological conditions.

In this work, rat tibialis anterior muscle has been characterize both in passive and active concentric contraction. Results of experimental tests allow to validate a 3D Finite Element model.

Materials and methods

Tendon and muscle samples were extracted in order to determine its mechanical properties under uniaxial tension till fracture. A finite strain hyperelasticity model for soft biological tissues[2] has been employed to characterize this behaviour.

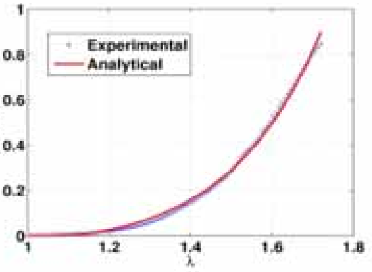

Fig. 1: Passive muscle Stress-Stretch curves, experimental and analytical hyperelastic model.

Using an electro-mechanic testing machine, in vivo tests of tetanic force at different muscle lengths were performed. Muscle was electrically stimulated under certain conditions through the sciatic nerve.

Results and discussion

Tendon and muscle passive material parameters where fitted to the experimental stress-stretch data as can be seen in Fig. 1. These tests determine basic properties to implement the numerical model. Fig. 2 represents total tibialis anterior muscle force under activation conditions.

Conclusion

The numerical model of the rat tibialis anterior muscle simulate real behaviour of the tissue according in vivo tests. This model allows to predict levels of stress inside the tissue for different working conditions.

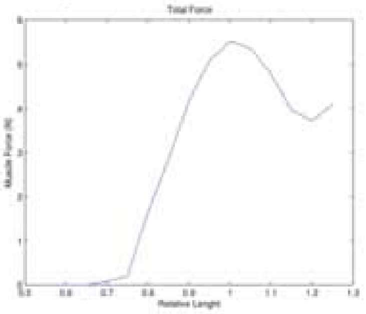

Fig. 2: Total muscle force versus Relative length.

Fig. 3: 3D Finite Element mesh of tibialis anterior.

References

[1] Zajac, F. E., 1989. I. Critical Reviews in Biomedical Engineering 17, 359–411.
[2] Weiss, J. A., et. al, 1996. Comput Methods Appl Mech Engrg 135, 107–128.

Intramuscular architecture of the autochthonous back muscles in humans

H. Stark[1*], R. Fröber[2], N. Schilling[1]

Friedrich-Schiller-Universität Jena, Germany
[1]Institut für Spezielle Zoologie und Evolutionsbiologie, Erbertstr. 1, 07743 Jena
[2]Institut für Anatomie I, Teichgraben 7, 07743 Jena
*heiko.stark@uni-jena.de

Introduction

Various training concepts in preventive medicine and rehabilitation take muscle properties such as contraction speed (fast *vs.* slow) or the topography of the muscles (mono- or biarticular) into account to achieve optimal training outcome. So far, the internal architecture of muscles has largely been ignored although it is well known that parameters such pennation angle or length of muscle fascicles but also the proportion of fleshy to tendinous parts have a major impact on the contraction behaviour of a muscle. Based on the fascicle arrangement, pennated and non-pennated muscles are distinguished. This distinction is crucial for a muscle's force production since the fascicles transmit the force to the tendon at different angles. The length and the pennation angle of the fascicles specify the velocity, distance, and the force during a muscle's contraction. Pennated muscles are well suited for high forces over short contraction distances, while a non-pennated architecture is well suited for high contraction velocities and long distances. To estimate these contraction parameters for a given muscle, often the superficial fascicle orientation is used although several studies have shown that the internal architecture cannot necessarily be inferred from the superficial arrangement. In many cases, the inner fascicle architecture is much more complex comprising for example so-called intramuscular in-homogeneities (i.e., local differences in pennation and fascicle length)[1,2]. With our 3D-reconstruction, we aim to increase our knowledge of the intramuscular architecture of the autochthonous back musculature in humans in order to allow the incorporation of these properties in training concepts and biomechanical modelling.

Materials and methods

One adult male cadaver (57 years) was studied. After removal of skin, subcutaneous fat, and the mm. trapezius, latissimus dorsi et serratus posterior inferior, titan-screws were placed on palpable landmarks along the spine and pelvis.

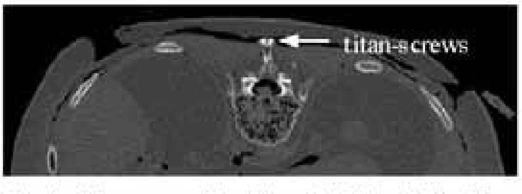

Fig. 1: CT-cross section through T11 with the titan-screws on palpable landmarks.

A CT-scan was recorded from the complete torso, and the skeleton including the makers was reconstructed from the image stack (Fig. 1). To reconstruct the complex system of the autochthonous back musculature, several 3D-coordinates along the fascicles were measured using the 3D-digitizer 'Microscribe' while the muscles were dissected in layers on both sides of the body. The data were further processed, artefacts removed, and the fascicles aligned using the self-written software 'Cloud'. To visualize the skeleton and the muscles, the open source program 'Pov-Ray' was used (Fig. 2).

Results and discussion

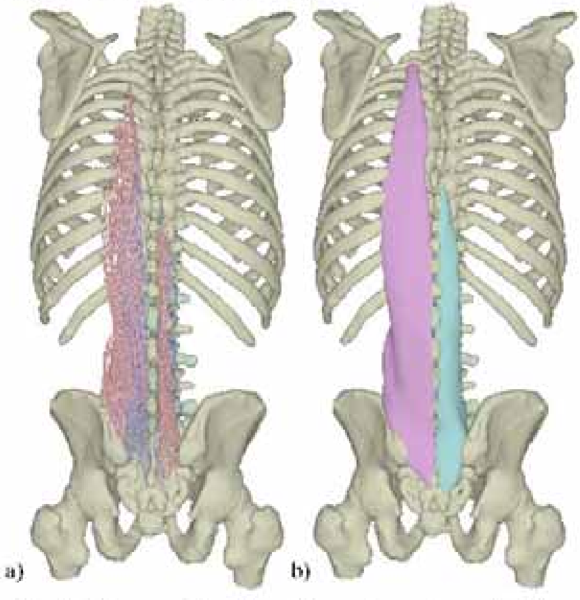

*Fig. 2: 3D-reconstruction of the male cadaver skeleton including the titan screws on palpable landmarks - spinous processes and crista iliaca (in yellow). The lumbar vertebrae L1, L3, and L5 are shown in green. Reconstruction of the m. longissimus thoracis (left) and the m. multifidus thoracis et lumborum (right) illustrating their **a)** fascicle architecture (fleshy parts in red, tendinous parts in blue) and **b)** muscle surface surrounding all fascicles.*

Of the epaxial musculature (m. spinalis thoracis, m. iliocostalis lumborum, m. longissimus thoracis, m. semispinalis thoracis, m. multifidus thoracis et lumborum, mm. rotatores, mm. interspinales, mm. intertransversarii), altogether 1082 fleshy (591 left, 491 right) and 339 tendinous parts (only right side) of all fascicles were measured. Compared to the multifidus muscle, the longissimus muscle has considerably longer fascicles and a lower pennation angle (mainly in the caudal part). Whereas the relatively short fascicles of the multifidus muscle connect more or less linear between their origin and insertion, both, the fascicle curvature and torsion, are clearly higher in the longissimus muscle. As a result, the longissimus has distinct S-shape. The ongoing statistical analysis of a variety of parameters will allow the comparison between body sides and among different muscles. Afterwards, conclusions about in-homogeneities or the number and size of morpho-functional (sub-)units per muscle or muscle group can be drawn to deduce and extract essential architectural parameters necessary for muscle modelling and simulations. The results will provide a data base to create improved, i.e. more detailed muscle models such as a Finite Element Mesh incorporating further parameters, and allow to compare this data base with other studies[3,4,5,6,7].

Acknowledgements

The study was supported by the Berufsgenossenschaft für Nahrungsmittel und Gaststätten Erfurt. For his help with the CT-scans, we thank PD Dr. Schulz from the Institut für Diagnostische und Interventionelle Radiologie, Universitätsklinikum Jena. The titan-screws were kindly provided by R.D. Bader from the Gesichts- und Kieferchirugie, Universitätsklinikum Jena. Technical assistance by S. Müller and A. Wiegand is gratefully acknowledged.

References

[1] van Eijden TMGJ *et al.*, Anat. Rec. 248 (3):464-474, 1997.
[2] Gorb SN *et al.*, Zoomorphology 120 (2):91-97, 2000.
[3] Bogduk N *et al.*, Spine 17 (8):897-913, 1992.
[4] Dumas GA *et al.*, Spine 16 (3):293-303, 1991.
[5] Hansen L *et al.*, Spine 31 (17):1888-1899, 2006.
[6] McGill SM *et al.*, Clin. Biomech. 8 (4):171-178, 1993.
[7] Stokes IAF *et al.*, J. Biomech. 32 (3):311-316, 1999.

Cooperation and variability within the sarcomere network – investigated by isolated mini muscle cells

Fabian F. Dettwiler [1], **Jachen Denoth** [1*]

[1*] Institute for Biomechanics, Swiss Federal Institute of Technology Zurich, Switzerland,
jdenoth@ethz.ch

Introduction

We investigate the cooperation and variability of sarcomeres within the contractile apparatus of the living muscle cell. The relationship between the dynamics of the 'sarcomere network' and muscle performance is explored.

We believe that these coherencies are crucial for the understanding and further investigation of the molecular function and pathologies of the contractile apparatus.

To overcome classical limitations in live-cell muscle mechanics, we establish an experimental framework to investigate the 'sarcomere network' of muscle cells only containing 1-5 short myofibrils.

Materials and methods

The marine invertebrate Lanceolatum Branchiostoma is introduced as a model organism. Its muscle for body movement consists of cells that are in the magnitude of 1x1x100 μm^3 and usually contain only 1-5 short myofibrils (Fig. 1).

Single cells are obtained enzymatically by tissue disaggregation and continuously held in artificial sea water at 15°C. Cells are mounted between a MEMS force sensor[1] a and a stiff borosilicate tip within a petri dish (Fig. 2). Both tips are surface modified to allow natural adhesion.

Simultaneously, a single isometric contraction is induced by electrical activation, force is acquired and the kinematics of the 'sarcomere network' is captured by high-speed videomicroscopy in phase contrast and DIC mode. The measurement is repeated at different temperatures.

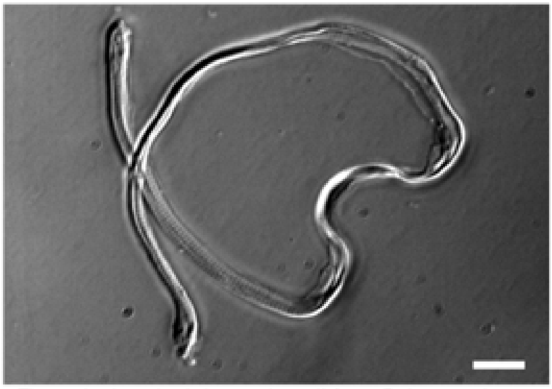

Fig. 1: Isolated mini muscle cell from B. Lanceolatum. Scale bar: 10 µm

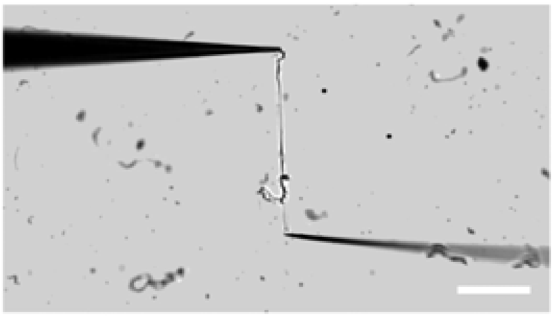

Fig. 2: Mini muscle cell mounted between a glass (above) and MEMS force sensor tip (bellow). Scale bar: 50 µm

Results and discussion

We are going to present and discuss the outcome of our first experiments i.e. the quantification of the cooperation of sarcomeres during the isometric contraction at different temperatures. The results will be compared to those from isolated myofibril experiments and the current conceptions.

There will also be reference to the impact and origin of variability within the 'sarcomere network'.

Conclusion

We will discuss the potential of muscle cells from Branchiostoma Lanceolatum as a model system to investigate the dynamics of the 'sarcomere network' but also muscle biology in general.

Acknowledgements

Thanks to the Swiss National Science Foundation, Prof. Dr. Viola Vogel ETH Zurich, Prof. Dr. Urs Greber and Dr. Irina Agarkova University of Zurich

References

[1] Yu Sun *et al.*, Biomed. Mat. 2:1:16-22, 2007

Mechanical work as predictor of force enhancement and force depression

Kosterina N. [1], **Westerblad H.**[2], **Eriksson A.**[1*]

[1*] Mechanics, The Royal Institute of Technology, Sweden, anderi@mech.kths.se
[2] Department of Physiology and Pharmacology, Karolinska Institutet, Sweden

Introduction

The main function of the skeletal muscle is to provide force during walking, running and other everyday movements, and it is important to know the mechanism underlying such processes as muscle shortening and stretch. In particular, the understanding of transient force production under various length regimes is a necessity for improved description of muscular action in numerical simulations of movement[2].

We investigate a history dependence of skeletal muscle force production, specifically, the steady-state force after active muscle shortening and stretch not being equal to the isometric force[1]. We show that the isometric force production is not only dependent on current muscle length and length derivative, but depends on memory of preceding contraction history.

Materials and methods

The Isolated extensor digitorum longus and soleus muscles from mice (NMRI strain) were used to investigate the force produced by a muscle, and some parameters hypothetically influencing this history-dependent force modification.

The muscles were pre-stimulated at fixed length, then a stretching/shortening history was introduced, whereafter induced changes of active force were recorded while the muscles were held isometrically to reach a steady-state force before de-stimulation. The series of experiments can be divided into four sets according to the length variation in the stimulated state: 'Shortening', 'Stretch', 'Stretch-Shortening' and 'Long Shortening'.

The mechanical work during active stretching and shortening was evaluated by integrating the product of force and ramp velocity over the length-varying period:

$$W = -\int_{t_{ini}}^{t_{fin}} F(t) \cdot \frac{dl}{dt} dt$$

giving positive work for shortening, negative for stretch.

Results and discussion

The results show a negative linear correlation between the force modification and the mechanical work produced by or on the muscle, continuous between shortening and stretching (Fig. 1). This suggests a common mechanism underlying the force depression with concentric contraction and the force enhancement with eccentric contraction, which is in contrast to the general idea that the force modification following shortening and stretches involves different mechanisms.

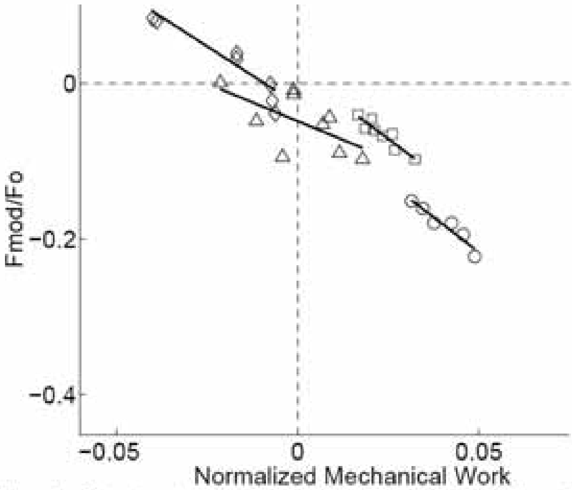

Fig. 1: Steady-state force modification as a function of normalized mechanical work of mouse SOL muscles (average values for groups of 5-6 muscles). Data points represent mean values for the groups of experiments: Shortening - squares, Stretch - diamonds, Long Shortening - circles, Stretch-Shortening - triangles.

Modification of the passive force component following each stimulation was also observed. Experiments show that the fully stimulated redevelopment of isometric force after transient-length contraction follows a time function similar to the creation of force when isometric muscle is initially stimulated.

Conclusion

The study confirms presence of the active and passive force modification following contraction with various length changes. The results show that muscular force does not only depend on length and length time differential. The steady-state force also takes into account the accumulated length history, as shown in transient-length contractions. Our results indicate that the mechanical work produced by the muscle during length variation is a good general predictor for the steady-state force modification induced by transient-length contractions.

Acknowledgements

The authors gratefully acknowledge technical support in preparing muscle specimens from Shi-Jin Zhang, and financial support from the Swedish Research Council.

References

[1] Kosterina N. *et al.*, J. Biomech. 44:2422-2429, 2008
[2] Kaphle M., Eriksson A., J. Biomech. 41:1213-1221, 2008

FORCE ENHANCEMENT IN A MYOFIBRIL – THE ROLE OF HALF-SARCOMERE DYNAMICS

Urs Stoecker (1), Jachen Denoth (1)

1. Institute for Biomechanics, ETH Zuerich, Switzerland

Introduction

Stretching of cardiac and skeletal myofibrils has been extensively studied experimentally (e.g. [Joumaa, 2008; Rassier, 2008; Telley, 2006a]) and discussed in different contributions (e.g. [Telley, 2006b; Telley, 2007]). To analyze the role of half-sarcomere dynamics during stretching of myofibrils one needs a multi-segmental model i.e. a model that consists of several contractile elements in series that include cross-bridges kinetics. A generic framework regarding the muscle as a linear motor composed of serially coupled subunits has been presented to analyze inter-sarcomere dynamics for stationary conditions [Denoth 2002].

Methods

In this work an extended model of the former one is introduced. The Hill-type description of the contractile element is substituted by a Huxley-like formalism of two bound states [Nishiyama, 1977] to account for 'real' transient forces based on cross-bridge kinetics. Biological variability is taken into account by e.g. introducing individual force capacities of the single half-sarcomeres. The formalism allows calculation of the response of force and hS dynamics of a myofibril due to activation, relaxation and stretching.

In our model, we performed numerical simulations of a system of four half-sarcomeres in series under "physiological" conditions of a frog sartorius myofibril, while including structural parameters in our model [Linari, 2007]. These conditions were tested using classical protocols to determine force-length and force-velocity relationships.

Results

During activation, half-sarcomere length non-uniformities occur as has been partially known from previous experiments [Telley 2006a]. During stretching the force response shows the well known increase, even though individual sarcomeres are located on the descending limb of the force length relationship (Figure 1). The force dropped during stretching for longer amplitudes of the stretch.

After stretching, no "real" force-enhancement can be found in the simulations.

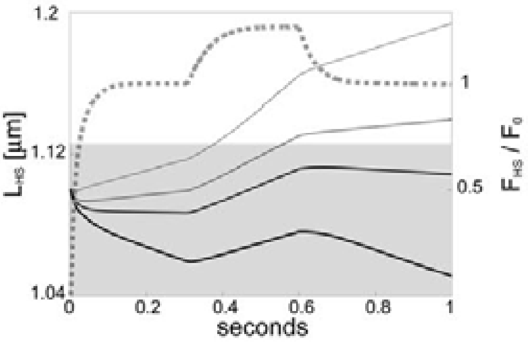

Figure 1: Slow stretching ($v=0.1L_0/s$, $\Delta L=0.3L_0$) of a system of 4 half-sarcomeres in series with different force capacities (thin grey the weakest, solid black the strongest). The grey dashed line denotes the force of the system. The grey band is the plateau of the force-length relation. The half-sarcomere non-homogeneity increases during stretching. After the stretch the force reduces to the force prior to the stretch.

Discussion

The spreading of the half-sarcomeres is a continuous process during activation as well as during stretching. The spreading is a result of the force capacities of the single half-sarcomeres and is not enhanced due to the stretching; however the spreading is slightly greater in the theoretical model than in adopted experiments.

Force-enhancement after stretching can only be found in specific conditions and is generally observed less in the theoretical model than in the experiments. A multi-segmental model in combination with an adapted 3-state-Huxley model cannot explain the aspect of force enhancement.

References

Denoth et al, J theor Biol 216:101-122, 2002.
Joumaa et al, Proc Biol Sci, 275: 1411-9, 2008.
Linari et al., Biophys J, 92: 2476-90, 2007.
Nishiyama et al., Biochim Biophys Acta, 460:523-36, 1977.
Rassier, Proc Biol Sci, 275:2577-86, 2008.
Telley et al, Biophys J, 90:514-30, 2006a.
Telley et al, J Physiol, 573.1:173-185, 2006b.
Telley et al, J Mus Res Cell Motil, 28:89-104, 2007.

Model of the muscle transversal deformation evoked by the muscle contraction.

Kaczmarek P.[1*]

[1*] Institute of Control and Information Engineering, Poznań University of Technology, Poland
Piotr.Kaczmarek@put.poznan.pl

Introduction

The muscle contraction phenomenon has been investigated for years. As the contraction is a complex process incorporating electrical, chemical and mechanical phenomena, it can be investigated by using different measurement techniques. Beside commonly used electrophysiological signals (EMG) there are also mechanomyographic signals (MMG) generated during muscle contractions. They are recorded by using laser distance sensors[4,7], accelerometers[2], or by microphones located over the muscle belly[3,5]. A very important feature of the MMG is that it reflects mechanical effects of the muscle contraction and thus it can provide an useful information related to the effective muscle contraction force. It was reported that the MMG signal is correlated with: the muscle contraction force, the fatigue level, the contraction type (isometric or isokinetic), the muscle length and the motor units (MUs) architecture. Moreover, the MMG is considered as a tool diagnostics the muscle diseases.

Majority of authors agree that the MMG is generated due to the transverse movement of the muscle surface evoked by MUs activity[1,5,6]. Nevertheless, the origin of this effect has not been fully described. So far, our group has proposed two models of the MMG generation process which were based on the mechanical approach. In fact, they are the first models explaining the MMG generation process. The first one described the MMG recorded with a piezotransducer by modeling a part of the muscle surface and an acoustic wave propagation in the paraffin oil medium generated by the muscle surface deformation due to an MU contraction[5]. The second one, which was also described in the present abstract, explained the MMG recorded with the laser distance sensor (LDS)[4].

Materials and methods

MUs which was recorded with the LDS during *in vivo* experiments revealed a diversity of the MMG waveforms. To explain this phenomenon, the hypothesis was made that the MMG profile is determined by both the muscle pennation and the MU location within the muscle volume. Therefore, to verify this supposition, the presented model accounts for these features.

For the sake of simplicity the muscle model was described here as a longitudinal cross-section of a medial gastrocnemius (MG) muscle of a rat (Fig. 1B). The MUs are localized in the same cross-section plane. They are parallel and connected only to the surface of the muscle with 19^{O} pennation angle. Thus, the contraction force even of a single MU, can be decomposed into two components ^{x}Q (the resulted contraction force measured with a transducer attached to the muscle tendon) and ^{z}Q (the force generating a local deformation of the muscle surface and consequently a transversal displacement of the whole muscle belly). Moreover, it was assumed that the MU occupies restricted area of the muscle volume and might be located in one of the 15 model segments, while the LDS recording the surface displacement was located over the middle part of the belly (Fig. 1B).

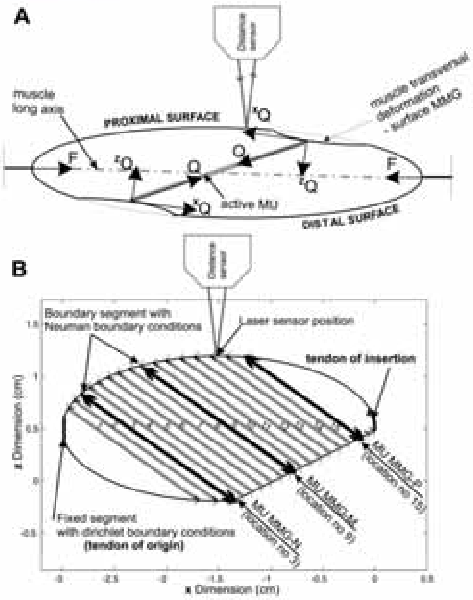

Figure 1: The MMG generation idea (A) and the longitudinal cross-section model of the MG muscle (B) with 15 MUs areas. The MU territory covers the area between two neighboring gray lines.

The dynamics of the whole system is described by the following parabolic equation:

$$D\frac{\partial \vec{u}}{\partial t}-\nabla(C\nabla\vec{u})=\vec{f}(\vec{u},t) \quad (1)$$

where $\vec{u}$ denotes the position vector $\vec{f}(\vec{u},t)$ is the external force vector, C and D are the constant elasticity and the dumping coefficients matrices respectively.

As the muscle is examined in the isometric condition, the segments connected to the tendons must satisfy the Dirichlet boundary conditions. The latter boundary segments are constrained by the Neumann boundary condition (NBC). Assuming the muscle surface motion is free, the NBC in the segments fixed to the muscle surface are defined by the following equation:

$$\vec{n}(C\nabla\vec{u})=\begin{bmatrix}{}^{x}Q\\{}^{y}Q\end{bmatrix} \quad (2)$$

where $\vec{n}$ denotes a versor in the direction normal to the boundary segment..

The model was implemented in MATLAB. The muscle geometrical parameters were kept similar to the size of a rat MG muscle. The muscle cross-section was partitioned into 833 nodes in which the equation (1) was solved numerically by using the PDE Toolbox. The model parameters (i.e. the viscosity and the elasticity coefficients) were estimated by using the standard Prediction Error Method (PEM) based on signals recorded *in vivo*. The model verification was performed for three MUs presenting different MMG waveforms recorded during the *in vivo* experiment. For the first one denoted as MU MMG-N the recorded distance between laser sensor and the muscle surface decreased with increase of the contraction force. In the second case (MU MMG-P) the distance increased with the force increase. For the third one the MMG was initially positive and then, when the contraction force exceeded a certain level become negative (MU MMG-M). The localization of the particular MU was estimated iteratively in the model to obtain the best correspondence between the model-generated and the *in vivo* recorded MMG signals. Finally, for the estimated MU location simulation results were compared with the MMG signals recorded *in vivo* during unfused and fused contractions of the particular MU.

Results and discussion

The muscle model parameters (the elasticity and dumping coefficients) were estimated for a single twitch. The fit of the MMG signal obtained with the muscle model compared to the MMG signal recorded *in vivo* reached the level of 86% for the single twitch contraction.

The estimated locations of the MUs MMG -N, -M and -P, is presented in the Fig. 1B. The comparision *in vivo* recorded and the model-generated MMG signals is presented in the Fig. 2. The results support hypothesis that the MMG profile is determined by the MU location. The fit of the MMG signals recorded in the experiment and generated by the model were above 75% for the twitch and unfused tetani contractions (at 1 Hz and 40 Hz stimulations, respectively). The fit error increased strongly for the fused contractions and was the highest for the MU MMG-P and the smallest for the MU MMG-M. The MMG of the muscle model grew more than in the experiment and the fit of the *in vivo* recorded and simulated MMGs decreased to 60%. Nevertheless, the profiles of the MMG recorded in the experiments and obtained with modeling were similar also in the case of the fused tetanic contractions. The discrepancy between the results from the computer model and these obtained *in vivo* can be attributed to the following modeling simplifications: 1) the homogeneous and constant model coefficients, neglected Poisson coefficient and hyperelastic properties of the muscle tissue, 2) the restricted MU areas and their discrete locations, 3) the simple gastrocnemius muscle geometry used.

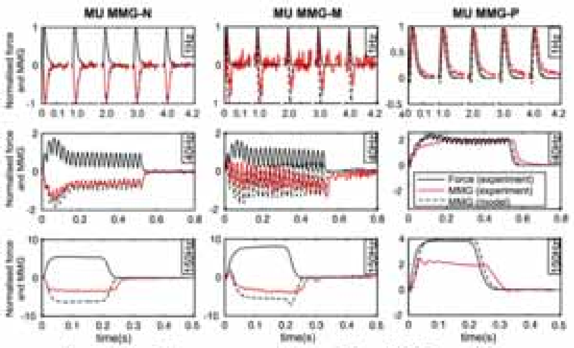

Figure 2: The comparison of the MMG and force signals recorded in the experiments with the model-generated MMG. The results are presented as relative changes of a particular signal to its maximum value recorded during 1 Hz stimulation.

Conclusion

The linear, distributed parameters model presented here, lets to explain the phenomenon of the MMG signal generation observed *in vivo*. However, the model reflecting the muscle nonlinearity (i.e. muscle tissue hyperelasticity) should significantly improve the accuracy of the simulation results. The proposed model may be applied to identification of the MU localization within the muscle belly. Moreover, the model enables to investigate mechanical effects generated by asynchronous contractions of a several MUs. This is an important issue for development of muscle state estimation methods.

References

[1] Beck TW. *et al. J Electromyogr Kinesiol*, 17:1 – 13, 2007.
[2] Cescon C., *et al. J. Neurosci.*, 159:19 – 25, 2007.
[3] Jaskólska A. *et al. J Electromyogr Kinesiol*, 16:89-102, 2006.
[4] Kaczmarek P. *et al. J Electromyogr Kinesiol*, Apr 2008.(in press)
[5] Kaczmarek P. *et al. J Electromyogr Kinesiol*, 15:617 – 630, 2005.
[6] Merletti R. *et al.* Wiley-Interscience, 2004.
[7] Orizio C., *et al. Eur J Appl Physiol*, 88:601–606, 2003.

Glycosaminoglycans do not Influence Collagen Fibril Load Transmission or Dynamic Viscoelasticity in Tendon

Fessel G. [1], Snedeker J. G.[1,2]

[1]* Department of Orthopedics, University of Zurich, Switzerland
[2] Institute for Biomechanics, ETH Zurich, Switzerland, gfessel@research.balgrist.ch

Introduction

Tendon is a complex connective tissue composed primarily of collagen fibrils, proteoglycans and water. Two glycosaminoglycans of small leucine-rich proteoglycans, dermatan sulfate and chondroitin sulfate, have been increasingly posited[1-3] to contribute to tensile mechanical behavior of collagenous tissues, potentially acting as molecular cross links between discontinuous collagen fibrils.

While such a contribution of proteoglycans to both elastic and viscoelastic behavior has been hypothesized, experimental studies have offered widely conflicting evidence that alternately support or reject these hypotheses. The current study sought to systematically test this theory of tendon structure-function by investigating the mechanical repercussions of enzymatic digestion of tendon glycosaminoglycan complexes.

Materials and methods

Twenty single rat tail tendon fascicles, randomly separated into two groups, were tested in a dynamic uniaxial testing machine (Electro Force 3220-EM, Bose Corp, USA). The test group consisted of fascicles that were depleted of dermatan and chondroitin sulfate chains by the enzyme chondroitinase ABC. The extent of GAG removal was verified by relevant assays and transmission electron microscopy.

Potential influence of GAG content in both the "heel" and "elastic" regions of tendon was investigated at two levels of tendon strain. First, a mean level of 1.8% strain was implemented to characterize the linear region of the fascicle material curve and then a mean level of 0.4% strain was implemented to characterize the heel region of the material curve. Around these mean strain levels, sinusoidal strains were applied with amplitudes of 0.5%. Strain-rate dependent (dynamic viscoelastic) behavior was assessed over two orders of magnitude with applied sinusoidal frequencies of 0.1, 1 and 10 Hz. These were selected to represent quasi-static loading, "physiological" loading, and quasi-impulsive loading. These frequencies and strain magnitudes translated to approximate mean strain-rates of 0.05, 0.5 and 5% s^{-1}.

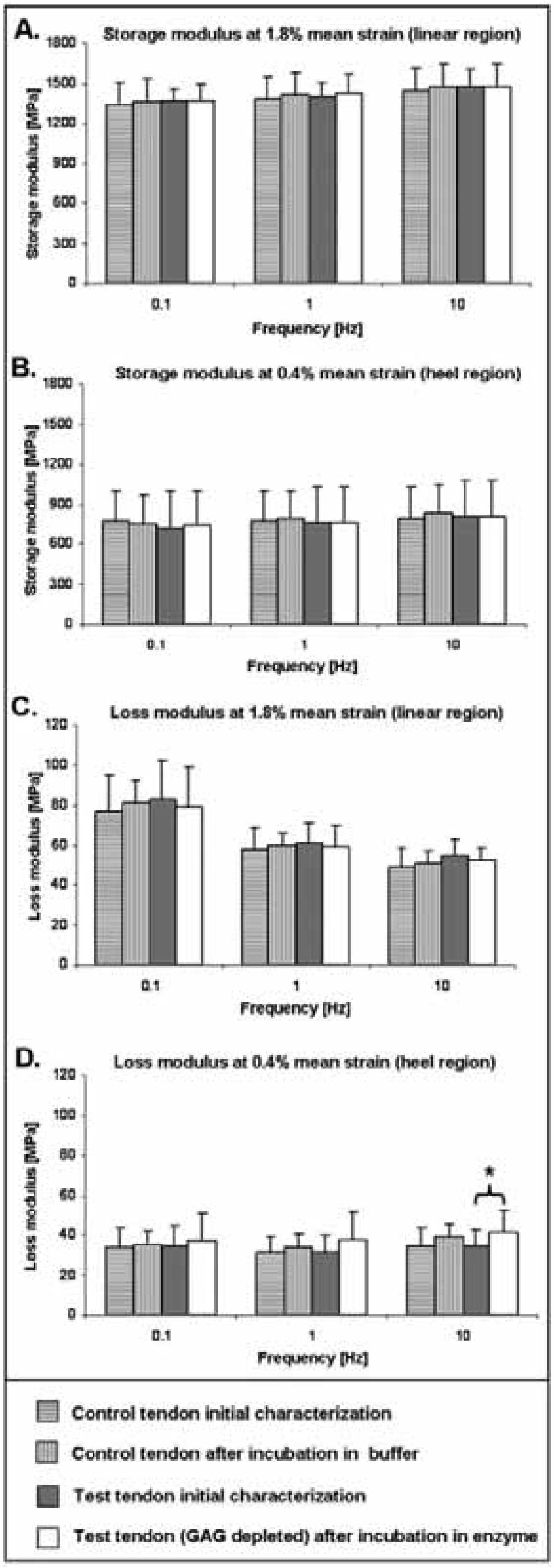

*Fig. 1: Comprehensive test results: * = significant difference pre-post treatment in the paired statistical analysis (p<0.05).*

Fourier analysis was applied to the force and displacement time histories to determine the complex stiffness (N/mm), a measure of the relative elastic and viscoelastic specimen behavior. Complex stiffness was later normalized by fascicle length and cross sectional area to obtain complex modulus (MPa). Complex modulus was finally separated into storage modulus and loss modulus to quantify respective measures of elastic and viscous behavior for each specimen.

Results and discussion

Dynamic viscoelastic tensile tests on glycosaminoglycan depleted rat tail tendon fascicle were not mechanically different from controls in storage modulus (elastic behavior) over a wide range of strain-rates in either the linear or nonlinear regions of the material curve. Loss modulus (viscoelastic behavior) was only affected in the nonlinear region at the highest strain rate, and even this effect was marginal.

Conclusion

Glycosaminoglycan chains of small leucine rich proteoglycans do not appear to mediate dynamic elastic behavior nor do they appear to regulate the dynamic viscoelastic properties in rat tail tendon fascicles.

References

[1] Ruggeri A., Collagen-proteoglycan interaction. (ed. Ruggeri A.) Martinus Nijhoff, 1984.
[2] Scott, J. E. Faseb J 6, 1992.
[3] Redaelli, A. et al., J Biomech 36, 2003.

Anatomically-based modeling of soft-tissue muscle deformations in the lower limbs during walking

Oberhofer K. [1*], **Mithraratne K.** [1], **Stott S.** [2], **Anderson I. A.** [1]

[1*] The Bioengineering Institute, University of Auckland, New Zealand, k.oberhofer@auckland.ac.nz
[2] Department of Surgery, University of Auckland, New Zealand

Introduction

Anatomically-based modeling of soft-tissue muscle deformation during walking is a major challenge because of the numerous muscles that are involved in gait, the large deformations that occur and the dependency of the muscle deformation on neighbouring structures [1]. While straight-line models, commonly used in gait research [2], highly simplify the 3D architecture of muscle structures, mechanics-based FE models are generally too complex for studying the deformations of all lower limb muscles throughout gait [1], [3].

The present study aimed at modeling the soft-tissue muscle deformations in the lower limbs during walking using a geometric free-form deformation method called the Host Mesh Fitting (HMF) technique. Free-form deformation methods have extensively been used in computer graphics research [4]; however, they have only recently been introduced in biomechanical studies of the musculoskeletal system [5], [6].

Materials and methods

The mathematical modeling environment CMISS (http://www.cmiss.org) was used for model generation, computation and visualization.

Anatomically-Based Model and Kinematic Data

An anatomically-based, parameterized (FE) model of the lower limbs of one female subject was developed from magnetic resonance imaging using the fitting techniques described in [6]. Kinematic data were acquired on the same subject using an 8-camera VICON Workstation Version 5.0 (Oxford Metrics, Ltd.) at 100 Hz.

The Host Mesh Fitting Technique

The HMF technique, previously described in [6], allowed the derivation of soft-tissue muscle deformation given the positions of so-called control points during walking as kinematic constraints (Fig. 1a). Thereby, 20 muscle structures in each leg were embedded into a simple skin-based host mesh (Fig. 1b). The host mesh was deformed throughout gait by minimizing the distances between control points in consecutive time frames in a least-squares sense. The enclosed muscle structures were updated according to the deformed host mesh configuration (Fig. 2).

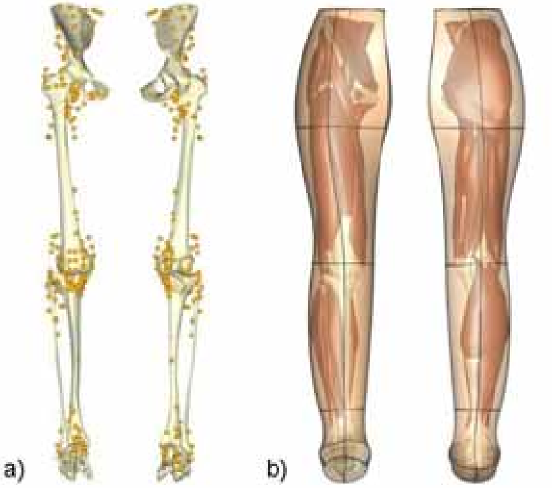

Fig. 1: a) Control points, assumed to be rigidly attached to one particular bone, and b) skin-based host mesh of the right leg from anterior and posterior view

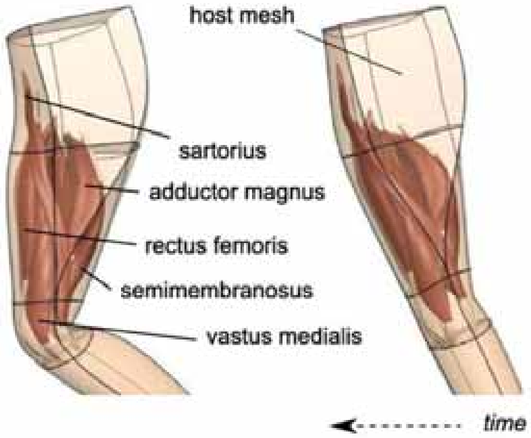

Fig. 2: The HMF technique allowed the deformations of several muscles according to the deformation of a simple surrounding host mesh.

Results

The geometric HMF technique resulted in a realistic simulation of the anatomically-based lower limb model during walking (Fig. 3). The solution for deforming the host mesh throughout one gait cycle was 63 sec on a desktop with an Intel Pentium 4 Processor (3.4 GHz). Updating the geometry of one muscle structure according to the host deformation took 53 sec.

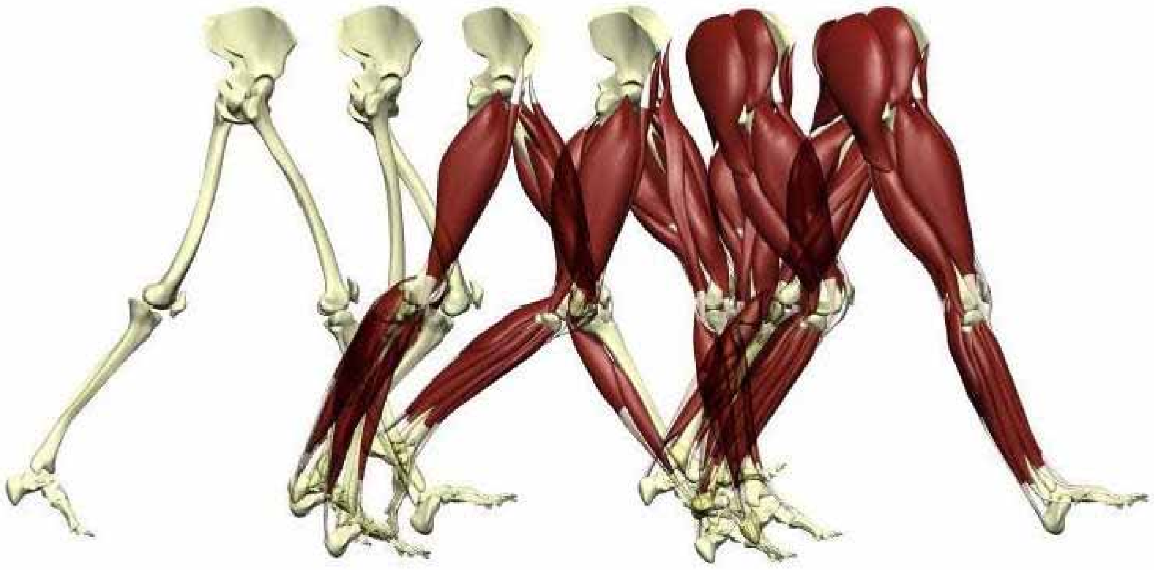

Fig. 3: The anatomically-based lower limb model during walking, with the muscle deformations being derived from segmental kinematics using the geometric HMF technique.

Discussion and Conclusion

The present results demonstrate that the geometric HMF technique is a computationally efficient method for deriving soft-tissue muscle deformations in the lower limbs during walking. Muscle-muscle collision detection, which has been a major limitation in previous studies [6], [7], was avoided by embedding all lower limb muscles into the same host mesh.

The HMF technique is mainly limited by its non-physiological nature as it does not comply with the conservation principles of continuum mechanics and does not account for the intrinsic material properties of muscle tissue. The success of the HMF method purely depends on the kinematic constraints, including the number and distribution of the control points and the design of the host mesh [6].

The geometric HMF solution may be used in future work as displacement boundary condition for solving the governing equations of finite elasticity. The successful convergence of nonlinear boundary-value problems in continuum mechanics is more likely to be achieved if the initial guess is already close to the final displacement [5]. Such a hybrid approach would allow for investigations of stresses and strains within muscles during walking.

The present lower limb model, in particular its implementation into the FE modeling software CMISS, is considered a first step towards the next generation of musculoskeletal models in biomechanical and clinical gait analysis. The gained insights from anatomically-based models during walking may help for improving treatment strategies in patients with musculoskeletal impairments and for more accurately defining soft-tissue constraints in orthopaedic research.

Acknowledgements

Funding for this study was provided by the NZ Foundation for Research, Science and Technology. Grateful acknowledgment is made to M. Moreau for her support with the acquisition of kinematic data.

References

[1] Blemker S. *et al.*, Annals of Biomedical Engineering. 33(5):661-673, 2005

[2] Delp S. L. and Loan J. P., Computers in Biology and Medicine. 25(1):21-34, 1995

[3] Roehrle O. and Pullan A. J., Journal of Biomechanics. 40:3363-3372, 2007

[4] Sederberg T. W. and Parry S. R., ACM Computer Graphics. 20:997-1015, 2000

[5] Fernandez J. W. *et al.*, Biomechanics and Modeling in Mechanobiology. 4:39-56, 2005

[6] Fernandez J. W. *et al.*, Biomechanics and Modeling in Mechanobiology. 2:139-155, 2004

[7] Dong F. *et al.*, IEEE Trans Visualization and Computer Graphics. 8(2):154-170, 2002

Modelling proximal femur deformities in spastic diplegic children

Carriero A. 1*, Zavastky A. 2, Stebbins J. 3, Theologis T. 3, Lenaerts G. 4, Jonkers I. 4, Shefelbine S. 1

1* Imperial College London, UK, a.carriero@imperial.ac.uk
2 University of Oxford, UK
3 Nuffield Orthopaedic Centre, Oxford, UK
4 Katholieke Universiteit Leuven, BG

Introduction

Children with spastic diplegic cerebral palsy (CP) walk with altered gait due to muscle spasticity and contractures. They frequently develop a range of bone deformities including increased femoral anteversion angle (FAA) and coxa valga (increased femoral neck-shaft angle (NSA)).

We hypothesized that spastic muscles affect bone growth by exerting abnormal stresses on the developing bones.

The objectives of this research were to:

1. estimate hip muscle loads and contact forces from gait analysis of CP and healthy children;
2. determine how the loading conditions of different gait patterns alter the stresses in the growth plate of the proximal femur.
3. simulate the growth of the proximal femur in CP children, implementing mechanobiological principles into a finite element model.

Understanding the mechanism by which bone deformities develop may help clinicians prevent or correct deformities before they affect function and to preserve the appropriate mechanical environment for the growing bone.

Materials and methods

One healthy child and three spastic diplegic children with different gait abnormalities were included in this study. The gait pattern of the first CP child was predominantly characterised by increased knee flexion at initial foot contact with the floor (jump knee), the second by hip adduction and equinus and the third by pelvic rotation and obliquity.

Three-dimensional gait analysis (Vicon 370 - Vicon Motion Systems, Oxford, UK) was performed for each child to determine ground reaction forces and kinematics. A child musculoskeletal model was created by isotropically scaling a generic adult model. The model included 86 muscles and 16 degrees of freedom and was based on marker positions measured during a static pose. In an inverse dynamics analysis, kinematics and kinetics from the gait analysis were imposed on the model to estimate joint moments, joint forces, maximal muscle force and muscle moment arms for each muscle over the entire gait cycle (SIMM, MusculoGraphics, Inc., Santa Rosa, CA). Muscle activation patterns of 43 muscles (right leg) were computed over the gait cycle, using a static optimization algorithm, minimizing the sum of the muscle activations [1]. The muscle forces resulting from the calculated muscle activation patterns and the external forces were then imposed and the hip contact forces were calculated.

A three-dimensional finite element model representing the proximal femoral geometry was generated based on the generic femoral geometry used in the musculoskeletal model (Rhinoceros, McNeek, Barcelona, Spain; Truegrid, XYZ Scientific Application, Inc., Livermore, CA). The model had femoral anteversion equal to 20° and neck-shaft angle equal to 120°. Cortical (E = 20 GPa, ν =0.3) and trabecular (E = 600 MPa, ν = 0.3) bone were assumed to be homogeneous, isotropic and linear elastic. The growth plate at the proximal femur was modelled as cartilage (E = 5 MPa, ν = 0.49), and a transition zone was modelled on either side of the growth plate to avoid stress concentrations. FE analysis was performed for all the children at 10%, 30%, 45% and 70% of gait cycle (Fig. 1). The chosen percentages of gait cycle correspond respectively to the instances of maximal muscle activity, the first and second peak in ground reaction forces and the initial swing phase and have been used previously to represent a gait cycle [3, 4]. In order to make the results comparable, the muscle and the hip contact forces were normalised (as percentage of the body weight).

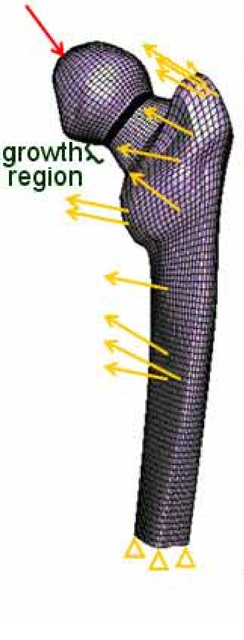

Fig. 1: Muscles forces and hip joint contact forces imposed on the FE model. The muscles considered in this study were gluteus maximus, medius, minimus, divided into anterior, medial and posterior, adductor brevis, adductor magnus anterior, pectineus, iliacus, psoas, quadratus femoris, gemellus, and piriformis. All the muscle loads were applied as concentrated loads on the femur [2, 3]. The hip joint contact loads were spread over the nodes closer to the point of application of the resultant. The model was fixed at the bottom extremity [3].

We used a previously developed mechanobiological model of growth in which cyclic octahedral shear stress (σ_s) promotes grow and cyclic hydrostatic compressive stress (σ_h) inhibits growth [4]. Growth potential was determined by the osteogenic index

$$OI=\sigma_s+0.5*\sigma_h \qquad [4].$$

The maximum octahedral shear stress and minimum hydrostatic stress over the four loads were determined at each node in the growth plate for normal and CP loading.

The direction of growth was determined by the average deformation of the neck that resulted from the four loading conditions.

For each iteration, one row of elements in the growth plate "grew" by an amount determined by the sum of the osteogenic index and a constant biological growth rate. Growth was simulated over 16 iterations, representing about ten months of growth [5].

Results and discussion

The loading conditions for the healthy child agreed with previous studies [1, 6], while the hip contact and muscle forces in CP children were different from the healthy values and each other, reflecting different walking strategies.

Averaged deformation, which determined the direction of growth, and osteogenic index in the growth plate, or the growth map, for the four children are shown in Fig. 2. In normal-loading, the resultant hip joint contact loads had a large negative vertical component (causing the neck to bend downward) and a large posterior component (causing the head to rotate posteriorly). The direction of growth therefore resulted in a smaller NSA and a decrease in anteversion. In CP loads, the vertical component was smaller (not as much bending of the neck) and more anteriorly directed (not as much rotation of the head) resulting in a large NSA and more anteversion than in healthy.

The predicted growth for the healthy child was high on the lateral and posterior side. With CP-loading conditions, the osteogenic index distribution was similar to the normal-loading condition but growth was promoted less on the anterior and lateral side of the growth region.

The growth front progressed about 3.5 mm in 16 iterations. Under normal-loading conditions the neck-shaft angle decreased 3.5° during growth (Fig 2, average deformation, frontal view). With CP-loading conditions, the femur NSA decreased by 1° for CP-jump knee and increased by 1°and 2° for the other two CP children. FAA increased in CP children by 2°-5° more than the healthy child.

This model is sensitive to both the load magnitude and load direction because the magnitude influences growth rate and therefore the amount of growth while the load direction affects the direction of deformation, and therefore the direction of growth.

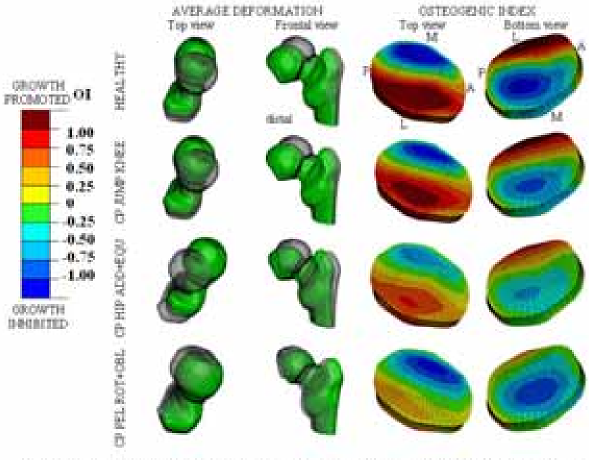

Fig. 2: Average deformation and osteogenic index for healthy, CP-Jump knee, CP-Hip adduction and equinus, CP-Pelvic rotation and obliquity children. A=anterior, P=posterior, M=medial, L=lateral

Conclusion

These results compare well with observations during skeletal growth, in which the FAA and the NSA decrease in healthy children and may increase in children with CP [4]. Morphology of the proximal femur is crucial for hip joint function and affects motor function in general. Understanding skeletal morphogenesis may help in preventing bone deformities and improving function in children with affected gait.

Acknowledgements

This work was funded in part by the Cerebra Charity Organization, UK.

References

[1] Lenaerts G. *et al.*, J. Biomech. 41: 1243-1252, 2008
[2] Duda G.N. *et al.*, J. Biomech. 30: 933-41, 1997
[3] Polgar K. *et al.*, Proc. Inst. Mech. Eng. [H]. 217: 173-89, 2003
[4] Shefelbine S. *et al.*, Ann. Biom. Eng. 32: 297-305, 2004
[5] Pritchett J.W., Clin. Orth. Res. Relat. 275: 274-79, 1992
[6] Bergmann G. *al.*, J. Biomech. 34: 859-871, 2001

Femero-Acetabular Impingement: Motion as an Initiator of Hip Joint Degeneration

Chegini, S.[1], **Ferguson, S.J.**[1]*

[1] Institute for Surgical Technology and Biomechanics, University of Bern, Switzerland,
stephen.ferguson@artorg.unibe.ch

Introduction

Recently, the concept of femoroacetabular impingement has been introduced by Ganz et al [1] as a potential initiator of hip osteoarthritis. The concept focuses on the problem of morphological variations of the hip joint which fall outside the range of "normal" acetabular and femoral geometry motion of the hip, and motion rather than load as a principal factor in the aetiology of degeneration. While the hypothesis is well supported by clinical observations, to date no biomechanical study has been undertaken to investigate this potential mechanism. The primary goal of this work was to verify a correlation between morphological variations of the bony components of the hip joint and resultant stresses within the soft tissues of the hip joint during dynamic loads and motions of routine daily activities. The secondary goal was to find the range of morphological parameters of the hip joint for which the tissue stresses are minimized.

Materials and methods

Three-dimensional computational models of normal and pathological hip joint geometries were developed. These geometries were varied based on changes in the morphological parameters defining the femoral head / neck junction (Alpha angle) and the degree of acetabular coverage (CE angle). The CE angle was varied from 0° (dysplastic joint) to 40° ("pincer" joint with severe acetabular over-coverage). The Alpha angle was varied between 40° (normal joint) and 80°, which is typical of a "cam" type joint with a marked aspherical protuberance on the anterior-superior aspect of the femoral head / neck junction. The model comprised the femoral head and neck, the acetabulum, the two articular cartilage surfaces and the acetabular labrum. Bone components were assumed to be rigid, soft tissue structures were modeled as linear elastic, due to the short duration of loading, with material properties derived from literature values.

Dynamic loads and motions of daily activities, including walking and standing-to-sitting, were imported from in vivo data, transformed to the model coordinate system and the full loading profiles were applied to all joint configurations. The contact pressures and stresses within the cartilage layers were calculated and cross-validated with previous experimental and computational findings and also compared to elucidate the effect of morphology on stress distribution.

Results and discussion

The distribution of cartilage layer stresses is shown in Figure 1 for the standing-to-sitting motion for all joint geometries. With a constant Alpha angle, increasing the CE angle leads to higher stresses at the acetabular rim, due to a direct collision of the femoral neck and the labrum (pincer impingement). As the Alpha angle is increased for a constant CE angle, an intrusion of the non-spherical portion of femoral head into the acetabulum results (cam impingement), with a consequent concentration of sub-surface cartilage stresses at the anterior border of the acetabulum at maximum flexion. For normal walking motion, impingement does not occur and maximum cartilage stresses depend only on the degree of acetabular coverage (dysplastic vs. normal).

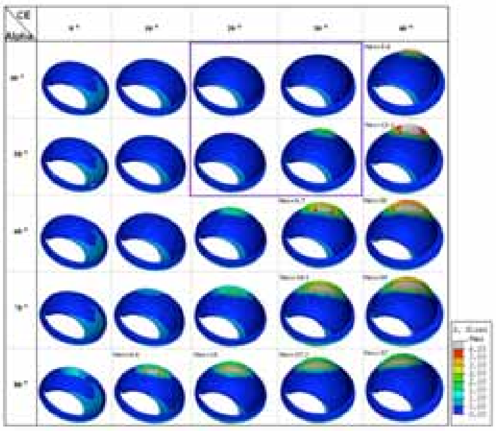

Fig. 1: Distribution of von Mises stresses (MPa) within the acetabular cartilage during standing-to-sitting for all simulated joint geometries. The joints considered as normal are encompassed in a blue rectangle.

Conclusion

For specific pathological morphologies of the hip joint (e.g. impinging hips), motion rather than axial overload may be the critical factor in the development of osteoarthritis.

Acknowledgements

Funding was provided by the Swiss National Science Foundation (NCCR CO-ME) and the Synos Foundation.

References

1. Ganz R. *et al*, Clin Orthop Relat Res 417:112-120, 2003.

Title: Effects of gravity on ulnar nerve latency of activation. Preliminary results of an in-vivo study

Mastrandrea F.[1*], Pandis C.[2], Metastasio A.[3]

[1]University of Perugia Faculty of Engineering Department of Mechanics Perugia, Italy,
francesco.mastrandrea@gmail.com,
[2]South Essex Partnership NHS Basildon and Thurrock University Hospitals,
[3]Cambridgeshire and Peterborough Mental Health NHS Trust Cambridge, United Kingdom.

Introduction

Nerve conduction is very important variable in the physiology of the nervous system. Is therefore essential, to understand the response of the human peripheral nervous system exposed to altered gravity conditions to analyse different aspects of the nerve conduction. A previous in vitro study demonstrated that microgravity conditions influence the interval between a stimulus and a response.

To discover whether nerve latency is influenced by the gravity in vivo, we measured the latency of activation along the motor component of ulnar nerve during three different gravity conditions (0g, 1g and 1.8g)."

Materials and methods

The setting of the experiment was an ESA airbus A-300 O G performing parabolic flights. To fulfil our scientific goal we used an evoked EMG coupled with an accelerometer which stimulated the ulnar nerve in two different sites: elbow and wrist, in three healthy male adults. The data set were acquired in each phase of the parabolic flight and were analysed using the ANOVA test.

Results and discussion

Our results evidenced that the latency of activation changes with the gravity conditions. In detail, during the wrist stimulation was measured a statistically significant longer latency of activation in 0 g condition in all the three subjects. The data obtained from the elbow stimulation in 0g also showed a statistically significant longer latency time in two out of three subjects. In the third subject the latency was longer in 2 g conditions.

Conclusion

The data presented demonstrate that the latency of activation is gravity influenced; this is in agreement with previous *in-vitro* studies. The microgravity phase shows a statistically significant longer latency of activation which is consistent with both sites of stimulation. However the elbow stimulation in one subject showed a shorter latency compared with the 2g measurement. This difference could be explained by technical difficulties during the data acquisition. Further experiments with a larger number of subjects and other parameters to measure (e.g. velocity of conduction, amplitude, temporal dispersion) are needed to confirm our results and to elaborate a physiological explanation of the observed phenomenon. In prospective also sensory nerves should be considered in similar studies.

References

Meissner K, Hanke W (2005). Action potential properties are gravity dependent. Microgravity sci. technol. XVII-2: 3-8.
Hanke W, Fernandes de Lima VM, Wiedemann M, Meissner K (2006). Microgravity dependence of excitable biological and physicochemical media. Protoplasma. 229: 235-42

The influence of recovery and training phases on body composition, peripheral vascular function and immune system of professional soccer players

Reinke S. [1,2,3], **Taylor W. R.** [2,3], **Karhausen T.** [1], **Doehner W.** [1], **Hottenrott K.** [4], **Duda G.** [2,3], **Reinke P.** [5], **Volk H.D.** [2,6], **Anker SD.** [1]

[1] Applied Cachexia Research, Department of Cardiology, Charité - Universitätsmedizin Berlin
[2] Berlin-Brandenburg Center for Regenerative Therapies, Charité - Universitätsmedizin Berlin
[3] Julius Wolff Institut, Charité - Universitätsmedizin Berlin
[4] Martin – Luther - University Halle-Wittenberg, Dept. Sportwissenschaft
[5] Dept. of Nephrology and Internal Intensive Care, Charité - Universitätsmedizin Berlin, Berlin
[6] Institut of Medical Immunology, Charité - Universitätsmedizin Berlin, CCM, Berlin, Germany

simon.reinke@charite.de

Introduction

Professional soccer players have a lengthy playing season, throughout which high levels of physical stress are maintained. The following recuperation period, before starting the next pre-season training phase, is generally considered short but sufficient to allow a decrease in these stress levels and therefore a reduction in the propensity for injury or musculoskeletal tissue damage.[1] We hypothesised that these physical extremes influence the body composition, blood flow, and endothelial/immune function, but that the recuperation may be insufficient to allow a reduction of tissue stress damage.

Materials and methods

Ten professional football players were examined at the end of the playing season, at the end of the season intermission, and after the next pre-season endurance training. Peripheral blood flow and body composition were assessed using venous occlusion plethysmography and DEXA scanning respectively. In addition, selected inflammatory and immune parameters were analysed from blood samples.

Results and discussion

Following the recuperation period a significant decrease of lean body mass from 74.4 ± 4.2 kg to 72.2 ± 3.9 kg was observed, but an increase of fat mass from 10.3 ± 5.6 kg to 11.1 ± 5.4 kg, almost completely reversed the changes seen in the pre-season training phase.

Remarkably, both resting and post-ischemic blood flow (7.3 ± 3.4 and 26.0 ± 6.3 ml/100ml/min) respectively, were strongly reduced during the playing and training stress phases, but both parameters increased to normal levels (9.0±2.7 and 33.9±7.6 ml/100ml/min) during the season intermission. Recovery was also characterized by rising levels of serum creatinine, granulocytes count, total IL-8, serum nitrate, ferritin, and bilirubin.

These data suggest a compensated hypo-perfusion of muscle during the playing season, followed by an intramuscular ischemia/reperfusion syndrome during the recovery phase that is associated with muscle protein turnover and inflammatory endothelial reaction, as demonstrated by iNOS and HO-1 activation, as well as IL-8 release.

Conclusion

The data provided from this study suggest that the immune system is not able to function fully during periods of high physical stress. The implications of this study are that recuperation should be carefully monitored in athletes who undergo intensive training over extended periods, but that these parameters may also prove useful for determining an individual's risk of tissue stress and possibly their susceptibility to progressive tissue damage or injury.

Acknowledgements

This work was supported by the Berlin-Brandenburg Center for Regenerative Therapies - BCRT. The authors would also like to thank the athletes that took part in this study.

Functional Imaging of Tendon for Improved Tissue Assessment

Harvey A. K. [1]*, Thompson M. S. [1], Cornell H. [2], Hulley P. [2], Cochlin L [3]., Tirlapur U. [1], Cui Z. [1], Brady M. [1]

[1] Department of Engineering Science, Oxford University, UK, harvey@robots.ox.ac.uk
[2] Botnar Research Centre, Nuffield Department of Orthopaedic Surgery, Oxford University, UK
[3]Department of Physiology, Anatomy and Genetics, Oxford University, UK

Introduction

Connective tissues constitute vital components of the musculoskeletal system; tendons enable skeleton movement by transmitting forces created in muscles to bones, and ligaments connect bones to each other. Tendons and ligaments suffer from a wide range of clinical problems, including rupture and degenerative pathology. The anterior cruciate ligament (ACL) rupture is an injury resulting from abnormal mechanical loading at the knee, often incurred during sporting (eg. football, rugby, basketball) activities such as turning and rapid deceleration. More than 200,000 ACL ruptures occur annually in the United States alone[1]; the higher level of competitive sport, the greater the risk for the athlete. Depending on the sport, women are up to 8 times more likely to suffer an ACL rupture than men[2].

The most common treatment for ACL rupture patients is surgical reconstruction, whereby a tendon graft is positioned within the knee to replace the damaged ACL. During rehabilitation, the tendon graft undergoes an adaptive process called ligamentisation[3]; It acquires some chemical and mechanical properties of the original ACL. Despite refinements in ACL surgical techniques, long-term successful outcomes are achieved in only 75 % - 95 % of cases[4]. Underlying reasons for this are not well defined, but are likely to be linked to extracellular matrix (ECM) remodeling processes occurring 2-3 months post-surgery[5]. Therefore, there is a growing demand for methods to functionally characterise tendon *in vivo* and/or non-invasively, and monitor the adaptive ligamentisation process in response to loading.

Magnetic resonance imaging (MRI), and in particular dynamic contrast-enhanced MRI, may provide insight into these underlying physiological mechanisms. Whilst there is much literature on *in vivo* MRI of cartilage, specifically delayed Gd(DTPA)$^{2-}$-enhanced MRI of cartilage (dGEMRIC), for quantifying degeneration related to glycosaminoglycan (GAG) depletion[6], there are no equivalent frameworks for tendon and ligament, despite their similar biochemistry.

Our work is currently focussed on multi-scale and functional imaging of tendon. We exploit the capability of near infra-red multiphoton laser scanning multi-photon microscopy (NIR-MPLSM) to induce second harmonic generation (SHG) from fibrillar collagen[7], the most abundant structural protein in tendon, to validate novel MRI protocols. We propose a novel, physiologically robust interpretation framework for analysing the SHG images. From a fitted surface model, we extract functional parameters related to the characteristic regular fibre crimping (waveform) and alternate light and dark banding pattern, which reflect tissue 'quality' and 'biomechanical integrity' (Figure 1).

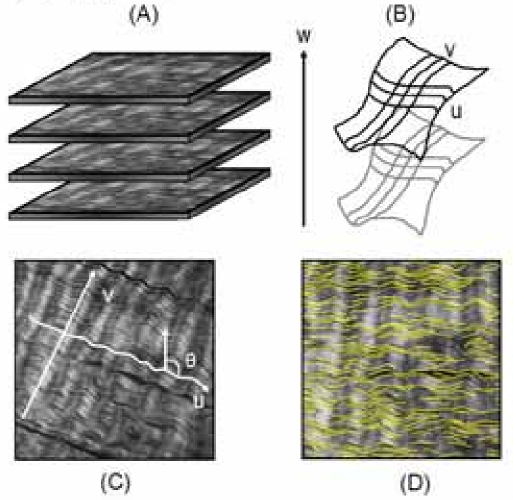

Fig. 1: Surface model for tendon SHG images. (A) NIR-MPLSM image stack. (B) Schematic description of parallel surfaces with intrinsic tissue co-ordinates (u,v,w). (C) Co-ordinates u and v represent local fibre orientation at angle, θ, and light/dark banding pattern, respectively. (D) Spline curves fitted to crimp waveform.

In this paper, we investigate *ex vivo* tendon samples using different imaging modalities: MRI, NIR-MPLSM and light microscopy. We compare the imaging results from normal and digested tendon, in order to establish a framework for interpreting and quantifying tendon tissue 'quality'.

Materials and methods

Phosphate buffer saline (PBS) treated and enzyme-digested (collagenase, trypsin, papain) tendon samples were imaged using MRI, NIR-MPLSM, and light microscopy at longitudinal and transverse orientations. MRI scans were carried out using an ultra-high field (7 Tesla) magnet.

Tendon samples used for NIR-MPLSM and light microscopy were dehydrated, cleared, and embedded in paraffin before sectioning. For NIR-MPLSM, sections were stained with Texas red Wheat Germ Agglutinin (TR-WGA, Molecular Probes). SHG and fluorescence emissions were captured in three channel setups corresponding to blue (400-430 nm), green (500-530 nm) and red (610-650 nm) light. Histology sections stained with Safranin-O were imaged with light microscopy.

MRI images were compared to NIR-MPLSM and histological images to enable interpretation of MR signal intensity at a smaller physiological scale. Analysis comprising spline curve fitting and differential geometry (Frenet-Serret equations[8]) was used to estimate functional parameters from the SHG images.

Results and discussion

Normal tendon MR images and corresponding Safranin-O stained sections are shown in Figure 2. MRI signal intensity is high at locations corresponding to the fatty surrounding sheath, and highlights the fibre directionality and fascicular bundling. Histological staining revealed the tendon cells, fibre direction and ECM GAGs.

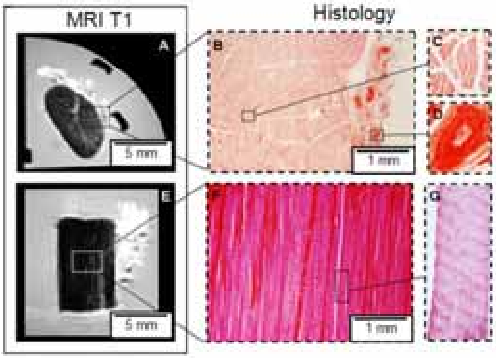

Fig. 2: Tendon MR images (A and E) and anatomically corresponding histological sections stained with Safranin-O (B, C, D, F, G). Transverse slice revealing surrounding sheath, blood vessels and fascicular bundles (top panel). Longitudinal slice showing fibre directionality and tissue integrity (bottom panel).

Figure 3 shows normal and digested tendon MR and SHG images, revealing differences between differentially digested tissues, at multiple scales. MR images depict the tendon macrostructure; SHG images show fibre directionality and ECM organisation. Enzyme-digested samples do not demonstrate the characteristic crimp waveform. Torsion and curvature values for these samples can be calculated using differential geometry, and related to the 'quality' of the tissue.

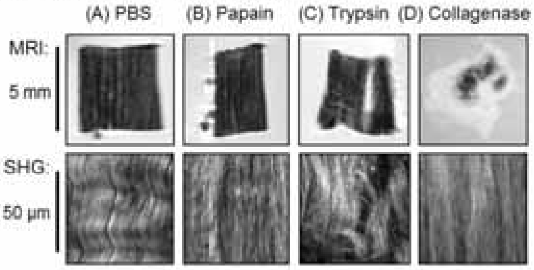

Fig.3: MRI and SHG images of (A) normal and (B-D) enzyme-digested tendon samples. Characteristic tendon crimping is revealed only in normal tendon (A).

Normal tendon stained with TR-WGA and imaged with NIR-MPLSM elicits fluorescence of different structures captured by the blue, green and red filters (Figure 4). Elongated tendon cells are aligned with fibre directions, ECM components are co-localised and image stacks are rendered in 3D.

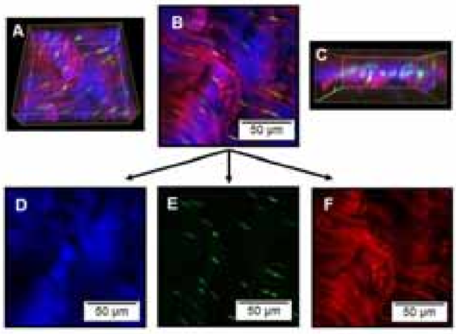

Fig.4: NIR-MPLSM with fluorescent staining allows different biochemical and physiological parts of tendon to be highlighted: (A, C) 3D rendered and colour-merged images, (B) merged image (D) collagen SHG, (E) tendon cells (F) polysaccharide residues.

Future work includes labeling specific mechanically important ECM components (eg. decorin, GAGs) with fluorescently conjugated antibodies. Having established a rigorous framework for interpreting and quantifying normal and enzyme-digested tendon, we are aiming to apply our protocols to clinical situations for classifying tendon samples excised during treatment of sports injuries. Further downstream, we are planning to bridge the gap between research and clinical MRI of tendon (and relate our work to ligament imaging), providing analysis tools which can assist clinicians in diagnosing injuries and predicting return-to-function.

Conclusion

In conclusion, the interpretation framework for tendon SHG images that we describe has the potential to improve *in vivo* imaging technologies. In particular, we are working towards a clinical validation of a specific MRI protocol for functional imaging of tendon. This has major implications for clinical assessment of tendon tissue, both in diagnosing injuries and monitoring repair.

Acknowledgements

We acknowledge the Life Sciences Interface Doctoral Training Centre and EPSRC for funding the D.Phil. studentship for A. K. Harvey.

References

[1] Cooper J. *et al.*, PNAS. 104:3049-3054, 2007
[2] Hewett T. *et al.* A J Sport Med. 34:490- 8, 2006
[3] Amiel, D. *et al.*, J Orth. Res. 4:162-172, 1986
[4] Wolf R. *et al.*, J Sth Orth. Ass. 11:25-32, 2002
[5] Bartlett R. *et al.*, J B J Surg. 83:625-634, 2001
[6] Burstein, D., MRM, 45:36-41, 2001
[7] Mullholland W. PhD Thesis, 2003
[8] do Carmo M. Diff Geom. Of Curves, 1976

Toward Intraoperative Functional Imaging of the Rotator Cuff Tendons

Li Y. [1,2*], **Wuergler-Hauri C.C.** [1], **Gerber C**[1]. **Snedeker JG** [1,2]

[1*] Department of Orthopedics, University of Zurich, Switzerland
[2] Institute for Biomechanics, ETH Zurich, Switzerland, yli@research.balgrist.ch

Introduction

Inappropriate tissue stiffness associated with inadequate healing of the rotator cuff tendons can result in increased susceptibility to re-injury[1]. The rat supraspinatus (SSP) tendon has emerged as a model in the study of rotator cuff[2,3], and the "standard" for assessing rotator cuff biomechanics is ex vivo testing. In contrast to ex vivo testing, non-destructive, in vivo biomechanical testing would open possibilities to gain essential information immediately prior to and following surgery, as well as over the time course of healing.

The present study aims to extend novel functional endoscopic imaging methods[4] to assess mechanical properties of the rat supraspinatus tendon in vivo. This method has been shown to provide high sensitivity to localized differences in tissue stiffness[5]. This study describes the implementation of this method to the rat shoulder and a preliminary validation of its use in assessing SSP tendon biomechanics in a partial tendon defect.

Materials and methods

All animal experiments were approved by the appropriate Swiss authorities. Four 16 week-old male Sprague-Dawley rats were anesthetized and the bilateral SSP tendons were surgically exposed. The rats were divided into two groups: uninjured and partially injured SSP, which underwent a partial defect using a 1 mm biopsy punch. The rat was placed supine on a custom made Supraspinatus Torque-Angle Device (STAD, Fig. 1), for measuring the range of motion in flexion and extension of the rat shoulder. Both the device and the scapula were orientated such that rotation about the device axis passively stretched the SSP tendon along its functional axis. A quantified external moment was then applied, over the full range of shoulder flexion and extension, while torque and shoulder angle were recorded.

To quantify the mechanical integrity of the component tendon tissues, a focused analysis of tendon surface strains was performed. The tendon surface was marked with Indian ink and marker displacement was recorded with an endoscopic video camera while load was applied to the SSP. The relative displacement of the tendon surface markers, and the corresponding tissue strains were calculated using a custom algorithm (Matlab v7.1).

Results and discussion

The shoulder joint could be reproducibly loaded in flexion and extension for both the intact and partial tendon defect groups (Table 1, Figure 1). Tendons with a partial defect showed no apparent change in shoulder range of motion, but showed less resistance to a given applied shoulder extension (Intact: 6.9±1.5 Nmm vs. Defect: 2.4±0.7 Nmm, p=0.1).

Analysis of the endoscopic images of the passively loaded SSP tendons is ongoing. Current image analysis Method could not show consistent increase in stiffness over time.

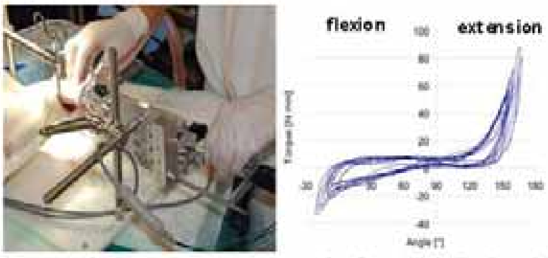

Figure 1. Torque versus angle from a left shoulder cyclically loaded in flexion and extension

Table 1: Peak angle and torque at shoulder range of motion extremes

	injured	Uninjured controls
angle [°]	-89.1+/-10.7	80.2+/-7.1
torque [Nmm]	-2.4+/-0.7	6.9+/-1.5

Conclusion

This pilot study explored a non-destructive method to assess in vivo biomechanical properties in passively loaded rat SSP tendons. To this end, we developed and implemented a device for quantifying and recording the moment-angle characteristics of the shoulder joint in flexion-extension. After configuring the device and positioning the animal in such a way as to passively stretch the SSP tendon along its functional axis, we were able to characterize some macroscopic parameters of shoulder joint biomechanics. While general trends are indicated, it must be noted that this pilot study lacked sufficient statistical power to draw definitive conclusions.

The shoulder range of motion did not markedly change with implementation of a partial defect, resistance to passive motion (quantified as joint torque) did appear to be considerably lower in the defect group. This indicates that the gross mechanical competency of the SSP tendon might be quantified using a non-invasive range of motion device such as the STAD. Specifically, the resistance of the shoulder joint to an applied angular excursion may provide a proxy indication of SSP integrity. Further studies are being performed to confirm this hypothesis.

With regard to the endoscopic assessment of local tendon mechanics, we hypothesized that a partial defect would shunt load to the surrounding intact tissues, and would give rise to higher tendon surface tissues strains. However, it is not shown in current image analysis. Additional methodological development is required to improve the sensitivity and accuracy of these measurements.

Acknowledgements

The authors gratefully acknowledge funding from the Balgrist ResOrtho foundation. Further thanks to Mr. HR. Sommer for his invaluable expertise in device construction.

References

[1] Gerber C et al. JBJS 82(4):505-15, 2000.

[2] Soslowsky LJ et al., JSES 5(5): 383-92, 1996.

[3] Thomopoulos et al. J Biomech Eng. 125(1):106-13, 2003.

[4] Snedeker JG et al. J Biomed Optics 11(6):4010, 2006.

[5] Thomopoulos S et al. J Orthop Res 21(3):413-9, 2003.


Innovation on the Move

Triceps-surae musculotendinous stiffness in women with different foot types

Aurélio F. [1*]**, Helena M.** [2]**, Ronaldo G.**[3]

[1*] Department of Sport Science – CIDESD, University of Beira Interior, Portugal, afaria@ubi.pt
[2] Department of Sport – CIDESD, University of Trás-os-Montes and Alto Douro, Portugal
[3]Department of Sport – CITAB, University of Trás-os-Montes and Alto Douro, Portugal

Introduction

In human locomotion the foot is the interface with the ground, as a result, differences in foot structures may lead to biomechanical differences of the entire lower extremity. Some authors[1-4] suggest that a low arch (LA) feet are flexible and more able to absorb shock dynamically while high arch (HA) is thought to be more rigid allowing considerably less motion and non-shock absorbent. A stiffer foot may be associated with increased overall lower extremity stiffness which may result in a stiffer gait pattern. Leg stiffness seems to differ between subjects with different foot orientations[5] and different foot arch structure[6] during running. However, to the author's knowledge, arch height calculated by dynamic arch index never was related with musculotendinous stiffness of the ankle. Therefore the purpose of this study was to investigate the relationship between musculotendinous stiffness and arch structure.

Materials and methods

This study was composed by one hundred and nine post menopause women [(mean ± SD) age 57.6 ± 5.6 years, mass 68.4 ± 11.3 kg, height 1.56 ± 0.05 m]. The body mass and height of each female was measured by a conventional balance and a stadiometer respectively.

To assess muscle-tendon unit (MTU) stiffness first was calculated maximal voluntary isometric contraction (MVIC) using one apparatus identical to the one of Fig.1. In this procedure a kistler force plate (type 9281b Kistler, Switzerland) with a sampling rate of 1000 Hz was used to assess vertical ground reaction forces. With the same equipment after MVIC calculation a damped oscillation technique was applied to assess "in vivo" MTU stiffness of plantar flexors. Free oscillation data was obtained using external pure gravitational mass equivalent to 30% of MVIC [7-9].

To evaluate plantar pressure a two-step protocol was used[10, 11] with two synchronized pressure platforms (footscan® 3D, RSscan International, Olen, Belgium) placed in series. The data was collected at a sample rate of 250 Hz. After obtain the plantar pressure data for each female the dynamic arch index was calculated for the right foot as a ratio of midfoot area to the total foot contact area, discharging the toes[12].

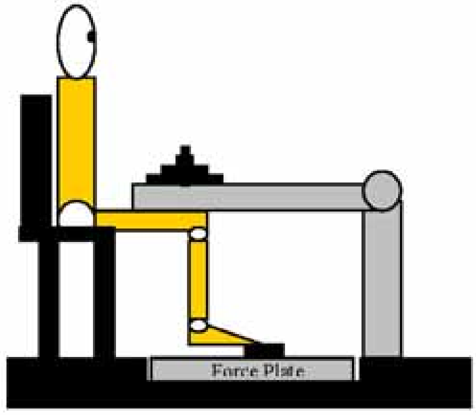

Fig. 1: apparatus to measure stiffness

Results and discussion

To notice if statistical differences in MTU stiffness imposed by foot structure exists ANOVA analysis were performed but no relationship was found, table 1.

Table 1: MTU stiffness for each foot type

Foot Type	**MTU stiffness** (mean ± SD)
Cavus (n =40)	20104 ± 5370
Normal (n =48)	18788 ± 4271
Planus (n =21)	21185 ± 4415

To account for possible influence of body weight in foot structure that could lead to variations in MTU stiffness this analysis were performed on obese and non obese female groups but no relation was also found.

According to literature[6] high-arched runners exhibit increased leg stiffness when compared with low-arched runners and some authors[13] refer that leg stiffness primarily depends on ankle stiffness. Nachbauer and Nigg[14] do not found however any relationship between either arch height or arch lowering and ground reaction force.

High values of stiffness are typically related to increased peak forces, loading rates and shocks[15]. The results of the present study appear to substantiate the previous two studies mentioned since no significant relationship between MTU stiffness and foot structure was found.

Conclusion

Based on the results of this study, it appears that there are no significant differences in MTU stiffness of plantar flexors that could be related with foot structure.

References

[1]Burns J., *et al.*, Clinical Biomechanics, 2005. **20**(9): p. 877-882.

[2]Cheung J.T.-M., *et al.*, Clinical Biomechanics, 2004. **19**(8): p. 839-846.

[3]Wilken J.M., 2006. **PhD**: p. 94.

[4]Williams D.S., *et al.*, Journal of Applied biomechanics, 2001. **17**(2): p. 153-163.

[5]Viale F., *et al.*, Foot Ankle Int, 1998. **19**(11): p. 761-5.

[6]Williams D.S., *et al.*, Gait & Posture, 2004. **19**(3): p. 263-269.

[7]Blackburn J.T., *et al.*, Clinical Biomechanics, 2006. **21**(2): p. 159-167.

[8]Hunter D.G., *et al.*, Physical Therapy in Sport, 2001. **2**(1): p. 15-22.

[9]McNair P.J., *et al.*, British Journal of Sports Medicine, 1996. **30(4)**: p. 313-317.

[10]McPoil T.G., *et al.*, J Am Podiatr Med Assoc, 1999. **89**(10): p. 495-501.

[11]Meyers-Rice B., *et al.*, J Am Podiatr Med Assoc, 1994. **84**(10): p. 499-504.

[12]Cock A.D., *et al.*, Gait & posture, 2006. **23**(3): p. 339-347.

[13]Farley C.T., *et al.*, Journal of Biomechanics, 1999. **32**(3): p. 267-273.

[14]Nachbauer W, *et al.*, Medicine and Science in Sports and Exercise, 1992. **24**(11): p. 1264-9.

[15]Butler R.J., *et al.*, Clinical Biomechanics, 2003. **18**(6): p. 511-517.

Specificity of loading and seasonal variation of vertical jumping performance in young women athletes

Rousanoglou E., Boudolos K.

Sport Biomechanics Lab, Department of Sport Medicine & Biology of Exercise, Faculty of Physical Education & Sport Science, National & Kapodistrian University of Athens, Greece
erousan@phed.uoa.gr

Introduction

Evaluation of physical abilities during the training season is a common practice [1-3]. The specificity of testing with regard to the training loading is often discussed [4,5]. For power athletes such as the volleyball players and the track & filed jumpers a critical physical ability typically tested is the vertical jumping performance [1-3].The aim of this work was to evaluate seasonal variation of vertical jumping performance with regard to specificity of training loading in young, elite for their age categories women athletes.

Materials and methods

Nineteen volleyball players and 13 track & field jumpers were tested three times, at the beginning, middle and ending of their training season (from August to March for the volleyball players and from September to June for the track & field jumpers). All athletes performed three tests of vertical jumping performance (CMJ, SJ and DJ) in each one of the three testing sessions (1st, 2nd, 3rd). A force plate (Kistler 9286AA, Bioware software, 750Hz) was used for data collection and analysis of the ground reaction force – time curve during the jump tests. The force and time parameters inserted for statistical analysis are presented in Table 1. Statistics applied aimed at the significance of the linear increase/decrease during the season as well as the pairwise differences between testing sessions (1st vs 2nd, 1st vs 3rd & 2nd vs 3rd). (SPSS 13.0) ($p \leq 0.05$).

Results and discussion

No seasonal variation was found in the CMJ and the DJ, for the volleyball players and the track & field jumpers, respectively, whereas the reverse was found for the significant variations (Table 1). The variations in the SJ appear similar for both athletic groups. Overall the main seasonal changes are noted between the 1st and the 3rd testing sessions of the training season.

Table 1. Significance of the linear increase/decrease and of the pairwise differences between testing sessions (1st vs 2nd, 1st vs 3rd & 2nd vs 3rd) ($p \leq 0.05$) in each one of the three jumping tests (CMJ, SJ, DJ) in the volleyball players and the track & field jumpers.

	Volleyball players			Track & Field jumpers		
	CMJ	SJ	DJ	CMJ	SJ	DJ
BW (N)	ns	ns	ns	ns	ns	ns
Jump height (m)	Linear increase	ns	ns	ns	ns	Linear increase 1st vs 3rd
Fz_{max} (BW)	Linear increase 1st vs 3rd	Linear increase 1st vs 3rd	ns	ns	Linear increase 1st vs 2nd	ns
RFD (BW/s)	ns	ns	ns	ns	ns	ns
P_{max} (Watt)	Linear increase 1st vs 3rd 2nd vs 3rd	Linear increase 1st vs 3rd	ns	ns	Linear increase 1st vs 3rd	ns
$t_{contact}$ (s)	Linear decrease 2nd vs 3rd	ns	ns	ns	ns	Linear decrease 1st vs 3rd
t Fz_{max} (s)	ns	ns	ns	ns	ns	ns
t Fz_{max} ($\%t_{contact}$)	ns	ns	ns	ns	ns	Linear increase 1st vs 3rd
t $P_{max\ (s)}$	ns	ns	ns	ns	ns	ns
Reactivity index ($t_{flight}/t_{contact}$)	ns	ns	ns	ns	ns	Linear increase 1st vs 3rd 2nd vs 3rd

Conclusion

When testing for the evaluation of jumping ability through the training season it appears that the most appropriate jumping test varies with regard to the specificity of training loading. Thus, the CMJ appears the most sensitive test for volleyball players perhaps due to the dominance of the stretch-shortening type of loading, whereas the DJ appears most sensitive for the track & field jumpers perhaps due to the necessity for loading of increased stiffness. These results further enhance previous similar findings [6, 7] and provide information for the specificity of athletic testing with regard to the particular training loading.

References

[1] Häkkinen K., J Sports Med Phys Fitness. 33:223-32, 1993.
[2] Marques MC, *et al.,*J Strength Cond Res. 22:1147-55, 2008.
[3] Viitasalo J.T. and Aura O., Can J Appl Sport Sci. 9:209-13, 1984.
[4] Abernethy P., *et al.,* Sports Med. 19: 401-17. 1995
[5] Murphy A.J. and Wilson G.J. J Sports Sci.15: 191-200. 1997
[6] Rousanoglou E. *et al.*, Isokinetics Exerc Sci. 14 261–267, 2006.
[7] Rousanoglou E. *et al.*, J Strength Cond Res. 22:1375-8, 2008.

Micromechanics Modeling of Axonal Injury in Brain White Matter

N. Abolfathi, A. Syed, G. Karami and M. Ziejewski

Department of Mechanical Engineering, North Dakota State University
Fargo, ND 58108-6050, USA. g.karami@ndsu.edu

Introduction

Diffuse Axonal Injury (DAI) can happen due to loading or sudden motion on the head. DAI is a major cause of fatality and severe disabilities. This injury can be translated in terms of biomechanical parameters such as the extent of axonal deformation, stresses, strains and separation from the surrounding extra cellular matrix (ECM). To study DAI, a microscale biomechanical modeling of tissue is forwarded. This modeling benefits from the studies on fibrous composite modeling procedure to examine the tissue and the fibrous axonal injury. Employing a developed micromechanics failure analysis for fibrous composites[1], the white matter of the brain is assumed as the composite with axon as the fiber and ECM as the matrix. The focus is on the interface and adhesion of the axon and ECM on the material characteristics of the tissue. The cohesive zone modeling (CZM) is employed to model the interface. The impact due to interface is studied in detail on the characteristics of the white matter of the brain. This modeling method enhances the previously proposed micromechanics modeling of brain tissue[2] and enables one to predict the impact due to sliding, and separation of the axons on the load transfer, stress and strain distribution of axon, ECM and tissue for a microstructural examination of DAI and tissue failure. This can improve the understanding of injury from mechanical perspectives and help in detail prediction of injuries in cellular level.

Modeling Procedure

Cell adhesion is a complex dynamic biological phenomenon. The adhesion of the cell to a surface occurs through specific intermolecular interactions. Employing continuum mechanics approximations, the discrete ligand-receptor bindings described by molecular interactions between the receptors and ligands, are expressed in terms of adhesion traction–separation as a constitutive law of the adhesive interface.

A representative unit cell of the tissue is assumed. This unit cell with the assumed constitutive properties for axon and matrix[3] will be subjected to axial and shear loading. A finite element analysis of this unit cell under periodic boundary conditions will be carried out. For the interface linear or bilinear traction separation can be assumed. Typical traction-separation curves are shown in Fig.1. Cohesive elements can simulate the stiffening as well as the delamination at the interface of axon and ECM. To predict damage initiation the maximum nominal stress/strain ratio or quadratic functional nominal stress/strain criterion is used. Damage can be predicted based on the extent of fracture energy, which is the size of the area under the traction–separation curve. Mixed-mode formulations were used, including the power law form of Benzeggagh–Kenane. The embedded cohesive elements incorporated in ABAQUS, the commercial FE code, are used in the analysis.

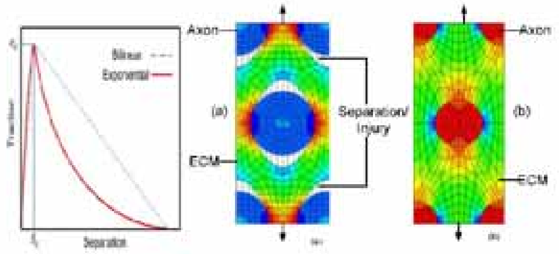

Fig.1. *Traction-separation curves of cell-substrate and stress distribution on the unit cell of brain tissue under transverse loading (a) with and (b) without incorporation of cohesive elements.*

Results and Discussions

The cross-sectional stress distributions of the unit cell under transverse axial loading are shown in Fig. 1 with and without CZ elements. CZ elements have definite impacts on the stress distribution and deformation. It is obvious once the separation of axon and ECM happens the venues for load transfer will change and so do the stress and deformation distribution. We have examined this separation phenomenon under different types of loadings, axial in all three directions, and shear and twist. For each loading, a separate conclusion can be made, due to nature of interfacial resistance. For example for shear, there is less tendency for the layers to separate than the axial loads.

Acknowledgement

Funding of the project is from AFOSR.

References

[1] Karami G *et al.* Appl. Comp. Mat., 15, 259–272, 2008

[2] Abolfathi N. *et al.* Comput. Meth. Biomech. & Biomed. Eng., 2009 (in press).

[3] Meaney, D.F. Biomech. Model Mechanobiol.1:279–293,2003

Effect of age, body composition and anthropometric variables in the biomechanic parameters of plantar pressure in obese postmenopausal women.

Monteiro M. A. [1]*, Gabriel, R. E. [2], Moreira, M. H. [1]

[1] CIDESD, Sport Sciences Department, University of Trás-os-Montes and Alto Douro, Portugal
[2] CITAB, Sport Sciences Department, University of Trás-os-Montes and Alto Douro, Portugal
* monteirom@iol.pt

Introduction

In women older than 50 years old, a muscle mass decline[1] and an increase of fat mass[2] is observed, which originates the sarcopenic obesity[3]. The impact of sarcopenic obesity is now emerging as an important public health problem[4] and apparently, in older people is stronger associated with physical limitations, such as balance lost, disability and gait disorders, comparing to the presence of one or other condition isolated[5].

An unsuitable force distribution caused by obesity, sarcopenia or both of them, may lead to an irregular movement, especially during the stance phase, which will cause an excessive stress and originate injuries in the soft tissues and muscles[6].

The aim of this work was to analyse in obese postmenopausal women: (1) the association of the biomechanic parameters (maximum peak pressure and absolute impulses) with age, anthropometric and body composition variables (body mass index, fat free mass, and relative skeletal muscle mass) and, (2) to identify if the age, the anthropometric and body composition variables have the ability to explain the biomechanic parameters variation.

Materials and methods

The sample was composed by one hundred and eighty nine postmenopausal women (age, 57.6 ± 6.9 years; height, 154.7 ± 4.7 cm and weight, 72.4 ± 9.9 kg).

A footscan pressure plate (RsScan International, 1m × 0.4 m, 8192 sensors, 253 Hz) was used and for each trial, a footprint was obtained from the pressure platform (Figure 1).

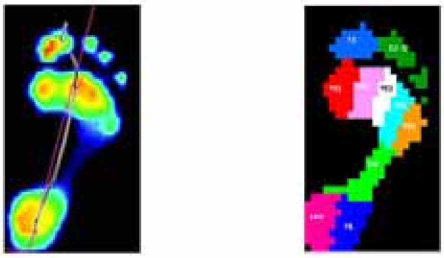

A b

Figure 1 – Peak pressure footprint (a) with the location of ten anatomical important areas (b).

The footprint was divided according to the predefined geometric criteria in ten anatomical pressure areas with the scalable mask automatically provided (Footscan Software 7.1, RsScan international) under supervision of the researcher, based on the peak pressure footprint.

These areas were defined as medial heel (HM), lateral heel (HL), metatarsal (M1, M2, M3, M4 and M5), the midfoot (MF), the hallux (T1) and the foot toes (T2-5).

The weight, relative skeletal muscle mass and fat free mass were evaluated resorting to the bioelectric impedance (InBody720, Biospace, Seoul, Korea) according to the research criteria established in the literature [7].

Height was measured without shoes to the nearest 0.1 cm with stadiometer SECA 220 (Hamburg, Germany) according to the anthropometrical posture, and total adiposity was evaluated resorting to body mass index (weight/height^2).

The degree of association between the variables (table 1) was examined through Pearson's coefficient of correlation *r*, and multiple regression analysis was developed.

Results and discussion

Table 1: Associations between anthropometric variables, body composition and biomechanic variables of plantar pressure.

Variables	Age (years)	BMI (kg/m^2)	FFM (kg)	SMM (%)
Maximum pressure				
T1	-0.65	0.08	0.07	-0.05
T2-5	0.51	0.11	0.18*	0.01
M1	-0.63	0.05	-0.05	-0.06
M2	-0.13	0.19**	0.24**	-0.09
M3	-0.11	0.23**	0.15*	-0.20**
M4	-0.03	0.29**	0.13	-0.29**
M5	0.16*	0.23**	0.08	-0.26**
MF	0.78	0.45**	0.13	-0.34**
HM	-0.14	0.06	-0.01	-0.07
HL	-0.09	0.12	0.01	-0.10
Absolute impulses				
T1	0.50	0.18*	0.07	-0.17*
T2-5	0.11	0.16*	0.16*	-0.08
M1	-0.07	0.14*	-0.05	-0.17*
M2	-0.07	0.33**	0.21**	-0.25**
M3	-0.06	0.31**	0.14	-0.30**
M4	0.06	0.34**	0.12	-0.36**
M5	0.22**	0.29**	0.10	-0.31**
MF	0.16*	0.49**	0.18*	-0.39**
HM	0.05	0.29**	0.13	-0.27**
HL	0.10	0.32**	0.12	-0.29**

BMI, body mass index; FFM, fat free mass; MM, absolute muscle mass and SMM, skeletal muscle mass

** ≤0.05, * ≤0.01

In the obese postmenopausal women, the anthropometric and body composition variables that presented more significant associations with the biomechanic parameters of plantar pressure, were: (1) body mass index (maximum peak pressure, M2, M3, M4, M5 e MF ($p \leq 0,01$) and absolute impulses, T1, T2-5, M1 ($p \leq 0,05$) M2, M3, M4, M5, MF, HM e HL ($p \leq 0,01$)); (2) relative skeletal muscle mass (maximum peak pressure, M3, M4, M5 e MF ($p \leq 0,01$) and absolute impulses, T1 and M1 ($p \leq 0,05$) and M2, M3, M4, M5, MF, HM and HL ($p \leq 0,01$)).

From the selected predictors to the regressions all of them revealed ability to explain the maximum peak pressure and absolute impulses variation (table 2).

Table 2: Multivariate regressions between the age, anthropometric and body composition variables and plantar pressure biomechanic variables

	Age (years)	BMI (kg/m^2)	FFM (kg)	SMM (%)	*R*	*R^2 Adjustedx 100*	*SEE*
Maximum pressure							
T1							
T2-5			0.18		0.18	2.5%	3.60
M1							
M2			0.27	-0.15	0.28	6.7%	7.52
M3		0.23			0.23	4.7%	7.51
M4		0.29			0.29	7.9%	5.08
M5				-0.26	0.26	6.2%	5.09
MF		0.45			0.45	19.6%	2.18
HM							
HL							
Absolute impulses							
T1		0.18			0.18	2.6%	1.14
T2-5			0.18		0.18	2.5%	3.60
M1				-0.17	0.17	2.3%	1.70
M2		0.33			0.33	10.4%	1.71
M3		0.31			0.31	9.2%	1.79
M4			0.20	-0.39	0.40	15.1%	1.46
M5	0.21		0.21	-0.32	0.41	15.5%	1.40
MF	0.16	0.49			0.52	26.1%	0.62
HM		0.29			0.29	7.7%	1.38
HL		0.32			0.32	9.6%	1.62

BMI, body mass index; FFM, fat free mass; MM, absolute muscle mass and SMM, skeletal muscle mass.

In the maximum peak pressure it is detachable the Midfoot which has obtained an adjusted coefficient determination (x100) of 19.6%, explained entirely by the body mass index, followed by the metatarsal 4 (7.9%), 2 (6.7%) and 5 (6.2%).

Among the control variables introduced as predictors in the absolute impulses it is noticeable again the midfoot (26.1%, explained by the age and body mass index), the metatarsus 5 (15.5%), the metatarsus 4 (15.1%) both explained by the fat free mass and relative skeletal muscle mass and the metatarsus 2 (10.4%, explained by body mass index).

None of the selected variables demonstrated ability to explain the modification of the maximum peak pressure in T1, M1, HM and HL.

Conclusion

Body mass index reduction and relative skeletal muscle mass maintenance or improvement is needed, in order to reduce the impact in the soft tissue, which might cause an excessive stress and originate foot pain and injuries.

Acknowledgements

This research was supported by the Portuguese Science and Technology Foundation (FCT) (PhD scholarship, SFRH/BD/38776/2007) and Operational Program for Science and Innovation 2010 (POCI 2010) co financed by Social European found (FEDER).

The authors acknowledge Dr. Ana Moutas Ribeiro for the technical support in this study.

References

1. Lees, S J, Rathbone, C R,Booth, F W. Age-associated decrease in muscle precursor cell differentiation. *American Journal of Physiology-Cell Physiology*. 2006; 290, (2): C609-C615
2. Aubertin-Leheudre, M, Audet, M, Goulet, E, et al. HRT provides no additional beneficial effect on sarcopenia in physically active postmenopausal women: a cross-sectional, observational study. *Maturitas*. 2005; 51, 140-145
3. Morley, J. The aging man and woman : are the differences important? *JMHG*. 2004; 1, 224-226
4. Roubenoff, R. Sarcopenic obesity: the confluence of two epidemics. *Obesity Research*. 2004; 12, 913-920
5. Baumgartner, R, *Age*, in *Human body composition*, Heymsfield, S, et al., Editors. 2005, Human Kinetics. p. 259-268.
6. Abboud, R J. Relevant foot biomechanics. *Current Orthopaedics*. 2002; 16, (3): 165-179
7. Heyward, V,Wagner, D, *Applied Body Composition Assessment*. Second ed. Champaign: Human Kinetics. 2004.

Exact Modeling and Finite Element Analysis of C6-C7 Segment of Cervical Spine

Haghpanahi M.[1], **Hosseini B.**[2] , **Beizaee Sh.**[3] , **Shabanimotlagh M.**[4*]

[1] Mechanical Engineering Department, Iran University of Science and Technology, Tehran, Iran
[2] Mechanical Engineering Department, Iran University of Science and Technology, Tehran, Iran
[3] Applied Mechanics Department, Chalmers University of Technology, Gothenburg, Sweden
[4] Mechanical Engineering Department, Iran University of Science and Technology, Tehran, Iran,
m.shabani.m@gmail.com

Introduction

Automobile accidents, sports injuries and falls cause a majority of cervical spinal injuries. Recognition of the type of the injuries will help the experts decrease the injuries. There are four main methods to collect information about the injuries, using animal models, cadaveric models, clinical studies and mathematical Models (Such as FE models). To have in mind the expenses and availability, using the mathematical model seems to be the easiest method to collect information. Mathematical models are mostly used to find the external response to external loadings such as bending, rotation and flexion/extension. These are the most important external forces exerted to the cervical spine for example in a car accident or in falling. The accuracy of the model will help to take precise results and the results can be verified by the data obtained from a human cadaver. The preference of the FE models is that you can load it as many times as you want with as many forces needed and you can change the condition as may be deemed advisable. Also, FE models can be used to change the material properties and this will help us to model the surgically modified spines.

Method

Mimics interfaces between scanner data (CT, MRI, Technical scanner,...) and STL file format, CAD and Finite Element analysis software. This software is an image-processing package with 3D visualization functions that interfaces with all common scanner formats. Mimics is a general-purpose segmentation program for gray value images and provides several segmentation and visualization tools, also enables the user to control and correct the segmentation of CT-scans and MRI-scans.

In our work we used Mimics to model C6-C7 segment obtained from CT data which was provided from Noor Clinic [1]. Fig. 1 shows the resultant 3D model of the segment after some work and edition (Thresholding according to Hounsfield unit between 200 and 2000, Region Growing, separating interaction with other vertebrae, cleaning the noises, 3D calculation) on pure CT data. We used Remesh command to provide some surface mesh, and using Triangle Reduction and Smoothing commands we created a finer mesh (mesh with higher quality, i.e. using more elements) to export to PATRAN.

Now in PATRAN space we have a 3D triangular surface mesh. We use PATRAN mesher to make volume mesh of the 3D model.

Data given from CT Scan shows just the hard parts of spinal column, therefore we should make the disk manually. By using the bottom surface of body of C6 and the upper surface of body of C7 we make disk between two vertebrae. The disk is made of two parts, the inner part is called Nucleus, and the outer part which is the harder part of the disk is called Annulus. The material properties of these parts are given in Table 1 [2]. Each vertebra has three main parts, the Cancellous bone which is the softest part of vertebra is located in the anterior part, Cortical bone which surrounds the Cancellous, and the third part is posterior elements part. The material properties of each part are given in Table 1 [2]. Also to model the types of ligaments between C6 and C7, which are shown in fig 1, we used six kinds of springs with different stiffness coefficients that are given in Table 2 [2]. Furthermore, to prevent the difficulties of contact analysis between disk and vertebrae we used MPC (Multi Point Constraint).

The bottom surface of the body of C7 is clamped. The pure bending load is applied on the sagittal plane with the magnitude of 0.5,1,1.5,2 N.m. Bending moment is provided by two identical point forces with opposite directions, applied on the top surface of C6. To have more precise results we used ten node tetrahedral elements. Consequently the model consists of 61295 elements and 97339 nodes, which should be solved using finite element method with linear analysis to obtain the displacement response. The results are taken for the end of posterior part of C6 vertebra, which is the most critical point (i.e. the maximum displacements arise).

Results and discussion

For our analysis we used four different case studies to produce 0.5, 1, 1.5, 2 N.m bending moments. To create them on the segment, we located two parallel point forces with opposite directions, by the magnitudes of 56.18, 112.36, 168.53, 224.72 N at two nodes on the upper surface of C6 vertebra with 8.9 mm distance.

Table 3 shows the maximum displacements for the loadings. As expected, the maximum displacement occurs at the end of the posterior part, Fig. 2 shows the displacement profile of C6-C7 segment under bending moment of 2 N.m. In order to calculate the deviation angle of vertebrae, α, we use α = D/R equation, where R is distance between the center of segment and the end of posterior part, and D is the displacement at the end of posterior part, that is taken from the analysis. In order to check the validity of the analysis we compared them with the experimental results taken from [2], Fig. 3 shows the results. Considering that we have used linear spring to model the ligaments and taking into account that the ligaments are stiffer under larger forces, the more the moment, the closer treatment of ligaments to the linear springs used. So we have the most similar angle in the case of 2 N.m moments.

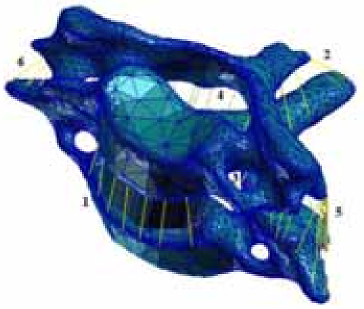

Fig. 1: Types of ligaments between C6 and C7 (numbering is based on names in Table 2)

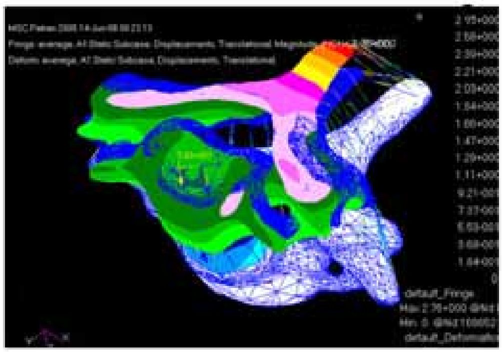

Fig. 2: Displacement profile of C6-C7 segment under bending moment of 2 N.m

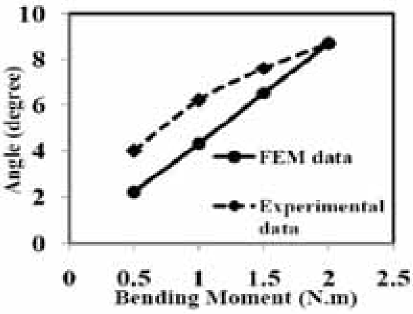

Fig. 3: Comparison between FEM and Experimental results for the deviation angle

Table 1. The material properties of different parts of disk and vertebrae

	Elasticity Modulus (MPa)	Poisson's ratio
Cortical Bone	10000	0.29
Cancellous Bone	100	0.29
Posterior Elements	3500	0.29
Disk Annulus	3.4	0.4
Disk Nucleus	1	0.499

Table 2. Stiffness coefficient of ligaments

	Ligaments	Stiffness Coefficient (N/mm)
1	Anterior Longitudinal ligaments	54.5
2	Posterior Longitudinal ligaments	20
3	Capsular Ligaments	20
4	Ligamentum Flavum	1.5
5	Interspinous Ligaments	1.5
6	Supraspinous Ligaments	1.5

Conclusion

The current research indicates that in mechanical analysis of the C6-C7 segment, the end of posterior part is the most critical, since the maximum displacement occurs at this part of vertebra. Also it is seen that by using the FEM software not only the trend of displacement response of C6-C7 segment can be predicted, but also the quantity of the displacement and the critical moment (load) for segment can be estimated profitably. The above procedure can be used in simulation of cervical spine injuries made by car accidents.

References

[1] CT Scan data of Gheyasvand Hossainali A, 2007/11/01, Noor Clinic, Tehran, Iran

[2] John A. Wheeldon, Frank A. Pintar, Stephanie Knowles, Narayan Yoganandan, Experimental flexion/extension data corridors for validation of finite element models of the young normal cervical spine, Journal of Biomechanics 39 (2006) 375-380

Computational analysis of the electro-mechanical activation sequence of the myocardium

Marcé-Nogué J.*[1], Roure F.[1], Fortuny G.[2]

[1] Departament de Resistència de materials i Estructures a l'Enginyeria, Universitat Politècnica de Catalunya, Spain, jordi.marce@upc.edu
[2] Departament d'Enginyeria Informàtica i Matemàtiques, Universitat Rovira i Virgili, Spain

Introduction

In 1975 the valencian cardiologist F. Torrent-Guasp described the heart as a Helical Ventricular Myocardial Band (**HVMB**) in which "The ventricular myocardium is presented when it is unrolled under the form of a single big muscular band that, due to its special disposition, describes two cavities in the intact heart" [5]. It gives a different perspective of the morphology of the heart than the current and it could explain better and most coherently the propagation of the electrical stimulus which activates the shortening of the fibres, the complex deformation movement of the heart and maybe an explanation about understanding the cardiac contraction.

In order to continue contributing in the study of the **HVMB**, a computational model to simulate the behaviour of the myocardial tissue, mainly based in the fibre, is firstly presented and secondly defined and solved. The model should be able to describe the morphological particularities of the **HVMB**.

Finally, the results are compared with others in the literature to observe if the electro-mechanical activation sequence of the myocardium follows the path described by the **HVMB**.

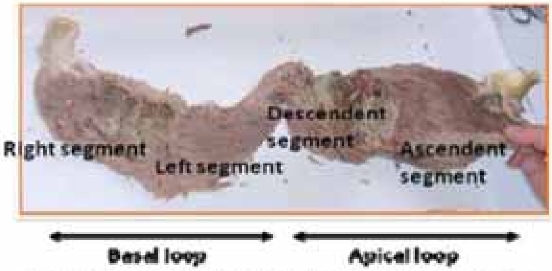

Figure 1 - The HVMB described by Torrent-Guasp

Materials and methods

The model should be able to describe two aspects of the myocardial tissue:

An active part due to the fibres. There is an internal electrical stimulus that activates the contraction of the fibres on a continuum way based on the interaction of (a) the electrical model that is described using the Aliev and Panfilov equations and (b) the mechanical model that is described using the rheological model of Hill-Maxwell and is based in the Theory of Huxley of the sliding filaments and the Cross Bridge model proposed by J. Bestel, F. Clément and M. Sorine[3].

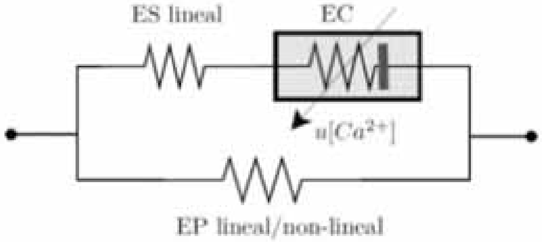

Figure 2 - Rheological model for the fibre

A passive part due to the connective tissue that controls the deformation of the tissue and keeps the cardiac fibres all together and is modeled as a three-dimensional continuum element formulated with the Finite Element Method as an isoparametric hexahedrical element of 8 nodes.

The interaction of the Active Part and the Passive Part in the model generates the following governing equation:

$$\rho \ddot{\underline{y}} - \nabla \underline{\underline{\sigma}} = 0 \quad ; \quad \underline{\underline{\sigma}} = \underline{\underline{\sigma}}_p + \sigma_a \underline{n} \otimes \underline{n}$$

Where σ_p is the passive stress of the connective tissue and σ_a is the active stress due to the contraction of the fibre. A mathematical model for the blood pressure based on the Windkessel model is included and the boundary conditions describing the behaviour of certain fixed points observed in real images are also included.

The geometry of the HVMB is defined starting from medical images and graphic reconstruction techniques in order to obtain a model simplification of the band.

Figure 3- Silicon and computational model of the HVMB

The equations are solved in a simplified HVMB continuum model meshed with 400 eight-node hexahedrical elements and 15 fibres inside meshed each with 50 two-node fibre elements. Propagation along the fibres of the Action potential *u(t)* is generated and a deformation following the same path of the stimulus and the fibres along the band is obtained.

The solution obtained is compared with others computational or experimental results published before in the literature.

The Action Potential propagation along the band is compared with a Fourier analysis of equilibrium radionuclide angiocardiography in order to compare the sequence of the myocardial contraction. Figure 4 shows the activation time of each part of the band in a slice that coincides with the activation times observed by Ballester-Rodés[2].

Figure 4 - Activation in one point

And the shortening of the fibres is compared with an integrated overview of the left ventricular mechanical sequence done by Sengupta [4] in which is investigated whether the onset and progression of regional left ventricular shortening and lengthening parallel the apex-to-base differences in depolarization and repolarisation. Figure 5 shows that shortening of the fibre appears first in the base (time=0.15 sec.) and last in the apex (time=0.35 sec.).

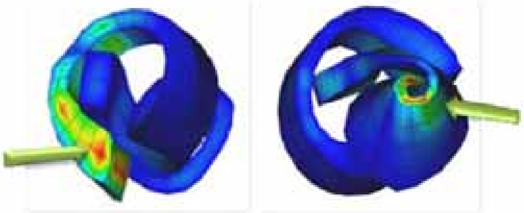

Figure 5 – Principal strain in the myocardial tissue

Results and discussion

If the path followed by the propagation of the action potential coincides with the same path described by the **HVMB**, the activation sequence of the myocardium coincides with the observed in an angiocardiography by Ballester[2].

The generated deformation in each fibre following the propagation along the **HVMB** coincides with the observations done by Sengupta about the mechanical sequence of the myocardium[4].

As a consequence of solving the computational model of the **HVMB** it can be concluded that the results obtained in this simulation agree (in a qualitative way) with the expected results and the observations done in literature and it can be accepted that this simplified model of the **HVMB** is enough good in its first elastic and lineal approximation and the behaviour observed is enough close to the behaviour expected.

Therefore, and according to the observations done in this work, it can be concluded that the electro-mechanical activation sequence in the myocardium coincides with the path described by the Helical Ventricular Myocardial Band.

References

[1] Aliev, R. and Panfilov, A. Chaos, Solitons & Fractals, 7:293-301, 1996.

[2] Ballester-Rodés, M. et altri. The sequence of regional ventricular motion. European Journal of cardiothoracic Surgery, 29S:S139–S144, 2006.

[3] Bestel, J. PhD thesis, Université Paris-Ix Dauphine, 2000.

[4] Sengupta, P.P. et altri. Apex-to-base dispersion in regional timing of left ventricular shortening and lengthening. Journal of the American College of Cardiology, 47(1), 2006.

[5] Torrent-Guasp, F. El músculo cardíaco. Publicacions de la Fundació Joan March, 1972.

An Integrated FE Model for Blast Waves-Human Head Biomechanical Interactions

M. S. Chafi, G. Karami and M. Ziejewski

Department of Mechanical Engineering, North Dakota State University
Fargo, ND 58108-6050, USA. g.karami@ndsu.edu

Introduction

Blast waves due to explosions create highly dynamic loads imposing severe and complicated stresses and strains on the exposing human head and brain and thus cause trauma injury. In general, blast-induced injuries can be divided into three broad categories, of primary (non-penetrating) injury, in which the blast wave travels through impacting the body to cause internal damage with no visible external signs of injury; (II) secondary blast injury, in which the blast wave propels objects or fragments to impact the body and cause the injury; (III) tertiary blast injury, in which the incoming blast wave would displace the body and imparts injury upon its impact with solid objects. In this study, the focus is on the primary brain injury. Of the many types of blast-related injuries, diffuse axonal injury, contusion, and subdural hemorrhage are the most notable ones.

The biomechanical model

A paradigm where a head is exposed to incoming shock waves of a blast explosion is modelled. The explosion detonation, expansion of shockwaves and the fluid/structure interaction with the head are examined. In essence the following stages are modelled and in sequence[1]; (a) detonation of the explosive charge; (b) propagation and spread of the blast waves; (c) interactions of blast waves with the head, and the time-dependent response of the brain and head; and (d) propagation of the shock waves within the human head and the brain. Ls-Dyna finite elements code has been employed to simulate, model, and analyze the above stages. With this explicit code, the time step is computed at each step as a function of the smallest mesh size and its material properties to ensure the convergence. Stages (a) and (b) are modelled by employing the capabilities of multi material arbitrary Lagrangian Eulerian algorithm. Fluid-structure interaction coupling facilities will be used in stage (c), and the standard finite element solid mechanics analysis will be employed for stage (d). The important part of the procedure is stage (c), in which the solver will be combined with the Eulerian-Lagrangian coupling algorithm. This algorithm coupling provides the interaction of a structure simulated with a Lagrangian mesh to a propagating air (fluid) media represented with an Eulerian mesh. Proper material properties are assumed for skull, brain and other anatomical components of head. In particular, a hyper-viscoelastic material behaviour is assumed for the brain.

Results and discussion

This computational algorithm can provide various biomechanical components at different stages of this dynamic process. In particular, we focus on the intracranial pressure, stresses, strains at various points of the brain and other anatomical components of the head at any instance. Figures 1 are showing the air overpressure after the detonation generated with time due to blast measured at a point close to head. Figure 2 shows a typical intracranial pressure distribution at a particular instance which shows the coup and counter-coup overpressure nature at such incidents.

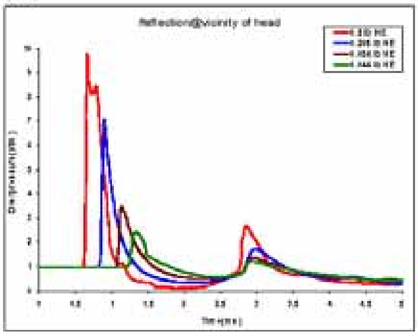

Fig.1. Highly explosive (HE) weight and air overpressure at two points in vicinity of the head.

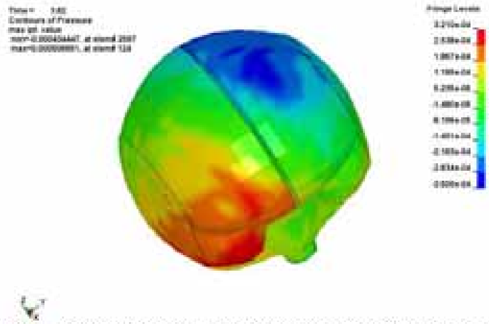

Fig.2. Typical pressure distribution on the brain at instant t=3.3msec after the blast

Acknowledgement

AFOSR has financially supported this work.

References

[1] M.S. Chafi, *et al.* Biomechanical Assessment of Brain Dynamic Responses Due to Blast Pressure Waves, Annals Biomedical Engineering, 2009 (submitted).

Title: On the influence of surgical trauma, age and gender on periprosthetic bone remodelling after THA

Szwedowski T. D. [1*], **Taylor W. R.** [1], **Matziolis G.** [2], **Heller M. O.** [1], **Müller M.** [2], **Janshen L.** [3], **Perka C.** [2], **Duda G.** [1]

[1*] Julius Wolff Institut, Charité – Universitätsmedizin Berlin, tomasz.szwedowski@charite.de
[2] Centrum für Muskuloskeletale Chirurgie, Charité – Universitätsmedizin Berlin, Germany
[3] Institut für Sportwissenschaft, Humboldt Universität zu Berlin, Germany

Introduction

Reduction of bone mineral density that can result from periprosthetic bone remodelling is thought to increase fracture risk, contribute to loosening and complicate revision procedures in total hip arthroplasty [1,2]. Minimally-invasive THA surgery aims to preserve soft tissues, and therefore muscle function [3], and lead to a more balanced mechanical environment that should be expressed as a greater retention of bone mass. Periprosthetic bone adaptation is thought not only to be influenced by the biological and mechanical attributes associated with age and gender, but also the level of soft tissue trauma incurred during more invasive surgical approaches.

Materials and methods

A randomized clinical trial prospectively followed 93 THA patients at post-operation and a 12 month follow-up period using DEXA BMD measurement of seven Gruen zone regions of interest. All patients received an elective, cementless arthroplasty employing the Zweymüller Alloclassic total hip endoprosthesis via either a transgluteal (n=46) or a minimally-invasive anterolateral (n=47) surgical approach from a pool of 10 surgeons. Patients were also grouped based on a threshold age of retirement (65) for a three factorial design consisting of: age (45 young; 48 old), gender (25 male; 68 female), and surgical approach. MANOVA with repeated measures was used to analyze all Gruen zones simultaneously and a partial η^2 analysis was performed to estimate the effect size for each factor.

Results and discussion

After implantation of a prosthesis, the estimates of effect on bone adaptation after 12 months were: combination of age and gender (η^2=0.21), gender alone (η^2=0.17), age alone (η^2=0.12), with all other interactions playing less of a role than surgical approach (η^2=0.10). Gender ($p<0.03$), as well as the interaction of age and gender ($p<0.01$) were shown to significantly affect the rate of remodelling (percentage of the initial postoperative BMD remaining after 12 months), whereas age, surgical approach and all other interactions between the three factors were not. Older women lost the most bone mineral in zones II and VII, whereas young men lost the most in I, III, IV, V and VI and older men retained the most in all zones.

Conclusion

Age and gender were found play an important role in influencing the course of a patient's periprosthetic bone remodelling. Furthermore, the results suggest that surgical approach is as important to the remodelling outcome as the patient's age alone. This study suggests that older women and especially younger men are potential beneficiaries of clinical decisions that mitigate bone loss through muscle sparing implantations. However, the role that age and gender play in internal loading must be better understood before preventative measures can be developed.

Acknowledgements

This study was partially funded by Zimmer Orthopaedics Inc. and the SFB 760.

References

[1] Brown, I. W., & Ring, P. A. J Bone Joint Surg Br, 67:218-221, 1985.
[2] Cooke, P. H., & Newman, J. H. J Bone Joint Surg Br. 70:386-389, 1988.
[3] Bertin, K. C., & Rottinger, H. Clin Orthop Relat Res. 429:248-255, 2004.

Numerical and experimental analysis of correlation between neck muscles activity and mechanical vertebrae loading conditions

Gzik M. [1], **Tejszerska D.** [1], **Świtoński E.** [1]

[1] Department of Applied Mechanics, Silesian University of Technology, Poland
marek.gzik@polsl.pl

Introduction

Human cervical spine is a delicate construction supporting the head. Many of clinical neurological problems as consequences of injuries or degeneration diseases are concerning the human part. Biomechanical relations between anatomical structures, responsible for this state are not completely identified. Anatomy and physiology of muscular system is quite well known but knowledge about biomechanical aspects concerning muscles mechanical influence on skeletal system is not complete. Many science institutions analysing neck muscles influence on head behaviour during situations corresponding to road accidents, less attention concentrate on physiological aspects. The paper presents methodology based on modelling and experimental researches, which the main purpose is identification of neck muscles forces and their influence on cervical spine during daily activity [1,2,6].

Modelling process

Modelling process was preceded by studies on anatomy of human cervical spine, properties of particular elements and kinds of living organisms modelling. 3–dimensional dynamical model of human cervical spine as author program was created on the basis of multibody methodology. Model consists of [1]:

- head, seven cervical vertebrae are treated as 6 degrees of freedom rigid elements and immovable trunk, movement of the elements is depended on muscles, intervertebral discs, facet joints and ligaments activity,
- muscles are divided in two main groups: first deep muscles treated as non-linear spring dumper elements and second group main muscles responsible for head and vertebrae movement. Muscles of second group are represented by forces calculating on the basis of optimization methods, coefficients was determined on the basis of experimental MRI and EMG methods[1,3,5],
- intervertebral disc is divided into isolated segments, representing anulus fibrosus as nonlinear spring element acting during extension and compression and nucleus pulposus as nonlinear spring - damper element acting only during compression, stiffness of discs was determined on the basis of experiments,
- facet joints is treated as nonlinear spring – damper element taking into consideration relative motion possibility of connected vertebrae, additional resisting moment appears when physiological relative motion between neighbour vertebrae is exceeded,
- ligaments are divided in parallel strips acting as forces only during elongation, stiffness was determined on the basis of experiments and literature data[2,3,8].

Experimental research

The model was verified on the basis of experimental researches as comparison of spine stiffness (using cadaver spines), vertebrae relative motion and action of muscles (on the basis of non-invasive tests on patients during routine medical diagnosis). Experimental researches were carried out on tenth human cadaver spines (five of women and five of man), age 55-65.

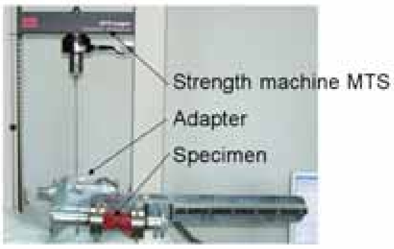

Fig.1 Experimental research on human anatomical spine

Necessary information about material parameters were obtained from tests on specimens of ligaments and discs fig.2.

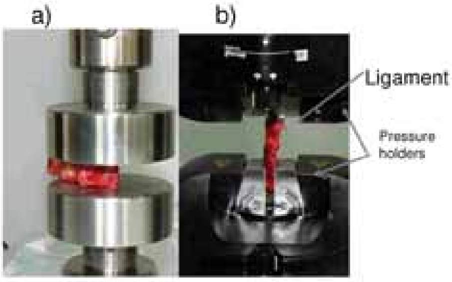

Fig. 2: a) Compression test of disc
b) Tensile test of anterior longitudinal ligament

Nowadays no exist technique which could allow measure individual muscles forces. Muscles role in movement could be recognize using mathematical models. Modelling process of muscles based on information about their anatomy and physiology. Physiological cross section area is important parameter in process of muscle force identification. Thank to cooperation with Voxel Diagnosis Centre in Bytom cross-section areas of male and female neck muscles were determined (fig. 3, tab.1) [3].

Fig. 3: MRI of Sternocleidomastoid with sign physiological cross section area

Table 1: Examples of average physiological cross section area of male and female neck muscles

MUSCLE		FEMALE [mm^2]	MALE [mm^2]
Trapezius -	**Right - R**	695	1095
	Left - L	731	1106
Sternocleidomastoid	**R**	275	364
	L	278	396
Semispinalis capitis -	**R**	62	93
	L	64	94
Splenius capitis -	**R**	77	94
	L	75	95
Obliquus capitis inf -	**R**	146	191
	L	148	185
Rectus capitis post. - major	**R**	74	108
	L	76	106

Moreover mentioned above experiments needle EMG (of Trapezius, Sternocleidomastoid, Splenius capitis) as well functional radiography of cervical vertebra in middle saggital plane were done.

Results and discussion

Created three dimensional model allow to carry out numerical simulation of forces in muscles and between anatomical human parts.

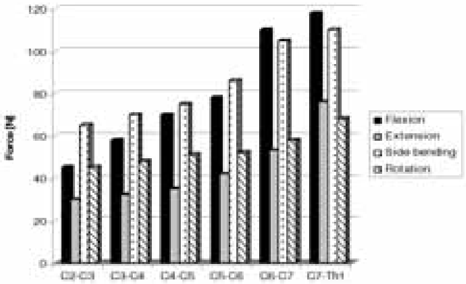

Fig. 4: Maximal forces in discs during flexion, extension, side bending and rotation of head

Comparison of discs and facet joints loads during different head movements for typical adult man are presented in figures 4 and 5.

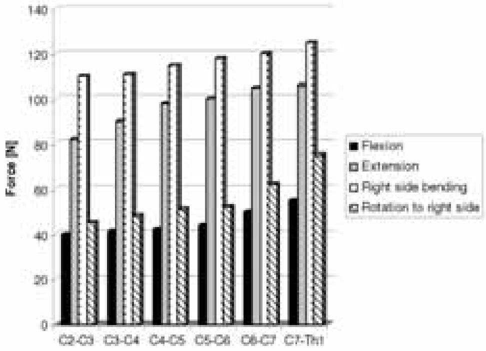

Fig. 5: Maximal forces in right facet joints during flexion, extension, right side bending and rotation of head

Conclusion

Methodology used in this work allows non-invasive diagnose of physical state of tissues in living organism. During work cognitive capabilities provided by modern diagnostics: functional radiography, magnetic resonance imaging MRI and electromyography EMG were used. Results of numerical simulations point out important role of muscles for neck loading conditions. Especially muscles tension, very often it is connected with emotional aspect. The research proved that side head bending generate negative cervical spine loads especially when is exposed through long time.

Acknowledgements

The researches were supported by Polish Ministry of Science and High Education project no. 4 T07B 01730

References

[1] Conley M. S., *et al.*: Noninvasive analysis of human neck muscle function Spine, vol.20, no.23, 1995.

[2] Gzik M., Biomechanics of human spine, Silesian University of Technology Publisher, Gliwice 2007.

[3] Gzik M., Identification of forces in anatomical structures of human cervical spine, Silesian University of Technology Publisher, Gliwice 2008.

[4] Panjabi M.M., *et al.*, Mechanical properties of the human cervical spine as shown by three dimensional load - displacement curves, Spine, vol.26, no.24, 2001.

[5] Seireg A., Biomechanical analysis of the musculoskeletal structure for medicine and sports, Hemisphere Publishing Corporation, New York 1989

[6] Wilkinson I., Lennox G., Essential Neurology, Blackwell Publishing, 2005.

[7] Zander T. *et al.*, Influence of ligament stiffness on the mechanical behavior of a functional spinal unit, Journal of Biomechanics 37, 2004.

In-vitro concept based on kinematic criteria comparison for artificial-intervertebral replacement testing

Holub O.[1]*,Otáhal M.[1] Otáhal S.[2]

[1]*Laboratory of Biomechanics, Department of Mechanics, Biomechanics and Mechatronics, Faculty of Mechanical Engineering, Czech Technical University in Prague, Prague, Czech Republic
ondrej.holub@fs.cvut.cz
[2] Department of Anatomy and Biomechanics, Faculty of Physical Education and Sport, Charles University in Prague, Prague, Czech Republic

Introduction

Presently, the biomechanics community is closely focused on scientific research of phenomena called the low back pain. The sphere of interest has turned to the whole spinal mechanism in order to develop a satisfactory solution for many people suffering from low back pain. This phenomenon has probably been explored from all points of view and there is plenty of works concerning the topic.

Therefore a scientific team has been set together in order to validate the inovative kinematic concept with a close connection to an experimental workplace.

This work is engaged in possibility of interconnecting measured data of in-vivo kinematics and spinal functional unit in-vitro. And that with closer analysis of behaviour of the instantaneous axis of rotation [Holub et al, 2008]. It was empirically found out that there is a very close relation between the IAR´s location and degenerative changes or by phenomenon called Whiplash [Gripp et al, 2008]. Irregularity of the IAR´s position has been associated with pain in majority of cases.

The concept of dual kinematics has been partially verified by a mathematical model[Otáhal 2006]. But the control mechaninism for such a sophisticated system was too sensitive to determination of mechanical properties and reaction time and the system became unstable. So that it was necessary to elaborate more presisely the methodology.

Materials and methods

A concept of "dual kinematics" has been drafted out for needs of closer understanding of behaviour of the vertebral system when loaded. The concept is similar to concepts in other joints. It strictly distinguishes between active and passive mechanical elements of the kinetic apparatus of the spine. The passive elements are tissues that define the pattern of the movement by their stiffness characteristics. The active elements are the muscles that are tuning the pattern directly or indirectly for specific kinematic needs. The spinal system is very sophisticated and interwoven by a dense net of proprioceptive feedback circuits. They provide prompt and exactly aimed reaction. Our work is thus based on the concept that the tuned kinematics maintains a balanced system in the operational space. The system is pre-defined by lay-out and history of the passive elements.

The method is based on a comparative analysis of the state that is considered as "real" in-vivo and of the simulated. We are analyzing influence of the different state of the model.

The measured and again applied kinematic pattern of a solid 'n' compared with solid 'n+2' helps us to compare behaviour of the solid between them. In case of our experiment these are three contiguous vertebrae focused on lumbar part of spine.

Presently the kinematic data in-vivo are obtained on open MRI, measured using the Siemens Magnetom Open viva 0,2T, for discrete position of lumbar spine with exposition of app. 3.5 minutes. In order to eliminate imperfections of imagining, the approximation of vertebra shape on each image with one with long exposition and backwards application of shape was needed. This method allowed us to apply the markers to approximated shape in order to eliminate errors in predicting the position of markers.

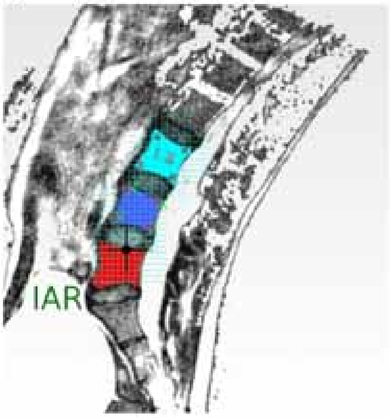

As mentioned above, the IAR provides a prompt and valid information about instantaneous behaviour of the system in discrete phases. For this purpose a system of scanning and calculation of the IAR from kinematic experiment for unipolar movements (inflexion- extension) has been designed.

Results and discussion

The method of the measurement of the spinal kinematics using open magnetic resonance does not bring quality data. Further we have found out that it is too lengthy to analyze the images when looking for key points from the magnetic resonance. And thus we are presently testing the system for new methods that would enable a more continuous movement. And thus they would significantly make the dynamic behavior of the tuned kinematics clear.

On contrary to it the method of calculation of the IAR and the comparative analysis have proved as strong and promising to the future for verification of the dual kinematics concept. It has shown possibilities of testing of artificial intervertebral discs and of influence of an operator´s mistake in positioning of the implants.

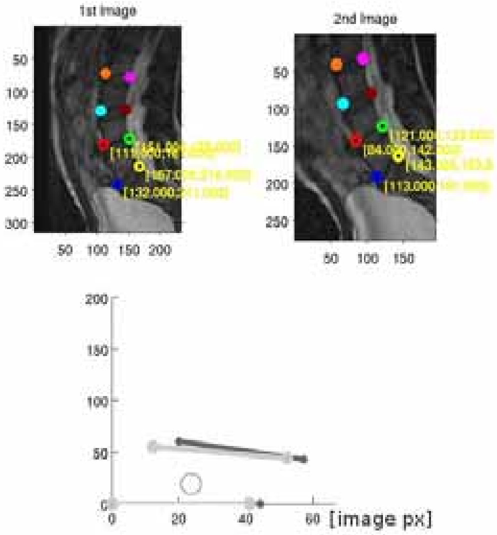

Fig. 1: IAR calculation from MRI data

Conclusion

A more detailed examination of intervertebral kinematics' behavior in-vivo connected to IAR leads to better understanding of complex mechanism of the whole intervertebral connection [Panjabi M.,1990].

The main aim of this work is an analysis of use of imaging methods for the IAR examination which is crucial for better understanding of kinematic behavior of the spinal system. Theoretical approach to intervertebral kinematics modelling has been already proved. But the need of practical verification has led us to practical extensions applicable for biomechanical testing. This work is based on the application of proved hypotheses and interlacing them with instantaneous axis of rotation as a key data for kinematic controlling system. These data are important for control and correlation of the model approach to modelling of the intervertebral kinematics.

Acknowledgements

Financial support for this project under grant MPO No. FT-TA3/131

References

[1] Adams M.A., *Spine Biomechanics,*Journal of Biomechanics, 38, 2005 ,1972-1983.

[2] Gripp et. al., Cervical helical axis characteristics and its center of rotation during active head and upper arm movements, Journal of Biomechanics, 38, 2008, 2799 - 2805.

[3] Holub et al, Instantaneous axis of rotation as a key data for intervertebral modelling, Conference HB2008, Prague, 2008

[4] Otáhal M., The system view of spinal system and the mathematical modeling of the spine, 2006

[5] White III A.A., Panjabi M.M. Clinical biomechanics of spine, 1990

Load Transmission: Morphological Adaption in Tarso-metatarsal Joints

Ebel C.[1], Müller-Gerbl M.[2], Wurzinger L.J.[1], Putz R.[1]

[1]Institute of Anatomy, Ludwig-Maximilian University Munich, Pettenkoferstr.11, D-80336 Munich, Germany, christine.ebel@med.uni-muenchen.de
[2]Institute of Anatomy, University of Basel, Pestalozzistrasse 20, CH-4056 Basel, Switzerland

Introduction

Undefined middle foot pain can lead to significant limitations in life quality and achievements of patients especially in the latter half of their lives [1]. Diagnosis is complicated by insufficient knowledge of the function of the tarso-metatarsal joints (Lisfranc's joint, TMT joint). This can lead to poor therapy choices and, consequently, unsatisfactory treatment. Too often pain symptoms will persist and intensify and become chronic, while mobility is pronouncedly limited [3].

The TMT joints are particularly important in the structure of the foot. This is emphasized in a 2001 study by Lakin [4].

The aim of our study was to obtain insight into the function of force transmission in this bridge region of the foot skeleton. We analysed the localization of degenerative changes of articular cartilage of the TMT joints and the distribution of density in their subchondral bone plates. We refer to a number of previous studies which show that quantitative distribution of subchondral density is an expression of these bones' 'loading history' [2], i.e. their accommodation to predominant dynamic stress [5,6]. By means of CT-osteoabsorptiometry (CT-OAM) after Müller-Gerbl [5,6], a precise and well established diagnostic tool, these distribution patterns can be shown both in vitro and in vivo. As the significance of undefined middle foot pain increases, our approach to analysis of the TMT joints should offer clinical relevance. We chose to focus on older individuals, as we were aware of the practical importance of painless and sufficient mobility at an advanced age.

Materials and methods

We used 7 formalin-fixed complete tarso-metatarsal joint series (Lisfranc's joint, TMT joint) from the undergraduate dissection course (average age 80.8). Applying the Collins schema, localisation of cartilaginous surface DMC was examined. For showing subchondral density patterns the well-established method of CT-osteoabsorptiometry (CT-OAM) was used.

Results and discussion

Far more than half of the articular surfaces examined showed a predominance of slightly changed cartilage surfaces. Moderate to heavy cartilage deterioration could be documented in approximately one third of cases. The cartilaginous surface DMCs were frequently located at the medial edges. Analysis of maximum density area localization, both proximal (ossa cuneiformia) and distal (ossa metatarsalia), allowed identification of four different types. Most frequent was type C, whose maximum is located along the medial edge with continuations towards the dorsal margin (Fig.1,2). There was a clear correlation of topical cartilage degeneration and subchondral density.

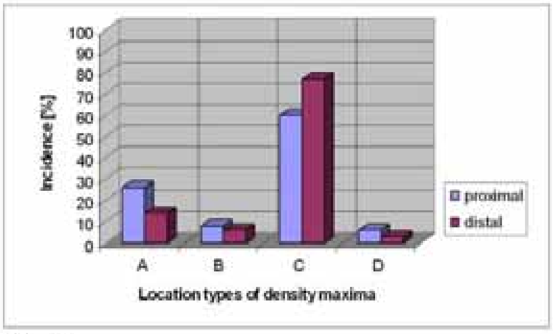

Fig. 1:
Localisation of maximum density areas (CT-OAM)

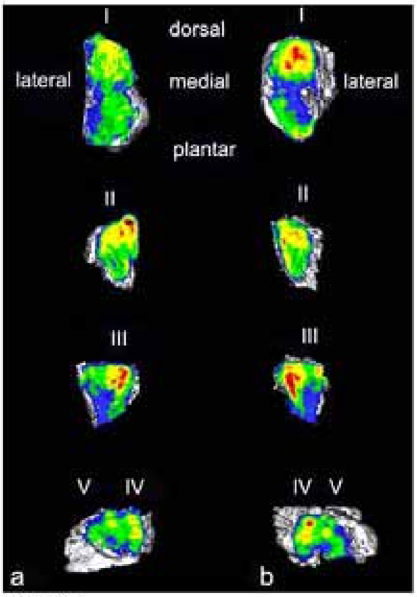

Fig. 2:
CT-OAM: ventral view, right foot:
typical distribution patterns: **a** Ossa cuneiformia I-III, Os cuboideum, **b** Ossa metatarsalia I-V

Conclusion

In summary, we observe that under dynamic conditions, in healthy feet the force transmission in the TMT joints appears to occur via the dorsal and medial edges. Considering the correlation of topical cartilaginous surface DMC and subchondral density patterns, clinical application of CT-OAM seems to be recommendable in the case of undefined middle foot pain.

As we could demonstrate, the individual material distribution of supportive tissue makes visible the manifestation of skeletal dynamics.

Acknowledgements

We want to thank Linda Jakobi for her excellent technical support at the workstation.

References

[1] Bowling A. et al., Age and Aging. 26:107-114, 1997
[2] Carter DR., J Biomech. 20:785-794, 1987
[3] Goossens, M. et al., Clin Orthop. 176:154-162, 1983
[4] Richter, M. et al, Foot Ankle Int. 22:392-398, 2001
[5] Lakin RC., J Bone Joint Surg. 83:520-528, 2001
[6] Müller-Gerbl M. et al., Skeletal Radiol. 18:507-512, 1989
[7] Müller-Gerbl M. et al., J Bone Miner Res 2:411-418, 1992

Advances in the biomechanical approach to standing human body vibration

Grimpampi E.[1]*, Sacripanti A.[1,2]

[1]*Facoltà di Medicina e Chirurgia, University of Rome "Tor Vergata", Italy, eleni.grimpampi@enea.it
[2]Dipartimento Tecnologie della Fisica e Nuovi Materiali (FIM), ENEA, Italy

Introduction

A human body is exposed to different kind of vibrations. In the last decades many studies have been conducted to investigate the effect of whole-body vibration exposure[1-4].

In this study the standing human body exposed to vertical vibration is examined, and the energy expenditure of the human body in a vibration environment is estimated, by means of a global and integrated approach. In particular, the variation in O_2 uptake, the variation in superficial temperature and the displacement of the markers related to the muscles are calculated and compared for different vibration frequencies.

Considerations and experiment set up

The human body can be considered as a complex organic structure. In order to understand how it responds to vertical vibration, it is useful to address the problem with an integrated and global approach. Estimating the energy expenditure of the subjects by means of the variation of the superficial temperature with the aid of infrared thermography, the displacement of the markers related to the muscles with the aid of the ViconMX® Motion Analysis System and the oxygen uptake with the aid of the CosmedK4® telemetric system, it is possible to obtain interesting results regarding the subject's behaviour under different vibration conditions.

The lack of consistency in whole-body vibration protocols in the current published studies makes the establishment of an appropriate protocol essential, and in this sense, an experiment set up was implemented. Six persons were subjected to vertical vibration ranging from 20 to 50 Hz and for an exposure time of 5 to 30 min. After the establishment of the final protocol a series of laboratory experiments took place. Two males were exposed in vertical vibration at three different frequencies: 20, 30 and 45 Hz and for an exposure time of 26 min (including the rest period before and after the vertical vibration).

For the measurements the following systems were used:

- vibrating plate which delivers vibrations across a range of frequencies (20 – 50 Hz);
- ViconMX® Motion Analysis System for the three dimensional kinematic motion analysis using 18 reflected markers attached on the athlete's body;
- two infrared thermography systems; and,
- CosmedK4® telemetric system for the measurement of the oxygen uptake.

As can be seen in Figure 1, the subject is placed on a vibrating plate with the reflective markers and the CosmedK4® face mask. A thermal image of the subject during the experiment can also be seen.

Fig. 1: Testing on a standing human body exposed to vertical vibration

Results and discussion

The most interesting findings regard the oxygen uptake, the superficial temperature evolution, and the transmissibility and dispersion coefficients for the acceleration of the muscles. Having information for these variables, the effects of the whole-body vibration to the human body can be understand from a global point of view. Regarding the oxygen consumption during the experiment, a linear relationship between the frequency of vibration exposure and the average oxygen consumption is found with a good approximation (Fig. 2).

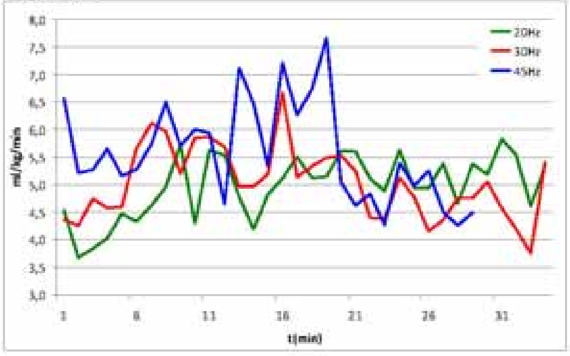

Fig. 2: VO_2 consumption at three different frequencies

Conclusion

The primary objective of this study is to develop and implement an appropriate whole-body vibration protocol and to study the effects of whole-body vibration to the human body in a standing position by means of energy expenditure. Because of the complexity of the human body structure, this problem could be affronted in a better manner by an integrated and global approach. This study is an essential step for applying this approach to a greater number of individuals, in order to achieve statistical validation.

Acknowledgements

The authors wish to acknowledge the technical support of the ENEA (*Italian Agency for Technological Innovation, Environment and Energy)* where the research has been carried out. Furthermore, the contribution of Dr. Ing. Ivan Roselli and Stefano Bonifazi of the ENEA, and Dr. Antonio Buglione of the University of Rome "Tor Vergata" in the data acquisition and analysis, is acknowledged.

References

[1] Griffin, M. J. Handbook of human vibration Academic Press, London, 1996

[2] Holmlund, P. and Lundström, R. Mechanical Impedance of the Human Body in the Horizontal Direction. Journal of Sound and Vibration. pp. 215 (4), 1998, pp. 801-812

[3] Bosco, C., Colli, R., Introini, E., Cardinale, M., Tsarpela, O., Madella, A., Tihanyi, J. and Viru, A. Adaptive responses of human skeletal muscle to vibration exposure. Clin. Physiol. 19 (2), 1999, pp. 183-187

[4] Kerschan-Schindl, K., Grampp, S., Henk, C., Resch, H., Preisinger, E., Fialka-Moser, V. and Imhof, H. Whole-body vibration exercise leads to alterations in muscle blood volume. Clin. Physiol. 21 (3), 2001, pp. 377-382

Intravertebral Distribution of Trabecular Bone Architecture in Vertebral Bodies of the Human Thoracic Spine – a MicroCT-Study

Doberauer J.[1], Wurzinger L.J.[1], Putz R.[1], Müller-Gerbl M.[2]

[1]Institute of Anatomy, Ludwig-Maximilian University Munich, Pettenkoferstr.11, D-80336
Munich, Germany, johannes.doberauer@med.uni-muenchen.de
[2]Institute of Anatomy, University of Basel, Pestalozzistrasse 20,
CH-4056 Basel, Switzerland

Introduction

Osteoporosis is a degenerative bone disease, affecting, in many different ways, a considerable share of the population of our western industrial nations. Lack of daily exercise, incorrect diet, nicotine abuse, alcohol abuse and at the same time heavy burden going beyond daily measure, result in clearly increased risk of bone fracture. Particularly the spinal column is affected, which combines in itself a compromise between static load-bearing capacity and kinematic possibilities [2]. It is possible that vertebral fractures burden affected patients with chronic back pain and functional complaint to a high degree [1] and that their quality of life is clearly reduced. Osteoporotic changes are based on processes of renovation in the trabecular structure, which can finally lead to vertebral bodies becoming unstable and collapsing under burden.

This study aimed at investigating regional differences in the trabecular structure inside the thoracic vertebral bodies and, on this basis, at collecting information on their stability.

Materials and Methods

For our study we used four female cadavers (aged 57-80, on average 64, 3) out of the supply of the students' dissecting course from the Institute of Anatomy in Munich. We examined the vertebral bodies of the four thoracic vertebrae T2, T5, T8 and T11. We excluded specimen with superficially visible degenerative changes, as well as with scoliosis and such indicating surgery. For the micro-tomographic imaging we used a micro-ct 20 from Scanco (Zürich, CH). The vertebral bodies were subdivided by transverse and sagittal sections in such a way that at T2 and T5 there could be investigated 24 regions each and at T8 and T11 36 each and individually. Thereby the analysis was restricted to the cancellous bone. We assessed the results of the structure parameters bone-volume-fraction (BV/TV), connectivity density (Conn.D.), structure-model-index (SMI), trabecular number (Tb.N.), trabecular separation (Tb.Sp.) and degree of anisotropy (DA) from their cranial to their caudal sections and we compared the difference between ventral and dorsal within the vertebral bodies.

Results and Discussion

Five of the seven structural parameters showed clearly perceptible tendencies from the cranial to the caudal sections. Thereby, near the endplates, Conn.D., SMI und Tb.N. showed high values, which decreased reaching the midtransverse section. In reverse, however, the values of Tb. Th. and Tb. Sp. were low near the endplates and increased reaching the midtransverse section.

The comparison of the values between the front and the back regions of the vertebral body showed that, in the dorsal regions, the structural parameters BV/TV, Conn.D. and Tb.N. tend to indicate clearly higher values, whereas Tb.Sp. and DA showed clearly lower values from the cranial to the caudal sections.
Considering the small number of cases this study didn't allow any statistical analysis and it remained to be descriptive. Nevertheless there could be found distinct tendencies due to a high number of separately analyzed regions of the vertebral bodies and clear homogeneity of the results. Therefore it became obvious, that the regions near the endplates as well as the dorsal zones of the cancellous bone in the vertebral body showed a substantially more dense structure than other regions.

Conclusion

Our results show clear patterns of distribution of the trabecular structure within the thoracic vertebral body. Particularly near the endplates and in the dorsal regions cancellous bone appears to make a major contribution to the load bearing capacity of the vertebral body. These findings could be of vital importance for the surgical therapy of osteoporosis induced vertebral fractures.

Acknowledgements

Special thanks go to Mrs. Prof. Dr. Magdalena Müller-Gerbl for her valuable contributions and helpful suggestions.

As well I would particularly like to thank Mr. Prof. Dr. Dr. Reinhard Putz for exceedingly interesting and informative conversations I was allowed to have with him.

References

[1] Health U.D.O., Clinician 22, 2004
[2] Putz R., Ann Anat 174: 40-47, 1992

AUTHORS INDEX

Social Event

A social event will take place on Monday evening. All participants are invited to have dinner together at Zurich Zoo. The social event will provide the opportunities to meet and discuss in a relaxed atmosphere.

Picture: Zürich Tourismus

Picture: Zoo Zürich; www.zoo.ch

PROGRAM: Monday 8th June 2009

18.15	**Entrance Zoo**
18.30 – 19.30	**Apéro at the lions enclosure (good weather) or at the penguins place**
19.30 – 20.30	**Guided tour**
20.30	**Banquette and more**

Map of the City of Zurich

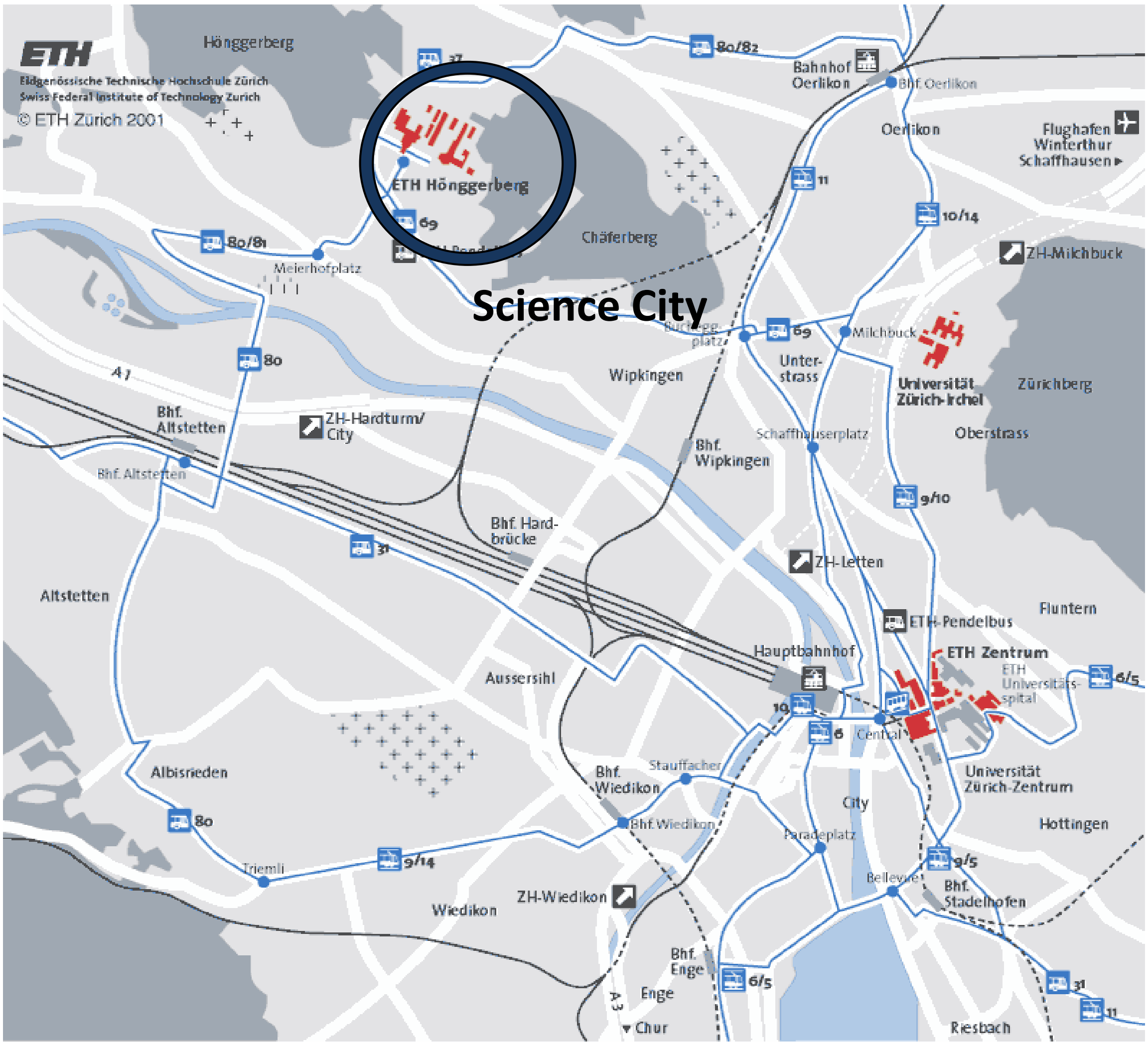

The conference venue is ETH Zürich, *Campus Hönggerberg, Science City, Institute for Biomechanics*.

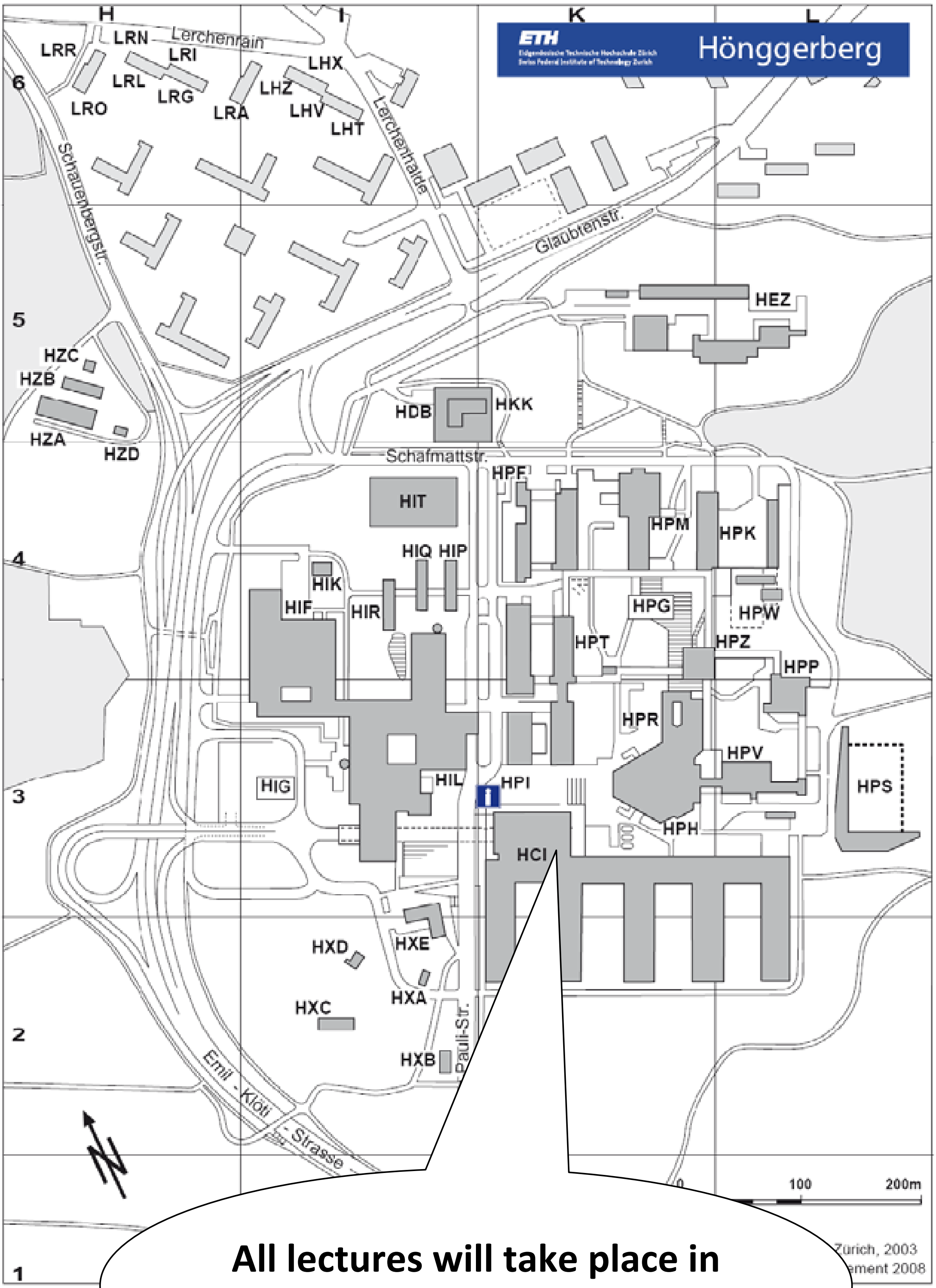

All lectures will take place in room HCI J7

Sunday, June 7 HCI J7 15:00 - 18:30

13:00 Registration

15:00

Opening ceremony

Tutorials

Introduction to the movement of the human body

Movement and loading during activities and its consequences on the musculo-skeletal system with a focus on soft tissues

15:15 T1 **Muscle loading; structural, functional and molecular implications as well as health consequences**
Hoppeler Hans

15:45 T2 **Muscle repair and hypertrophy following exercise and the role of mechano growth factor and the IGF-1 gene**
Goldspink Geoffrey

16:15 T3 **The movement and loading during activities and its consequences on the musculo-skeletal system with a focus on soft tissues - relevant medical problems of the soft tissues**
Goldhahn Jörg

Discussion

---------------- Break -----------------

Posters

17:00

Poster Talks

P1 **Triceps-surae musculotendinous stiffness in women with different foot types**
Aurélio F., Helena M. and Ronaldo G.

P2 **Specificity of loading and seasonal variation of vertical jumping performance in young women athletes**
Rousanoglou E. and Boudolos K.

P3 **Micromechanics modeling of axonal injury in brain white matter**
Abolfathi N., Syed A., Karami G. and Ziejewski M.

P4 **Effect of age, body composition and anthropometric variables in the biomechanic parameters of plantar pressure in obese postmenopausal women**
Monteiro M. A., Gabriel R. E. and Moreira M. H.

P5 **Exact modeling and finite element analysis of C6-C7 segment of cervical spine**
Haghpanahi M., Hosseini B., Beizaee Sh. and Shabanimotlagh M.

P6 **Computational analysis of the electro-mechanical activation sequence of the myocardium**
Marcé-Nogué J., Roure F. and Fortuny G.

P7 **An integrated FE Model for blast waves - human head biomechanical interactions**
Chafi M.S., Karami G. and Ziejewski M.

P8 **On the influence of surgical trauma, age and gender on periprosthetic bone remodelling after THA**
Szwedowski T. D., Taylor W. R., Matziolis G., Heller M. O., Müller M., Janshen L., Perka C. and Duda G.

P9 **Numerical and experimental analysis of correlation between neck muscles activity and mechanical vertebrae loading conditions**
Gzik M., Tejszerska D. and Świtoński E.

P10 **In-vitro concept based on kinematic criteria comparison for artificial-intervertebral replacement testing**
Holub O., Otáhal M. and Otáhal S.

P11 **Load-transmission: morphological adaption in tarso-metatarsal joints**
Ebel Ch., Müller-Gerbl M., Wurzinger L. J. and Putz R.

P12 **Advances in the biomechanical approach to standing human body vibration**
Grimpampi E. and Sacripanti A.

P13 **Intravertebral distribution of trabecular bone architecture in vertebral bodies of the human thoracic spine – a microCT-study**
Doberauer J., Wurzinger L.J., Putz R. and Müller-Gerbl M.

18:30 **Buffet Dinner**

Monday, June 8 HCI J7 09:00 - 17:30

Tutorials

Material response – mechanical effects of loading

What are the effects of movements and loading on the entire musculo-skeletal system with a focus on soft tissues; what causes health problems, what can be tolerated?

09:00	T4	**Tendon structure and function - an intricate balancing act** Snedeker Jess G.
09:30	T5	**Effects of movements and loading on the entire musculoskeletal system with a focus on muscle. What causes health problems, what can be tolerated?** Denoth Jachen

Talks

Session 1: Load Case

10:00	O1	**A novel method to compute muscle moment arms** Favre P. and Snedeker J.G.
10:15	O2	**A novel cable fixation technique reduces fragment dislocation in case of proximal humeral four part fractures** Baumgartner D., Schlüssel M., Gerber H. and Stüssi E.
		--------------- Break ----------------
11:00	O3	**Protocol for the shoulder valuation with an opto-electronic system and clinical application to the follow-up of traumatic patients** Anasetti F., Accetta R., Galbusera F., Meersseman A., Monti L., Aziz H.N. and Mineo G.V.
11:15	O4	**Evidence of mechanical load redistribution at the knee joint in the elderly while performing ramp and stairway locomotion** Karamanidis K. and Arampatzis A.
11:30	O5	**An investigation into the effects of a simulated effusion in healthy subjects on knee kinematics and muscle activity during jogging and running.** Coughlan G.F. , Mc Loughlin R ., Mc Carthy Persson U. and Caulfield B.
11:45	O6	**Prediction of foot instability and inbalance using biomechanical measurements** Rusu L., Marin M., Dragomir M. and Rusu P.F.
12:00	O7	**Movement optimization of multibody system with application to long jump** Pettersson R. and Eriksson A.
12:15	O8	**Intraarticular and muscle force reactions of the leg using different insoles** Wyss Ch., Roethlisberger M., Gerber H.

Lunch

Sponsors

Product Presentations

13:15	**QUALISYS: Real-time performance with optical mocap system**
13:45	**CADFEM: Calculation of boundary conditions for a Finite Element Analysis with the AnyBody Modeling System**
14:00	**SMITH & NEPHEW: Biomechanics & Research Europe**

Tutorials

14:15	T6	**Immediate and short term response of tendon and ligament to mechanical load** Birch Helen
14:45	T7	**Short term mechano-regulation of muscles due to movement** Flück Martin

Talks

Session 2: Muscle

15:15	O9	**Rat tibialis anterior muscle characterization, passive and active behaviour. 3D Finite Element Model.** Grasa J., Muñoz M. J., Soteras F., Osta R., Zaragoza P., Calvo B. and Doblaré M.
15:30	O10	**Intramuscular architecture of the autochthonous back muscles in humans** Stark H., Fröber R., Schilling N.
		--------------- Break ----------------
16:15	O11	**Cooperation and variability within the sarcomere network – investigated by isolated mini muscle cells** Dettwiler F. and Denoth J.
16:30	O12	**Mechanical work as predictor of force enhancement and force depression** Kosterina N., Westerblad H. and Eriksson A.
16:45	O13	**Force enhancement in a myofibril - the role of half-sarcomere dynamics** Stöcker U. and Denoth J.
17:00	O14	**Model of the muscle transversal deformation evoked by the muscle contraction** Kaczmarek P.
17:15	O15	**Glycosaminoglycans do not influence collagen fibril load transmission or dynamic viscoelasticity in tendon** Fessel G. and Snedeker J.G.
18:15		**Social Event, Entrance Zoo**

Tuesday, June 9 HCI J7 09:00 - 14:45

Tutorials

Tutorials: System adaptation – long term effects of loading

Long-term effects of load, adaptation of material (micro), development of injury, interventions and therapies (macro)

09:00	T8	**Long-term musculoskeletal adaptations to loading and unloading in humans** Narici Marco
09:30	T9	**Effects of musculoskeletal loading on the prevention and rehabilitation of muscle-tendon injury: biomechanical and neural aspects** Aagaard Per

Talks

Session 3: Mix

10:00	O16	**Anatomically-based modeling of soft-tissue muscle deformations in the lower limbs during walking** Oberhofer K., Mithraratne K., Stott S. and Anderson I.A.
10:15	O17	**Modelling proximal femur deformities in spastic diplegic children** Carriero A., Zavastky A., Stebbins J., Theologis T., Lenaerts G., Jonkers I. and Shefelbine S.
		---------------- Break -----------------
11:00	O18	**Femero-acetabular impingement: motion as an initiator of hip joint degeneration** Chegini S. and Ferguson S.J.
11:15	O19	**Effects of gravity on ulnar nerve latency of activation. Preliminary results of an in-vivo study** Mastrandrea F., Pandis C. and Metastasio A.
11:30	O20	**The influence of recovery and training phases on body composition, peripheral vascular function and immune system of professional soccer players** Reinke S., Taylor W. R., Karhausen T., Doehner W., Hottenrott K., Duda G., Reinke P., Volk H.D. and Anker S.D.
11:45	O21	**Functional imaging of tendon for improved tissue assessment** Harvey A. K., Thompson M. S., Cornell H., Hulley P., Cochlin L., Tirlapur U., Cui Z. and Brady M.
12:00	O22	**Toward intraoperative functional imaging of the rotator cuff tendons** Li Y., Wuergler-Hauri C.C., Gerber C. and Snedeker J.G.

Tutorials

12:30		**ESB Student Tutorial: The most important aspects when undertaking and completing a Ph.D.** Taylor William and Müller Ralph
		Lunch
13:30	T10	**Molecular basis of muscle contraction** Linari Marco
14:15		**Prize giving, Closure**
14:45		optional town tour, lab tour IfB or SMS Lab